공학박사 학위논문

Metabolic engineering of *Saccharomyces cerevisiae* for production of isobutanol and UV-absorbing chemical shinorine

Saccharomyces cerevisiae 의 대사공학을 통한 이소부탄올과 자외선 차단 소재 시노린 생산

2018 년 8 월

서울대학교 대학원

화학생물공학부

박 성 희

Metabolic engineering of *Saccharomyces cerevisiae* for production of isobutanol and UV-absorbing chemical shinorine

by

Seong-Hee Park

Advisor : Professor Ji-Sook Hahn, Ph.D.

Submitted in Partial Fulfillment of the Requirements

for the Degree of Doctor of Philosophy

in Seoul National University

August, 2018

School of Chemical and Biological Engineering

Graduate School

Seoul National University

ABSTRACT

Metabolic engineering of *Saccharomyces cerevisiae* for production of isobutanol and UV-absorbing chemical shinorine

Seong-Hee Park
School of Chemical and Biological Engineering
The Graduate School
Seoul National University

Saccharomyces cerevisiae is considered as promising host for production of biofuels and chemicals because it is a well-studied eukaryotic model system with high stress tolerance and robustness in harsh industrial conditions. In this dissertation, several strategies were developed and applied to produce isobutanol and shinorine in *S. cerevisiae*.

Firstly, *S. cerevisiae* CEN.PK2-1C, a leucine auxotrophic strain having a *LEU2* gene mutation, was engineered for the production of isobutanol and 3-methyl-1-butanol. An *ALD6* encoding aldehyde dehydrogenase and *BAT1* involved in valine synthesis were deleted to eliminate competing pathways. Transcription of endogenous genes in the valine and leucine biosynthetic pathways was also increased

by expressing Leu3Δ601, a constitutively active form of Leu3 transcriptional activator. For the production of isobutanol, genes involved in isobutanol production (*ILV2*, *ILV3*, *ILV5*, *ARO10*, and *ADH2*) were additionally overexpressed in *ald6Δbat1Δ* strain expressing *LEU3Δ601*, resulting in 376.9 mg/L isobutanol production from 100 g/L glucose. To increase 3-methyl-1-butanol production, leucine biosynthetic genes were additionally overexpressed in the final isobutanol-production strain. The resulting strain overexpressing *LEU2* and $LEU4^{D578Y}$, a feedback inhibition-insensitive mutant of *LEU4*, showed a 34-fold increase in 3-methyl-1-butanol synthesis compared with CEN.PK2-1C control strain, producing 765.7 mg/L 3-methyl-1-butanol.

Secondly, mitochondrial isobutanol production was improved by increasing mitochondrial pool of pyruvate, a key substrate for isobutanol production. Subcellular compartmentalization of the biosynthetic enzymes is one of the limiting factors for isobutanol production in *S. cerevisiae*. Previously, it has been shown that mitochondrial compartmentalization of the biosynthetic pathway through re-locating cytosolic Ehrlich pathway enzymes into the mitochondria can increase isobutanol production. Mitochondrial isobutanol biosynthetic pathway was introduced into *bat1Δald6Δlpd1Δ* strain, where genes involved in competing pathways were deleted, and *MPC1*, *MPC2*, and *MPC3* genes encoding the subunits of mitochondrial pyruvate carrier (MPC) hetero-oligomeric complex were overexpressed with different combinations. Overexpression of Mpc1 and Mpc3 forming high-affinity MPC_{OX} was more effective in improving isobutanol production than overexpression

of Mpc1 and Mpc2 forming low-affinity MPC_{FERM}. The final engineered strain overexpressing MPC_{OX} produced 338.3 mg/L isobutanol from 20 g/L glucose, exhibiting about 22-fold increase in production compared with wild type. Furthermore, to increase in Ilv3 activity, Nfs1 and Isd11genes, encoding cysteine desulfurase involved in iron-sulfur cluster assembly, were overexpressed, resulting in improved isobutanol production up to 435.2 mg/L.

Thirdly, isobutanol production was improved via construction of artificial cytosolic biosynthetic pathway by multi-copy integration system in *S. cerevisiae*. α-acetolactate synthase (ALS) is the key enzyme redirecting pyruvate flux to isobutanol production by competing with pyruvate decarboxylase (PDC) involved in ethanol production. To improve isobutanol production using the major pyruvate pool in the cytosol, cytosolic isobutanol biosynthetic pathway was constructed by overexpressing heterologous ALS (*alsS*) from *Bacillus subtilis* and *Lactococcus lactis*, and N-terminally truncated *ILV5* (*ILV5ΔN48*) and *ILV3* (*ILV3ΔN19*) lacking mitochondrial targeting signal with kozak sequence. Since overexpression of *alsS* from *B. subtilis* under the control of strong promoter promoted cell death, copper-inducible promoter, P_{CUP1}, was used to overexpress *alsS*. Cytosolic isobutanol biosynthetic pathway was constructed via delta- and rDNA-integration which are powerful tools for random multi-copy gene integration in *S. cerevisiae*, especially coupled with antibiotic selection. Multi-copy integration of *alsS* was screened by using antibiotic markers and also by selecting clones showing growth defects upon *alsS* induction by copper. The final engineered strain (JHY43D25-4) additionally

overexpressing *ILV5ΔN48*, *ILV3ΔN19*, 2-ketoacid decarboxylase (kivd), and alcohol dehydrogenase (Adh2) produced 265.5 mg/L isobutanol, exhibiting about 4.3-fold increase in production compared to control strain JHY43.

Lastly, *S. cerevisiae* was used as a host for the heterologous production of a UV-absorbing sunscreen material shinorine. By introducing heterologous shinorine biosynthetic genes from cyanobacteria, *Nostoc punctiforme* and *Anabaena variabilis*, into *S. cerevisiae*, yeast strain capable of producing shinorine was successfully constructed. Furthermore, to increase the pool of sedoheptulose 7-phosphate (S7P), an intermediate in pentose phosphate pathway used for shinorine production, xylose assimilation genes, xylose reductase (*XYL1*), xylitol dehydrogenase (*XYL2*), and xylulokinase (*XYL3*) were introduced to use xylose as a carbon source. In a fed-batch fermentation, the engineered JHYS17-1 strain produced 64.2 mg/L shinorine with highest content (14.3 mg/gDCW) ever reported in microbes. In addition, deletion of competing pathway producing erythrose-4-phosphate and fructose-6-phosphate from S7P, and overexpression of transcriptional factor (Stb5) for genes involved in pentose phosphate pathway and transketolase (Tkl1), contributed to enhancing shinorine production.

Keywords : Metabolic engineering, Amino acid metabolism,
Isobutanol, Mitochondrial pyruvate carrier, Shinorine, Xylose assimilation, Delta-integration, rDNA-integration, *Saccharomyces cerevisiae*

Student Number **:** 2014-30253

CONTENTS

LIST OF FIGURES

LIST OF TABLES

LIST OF ABBREVIATIONS

ADH	alcohol dehydrogenase
CRISPR	Clustered Regularly Interspaced Short Palindromic Repeats
DAHP	3-deoxy-arabino-heptulosonate 7-phosphate
DDG	2-demethyl 4-deoxygadusol
4-DG	4-deoxygadusol
DHAP	dihydroxyacetone phosphate
3-DHQ	3-dehydroquinate
E4P	erythrose-4-phosphate
EV	2-epi-5-epi-valiolone
F6P	fructose-6-phosphate
G3P	glycerol-3-phosphate
G6P	glucose-6-phosphate
GAP	glyceraldehyde-3-phosphate
GC	gas chromatography
GRAS	generally recognized as safe
His	histidine
HPLC	high performance liquid chromatography
KDC	ketoacid decarboxylase
2-KIV	2-ketoisovalerate

LTRs	long terminal repeats
Leu	leucine
MAAs	mycosporine-like amino acids-
MG	mycosporine-glycine
MPC	mitochondrial pyruvate carrier
OD	optical density
PCR	polymerase chain reaction
PDC	pyruvate decarboxylase
PEP	phosphoenolpyruvate
PPP	pentose phosphate pathway
qRT-PCR	quantitative reverse transcription PCR
qPCR	quantitative PCR
RBS	ribosome binding sites
Ri5P	ribulose-5-phosphate
R5P	ribose-5-phosphate
RI	refractive index
SC	synthetic complete
S7P	sedoheptulose 7-phosphate
Trp	tryptophan
Ura	uracil
X5P	xylulose-5-phosphate
YP	yeast extract-peptone

Chapter 1.

Research background and objective

In recent decades, metabolic engineering of microorganisms has greatly developed for the production of valuable material such as various chemicals, fuels, and pharmaceuticals [1]. Metabolic engineering aims to development of efficient cell factories by rewriting cellular metabolism to achieve high titer and yield of production. To this end, development of new tools for biosynthetic pathway optimization and genome engineering is essential.

Saccharomyces cerevisiae is considered as a great platform organism for metabolic engineering because of its well-studied genetics and physiology, developed abundant genetic manipulation tools, ease of cultivation, high tolerance to alcoholic compounds, and microbes generally recognized as safe [2]. Especially, since *S. cerevisiae* as eukaryotic organism has a endomembrane structure which is not possessed by bacteria, it provides various other environmental characteristics that can be applied to various studies.

The first objective of this study was to enhance innate isobutanol biosynthesis pathway for increase in isobutanol production. Isobutanol is considered as a promising alternative to ethanol as fuels. *S. cerevisiae* naturally produces isobutanol via valine biosynthesis and Ehrlich pathways, but its production is very small. In yeast, isobutanol is produced through the valine biosynthetic pathway and many enzymes involved in this pathway are transcriptionally inhibited by the accumulation of intermediates and products. Therefore, in order to increase the production of isobutanol in yeast, it is necessary to construct and reinforce isobutanol biosynthetic pathway that is not affected by such feedback inhibition.

The second objective of this study was to impeccably develop mitochondrial isobutanol biosynthetic pathway to improvement of isobutanol production. In *S. cerevisiae*, the valine biosynthetic process occurs in the mitochondria while the subsequent Ehrlich pathway occurs in the cytoplasm. Therefore, to increase isobutanol production, much of pyruvate, an important precursor for the production of isobutanol, must be imported into mitochondria. In addition, the intermediates of the Ehrlich pathway must be well exported to the cytoplasm. In order to overcome this problem triggered by subdivision of synthetic pathway, mitochondrial isobutanol production pathway was constructed by introducing enzymes involved in the Ehrlich pathway into the mitochondria. Compartmentalization of biosynthetic pathway is considered as a powerful strategy for increasing target products by facilitating fast reaction rates through concentration of substrates. However, to further increasing isobutanol using the mitochondrial biosynthetic pathway a sufficient mitochondrial pyruvate pool is required.

The third objective of this study was to construct artificial cytosolic isobutanol biosynthetic pathway. Another way to solve complexity of isobutanol biosynthetic pathway due to separation of the innate pathway by mitochondria in yeast is to establish a fully cytosolic isobutanol biosynthesis pathway. In order to perfect construction the exogenous pathway in the yeast, it is necessary to introduce a large amount of the gene into the genome. Integration of metabolic pathway genes with multi-copy in genome and the exact strain selection method is an essential component in metabolic engineering and synthetic biology. Although there are

several methods for screening yeast strains with multiple genes in genome, but a large amount of screening is still required to select the desired strains. Therefore, a screening method capable of accurately selecting strains having specific characteristics is needed.

The last objective of this study was to develop recombinant *S. cerevisiae* for the efficient production of shinorine. Shinorine is a promising natural sunblock material that can be used in cosmetic industry instead of chemical and physical sunblock material. Although a number of marine microorganisms such as cyanobacteria and algae can naturally produce shinorine, the most of them have been considered unsuitable for industrial-scale production because of difficulty of cultivation and genetic manipulation of these native producers. Therefore, it is necessary to develop efficient microorganisms as shinorine-producer.

The objectives of this study are summarized as follows.

- To enhance a innate isobutanol biosynthesis pathway for improving isobutanol production
- To develop a novel mitochondrial isobutanol biosynthetic pathway for efficient production of isobutanol
- To construct cytosolic isobutanol biosynthetic pathway by gene expression using copper inducible promoter and genes integration using multi-copy delta- and rDNA-integration for increasing isobutanol production
- To develop recombinant *S. cerevisiae* for the efficient production of sunscreen material shinorine

Chapter 2.

Literature review

2.1. Isobutanol production in microorganisms

2.1.1. Isobutanol

Isobutanol (2-methylpropan-1-ol in IUPAC name) also known as isobutyl alcohol 2-methylpropyl alcohol or isopropylcarbinol is a colorless sweet and musty odor and flammable liquid with the molecular formula $(CH_3)CHCH_2OH$. It has a high boiling point of 107.89˚C and a low freezing point of -108˚C. There are several isomers of isobutanol: *n*-butanol, 2-butanol, and *tert*-butanol, all of which are important in industry (Fig. 2.1).

Isobutanol is a promising valuable chemical that can be used in various areas especially as a liquid biofuel and a platform chemical. Because isobutanol has a high energy density of 31.6 kJ/g which is similar to gasoline (44.5 kJ/g) and higher than that of ethanol (29.7 kJ/g) it is considered to be an effective liquid fuel compared with bioethanol [3]. Also the low hygroscopicity of isobutanol makes it interesting for the use substitute for gasoline in the current petroleum infrastructure because of preventing the corrosion of engines and pipelines [3]. In case of using isobutanol as gasoline additive it can reduce the knocking of the engine and carburetor icing because it is a branched chain higher alcohol [4].

Isobutanol can be used in feedstock in the manufacture of isobutyl acetate which is used in the production of lacquer and in the food industry as a flavoring agent. Moreover, isobutanol can be precursor of derivative ester such as diisobutyl phthalate (DIBP) which is used as plasticizers in rubbers plastics and other

dispersions and also can be precursor of p-xylene, a building block for plastic bottles textiles and clothing. In addition, isobutanol is used as paint solvent, varnish, remover, ink ingredient, and paint additive.

2.1.2. Ehrlich pathway

Depending on the presence or absence of ammonium in the medium, some amino acids can be used as nitrogen source by assimilation and introduction into the biosynthesis of other amino acids. This catabolic process was first reported in 1907 by Felix Ehrlich and was thereby named as Ehrlich pathway (Ehrlich 1907). Ehrlich proposed that *S. cerevisiae* can be fermented in mixture of sole sugar and either leucine or isoleucine, one of branched chain amino acids (BCAAs), and, as a consequence, a higher amount of fusel alcohols was observed. Yeast can assimilate seven amino acids through the Ehrlich pathway, including valine, leucine, isoleucine, phenylalanine, tyrosine, tryptophan, and methionine (Table 2.1) [5]. The aromatic branched-chain alcohols and their derived esters made via the Ehrlich pathway is very important for the wine making industries by unique fragrance [6]. In general Ehrlich pathway is composed of three steps: initial transamination reaction, decarboxylation step, and reduction or oxidation of fusel aldehydes (Fig. 2.2). First, amino group from the amino acid is transferred into an acceptor, such as 2-oxoglutarate, by 4 enzymes consisting of Bat1, Bat2, Aro9, and Aro10, resulting in generation of α-keto acid. And then α-keto acid is converted to a fusel aldehyde

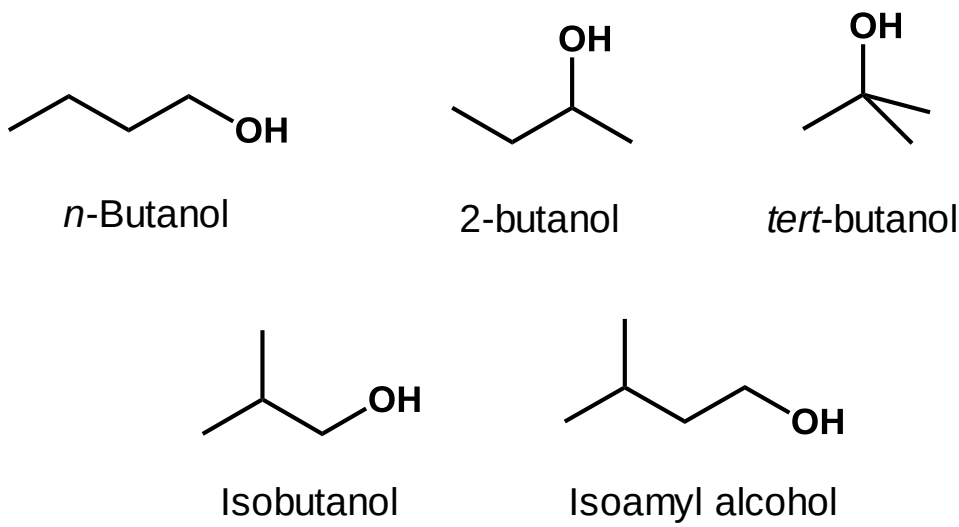

Figure 2.1 Struture of butanol isomer and branched-chain higher alcohols

by a decarboxylation reaction u and the last step can be either the aldehyde reduction to a fusel alcohol or the oxidation to a fusel acid (Fig. 2.2).

In case of catabolism of BCAAs the starting point of Ehrlich pathway is the deamination of the them which is performed by the transaminases Bat1 and Bat2. The amine group of the BCAAs is moved to a 2-oxoglutarate by Bat1 and Bat2, generating a glutamate, resulting in corresponding α-keto acids. In yeast, Bat2 is believed to be mainly involved in the BCAA catabolism in cytoplasm, and Bat1 is assumed to be responsible for synthesis of BCAAs in mitochondrial matrix. However, enzymatically both directions of both enzymes are possible and quite similar [7].

The second step of the Ehrlich pathway is the irreversibly decarboxylation of the α-keto acids to the corresponding aldehyde. There are five genes were already reported to be related to this step, composing *PDC1, PDC5, PDC6, ARO10,* and *THI3* in yeast [8]. Especially, the pyruvate decarboxylases (Pdc1, Pdc5, and Pdc6) are very active in *S. cerevisiae* and, therefore, they are the main decarboxylases of the amino acid catabolism [9]. Aro10 is known to be an enzyme that mediates catalytic reaction to a variety of substrates as α-keto acid decarboxylase. It is evidenced that Aro10 participates in Ehrlich pathway by its upregulation upon phenylalanine, leucine, or methionine use as sole nitrogen source [10]. Differently, Thi3 was described to be important decarboxylase for the 3-methyl-1-butanol production [11]. Besides, Thi3 is also important for sensing and the control of homeostasis and biosynthesis of thiamine in yeast and acts as a transcriptional factor

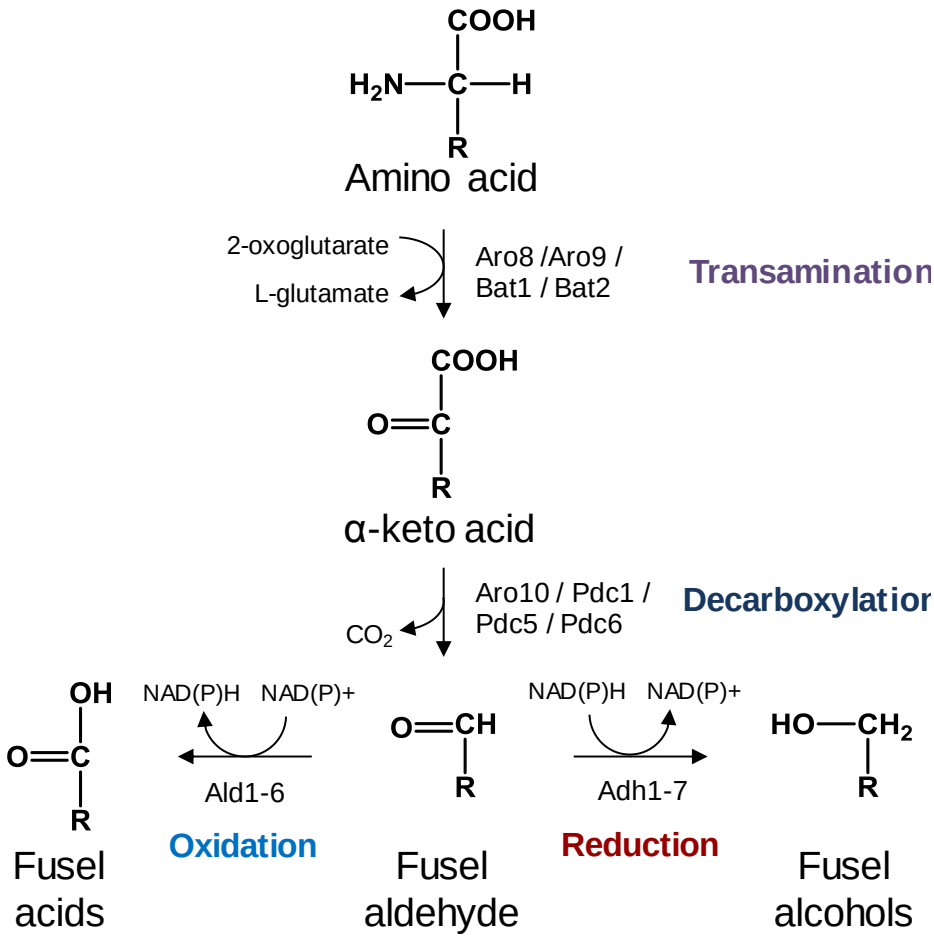

Figure 2.2 The Ehrlich pathway

Catabolism of amino acids is converted to fusel acids or fusel alcohols. The enzymes encoded of gene of each step are indicated.

Table 2.1 Ehrlich pathway intermediates and products

Amino acid	α-keto acid	Aldehyde	Fusel alcohol	Fusel acid
Valine	2-keto- isovalerate	Isobutanal	Isobutanol	Isobutyrate
Leucine	2-keto- isocaproate	Isoamyl aldehyde	3-methyl- butanol	Isovalerate
Isoleucine	2-keto-3-methyl- valerate	Methyl- valeraldehyde	2-methyl- butanol	Methyl- valerate
Phenylalanine	Phenylpyruvate	2-Phenylacetaldehyde	Phenylethanol	Phenylacetate
Tyrosine	*p*-Hydroxy-phenylpyruvate	*p*-Hydroxy-phenylacetaldehyde	Tyrosol	*p*-Hydroxy- phenylacetate
Tryptophan	3-Indole pyruvate	3-Indole acetaldehyde	Tryptophol	3-Indole acetate
Methionine	Keto-methylthio- butyrate	Methional	Methionol	3-methylthio- propionate

for the activation of the THI genes.

The final step of the Ehrlich pathway occurs either towards the reduction or oxidation of the fusel aldehyde (Fig. 2.2). The distinction between reduction or oxidation is depends on the environment yeast is in. In a glucose-rich fermentative condition the high glycolytic flux generates a rapid overload of NADH, which consequently redirect the Ehrlich pathway towards the fusel alcohol production. On the other hand, in glucose-limited growth, the Ehrlich pathway is redirected towards fusel acid production to increasing NADH pool. In *S. cerevisiae*, the alcohol dehydrogenases Adh1-7 are mainly involved in reduction of the fusel aldehydes to fusel alcohol (Fig. 2.2). Especially, Adh2, Adh6, and Adh7 are described as the most efficient for production of the branched-chain alcohols. On the other hand, relatively, oxidation of the branched-chain aldehydes are not well known. In yeast, six aldehyde dehydrogenases was reported, consisting of three cytosolic (Ald1, Ald2, and Ald6) and three mitochondrial (Ald3, Ald4, and Ald5) enzymes.

2.1.3. Isobutanol production in bacteria

Although several bacterial hosts had been employed for isobutanol production, the most frequently used microorganisms are *Escherichia coli* and *Corynebacterium glutamicum*. These microorganisms have the crucial limitation that they cannot naturally produce isobutanol because of inability to catalyze the decarboxylation of the α-keto acid. Therefore, the study of isobutanol production in bacteria is essential to the introduction of ketoacid decarboxylase (KDC).

For isobutanol biosynthesis, two molecules of pyruvate are condensed to α-acetolactate by α-acetolactate synthase (ALS), and then α-acetolactate is further converted to 2-ketoisovalerate (2-KIV) through valine biosynthesis pathway with two enzymes, acetohydroxyacid isomeroreductase (AHAIR) and dihydroxyacid dehydratase (DHAD). Finally, 2-ketoisovalerate decarboxylase and alcohol dehydrogenase catalyze the reduction of 2-KIV to isobutanol.

C. glutamicum is the main microorganism employed for production of several amino acids in large scale, such as, especially, L-valine production reaching at 0.3 g/g yield from sucrose [12]. Therefore, theoretically, *C. glutamicum* is expected to be a strain capable of producing high isobutanol titer via producing high amount of KIV. In *C. glutamicum*, isobutanol production with 77% of the theoretical yield was achieved by employed deletion of pyruvate competing pathways and overexpression of the *ilvBNCD* genes, encoding ALS, AHAIR, and DHAD, the *kivd* (KDC) from *Lactococcus lactis* and the endogenous alcohol dehydrogenase (*adhA*), and transhydrogenases (*pntAB*) from *E. coli* to relieving cofactor imbalance [13].

Meanwhile, the higher isobutanol yields were reported in *E. coli*. In order to isobutanol production in *E. coli*, acetolactate synthase from *Bacillus subtilis* (*alsS*) was employed instead of the endogenous *IlvB* and *IlvN* homologous, due to a higher affinity for pyruvate than the endogenous enzymes. In addition, overexpressing the *IlvCD, kivD,* from *L. lactis* and *ADH2* from *S. cerevisiae* increases a isobutanol production of 0.35 g isobutanol/g glucose with 86% of the theoretical yield in *E. coli* host [14].

Later on, research about isobutanol production with 100% efficiency was reported in *E. coli*. In this study, NADH-dependent mutants of *ilvC* from *E. coli* (*ilvC*^{6E6}) and adhA from *L. lactis* (*adhA*^{RE1}) were constructed. The use of this two mutants (IlvC^{6E6} and AdhA^{RE1}) in the isobutanol pathway resulted in 100% of the theoretical yield, under anaerobic conditions [15]. Previous studies on isobutanol production in several bacteria are summarized in Table 2.2.

Nevertheless, despite the high efficiency of isobutanol production in bacterial hosts, the higher alcohol tolerance of *S. cerevisiae* than these bacteria boosted the metabolic engineering studies for isobutanol production in yeast. Moreover, as already mentioned, yeast can be employed in fermentative processes with harsh conditions, which would allow future production of isobutanol with various biomass.

2.1.4. Advantages of *S. cerevisiae* as a host strain in metabolic engineering

As genetic manipulation is essential to produce a variety of chemicals through metabolic engineering using microorganisms, *E. coli* or *S. cerevisiae* strains that are easy to genetically manipulate are widely used as host strains. Both of these organisms possess the advantages of being very well-studied and genetically easy to handle, with many tools available for their genetic manipulation [16]. Compared to *E. coli*, *S. cerevisiae* has additional advantages as cell factory; (i) well-characterized eukaryotic model; (ii) a lower growth temperature (30 ºC optimum temperature); (iii)

industrial robustness such as its high tolerance to low pH, high osmotic pressure, and alcoholic compounds; (iv) easier cell separation because of larger cell size; and also (v) a lack of risk of phage contamination [2]. Furthermore, mating of haploid yeast strain allows leading to diploid and then can improve genes copy numbers, robust growth and increased adaptation [17]. Based on above-mentioned advantageous characters, *S. cerevisiae* has been used as a perfect host producing various natural or non-natural metabolites such as ethanol, 2,3-butanediol, 3-hydroxypropionic acid, isobutanol, lactic acid, n-butanol, and terpenoids by enhancing the innate pathway or introducing heterologous genes [16,18,19].

2.1.5. Isobutanol production in *S. cerevisiae*

S. cerevisiae, native producer of isobutanol produces isobutanol through glycolysis, valine biosynthesis, and the Ehrlich pathway, whereby glucose is converted to isobutanol via 2-ketoisovalerate (KIV), an intermediate of valine biosynthesis (Fig. 2.3). In bacteria, overproduction of isobutanol can be achieved by concomitant overexpression of enzymes involved in Ehrlich pathway, suitable ketoacid decarboxylase (Kdcs) and alcohol dehydrogenase (Adhs). On the other hand, in yeast, the isobutanol production pathway is more complicated, because the enzymes required for synthesis of KIV are located in mitochondria, while Kdc and Adh are located in cytoplasm. First, pyruvate has to be imported into the mitochondrial matrix and two molecules are condensed to α-acetolactate by acetolactate synthase (ALS), Ilv2, and then sequentially, α-acetolactate is converted to KIV by ketol

Table 2.2 Isobutanol production in bacteria

Strain	Substrates	Isobutanol			Description	References
		Titer (g/L)	Productivity (g/(L·h))	Yield (g/g)		
Corynebacterium glutamicum	Glucose	12.97	0.33	0.2	Batch, Anaerobic conditions, Construction of engineered strain Δ*aceE* Δ*pqo* Δ*ilvE* Δ*ldhA* Δ*mdh* overexpressing *ilvBNCD* and *adhA* and heterologous *pntAB*, and *kivd* genes	[13]
Bacillus subtilis	Glucose	2.62	0.086	0.07*	Fed-batch fermentation, Construction of engineered strain overexpressing *ilvCD* and *alsS* and heterologous *kivd* and *ADH2* genes	[20]
Escherichia coli	Glucose	22	0.2	0.35	Batch, Construction of engineered strain overexpressing *ilvCD* and heterologous *alsS*, *kivd*, and *ADH2* genes	[14]
	Glucose	13.4	0.55	0.42	Batch, Anaerobic conditions, Construction of engineered strain overexpressing mutants, $IlvC^{6E6}$ and $AdhA^{RE1}$	[15]
Synechocystis PCC 6803	Isobutyraldehyde	0.06	-	-	Overexpression of *kivd* and *ADH* (*slr1192*)	[21]

*approximate value

acid reductoisomerase (KARI), Ilv5, and dihydroxyacid dehydratase (DHAD), Ilv3 (Fig. 2.3). Afterwards, KIV is converted to valine by BCAA transaminases (Bat1) or exported back into the cytoplasm for isobutanol production via cytosolic Ehrlich pathway (Fig. 2.3). Therefore, for isobutanol synthesis in yeast, pyruvate has to imported into mitochondrial and also KIV must be exported to the cytosol.

In a first attempt to enhance synthesis of isobutanol in *S. cerevisiae*, without modification of the native compartmentalization of the pathways, isobutanol production was enhanced to six-fold (yield 3.86 mg/g glucose) by overexpressing the endogenous ILV genes (*ILV2*, *ILV5*and *ILV3*) compared to wild-type stain [22]. However, isobutanol production indicates less than 1% of the theoretical yield, possibly by raising the availability of KIV and degrading valine, which exerts a negative feedback regulation on Ilv2 via Ilv6.

Therefore, two major strategies have been engaged to minimize this transmembrane barrier: the relocation of the whole pathway either to the mitochondria or to the cytosol. The first attempt to relocate the whole isobutanol pathway to mitochondrial was reported. In this study, isobutanol production was increased to 65% with final isobutanol yield of 6.40 mg/g by construction of the complete mitochondrial pathway compared with by the native pathway [23]. Later, introduction of mitochondrial isobutanol biosynthetic pathway into yeast genome using delta integration led to increasing production of isobutanol (15 mg/g) by optimization of the mitochondrial isobutanol pathway [24].

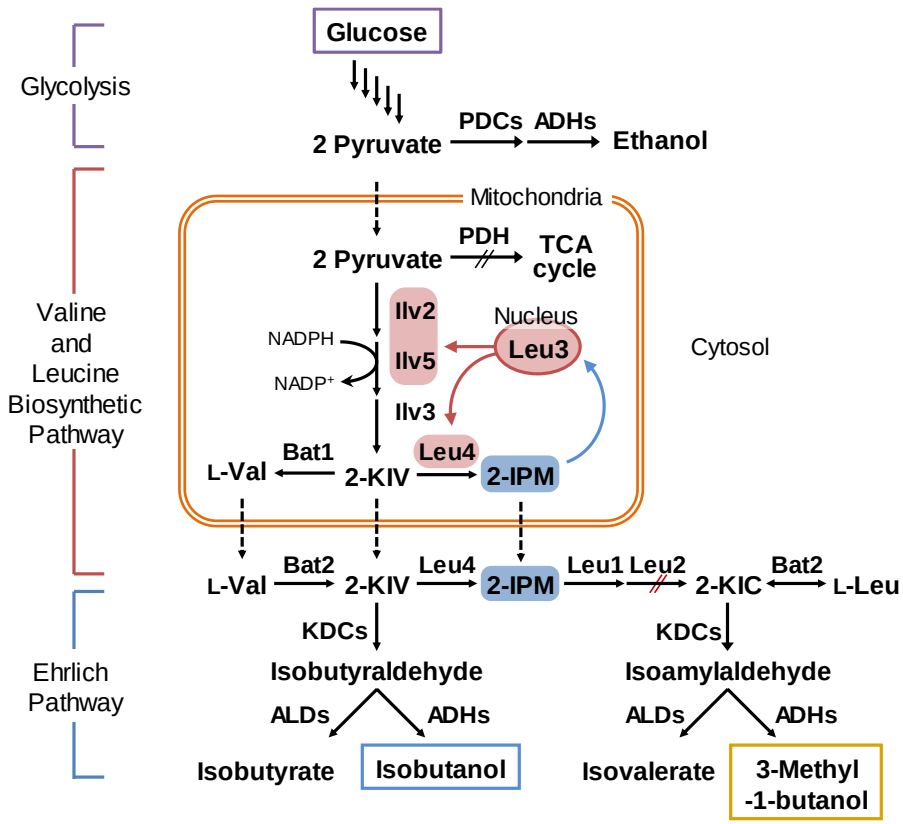

Figure 2.3 Metabolic pathway for isobutanol and 3-methyl-1-butanol in *S. cerevisiae* CEN.PK2-1C

Pyruvate produced from glucose by glycolysis, is mainly converted to ethanol via two steps, which consist of decarboxylation of pyruvate to acetaldehyde by pyruvate decarboxylase (PDC), and reduction of acetaldehyde to ethanol by alcohol dehydrogenase (ADH). Pruvate is converted to α-acetolactate by Ilv2 located in mitochondria, and then α-acetolactate is converted to 2-ketoisovalerate (2-KIV) by Ilv5 and Ilv3. Finally 2-KIV is converted to isobutanol by KDCs and ADHs via Ehrlich pathway. 3-Methyl-1-butanol also is synthesized from 2-KIV via leucine biosynthetic pathway and Ehrlich pathway.

In case of using mitochondrial isobutanol biosynthetic pathway to produce isobutanol, mitochondrial pyruvate pool is an important limiting factor. Therefore, various attempts have been made to construct the cytosolic isobutanol pathway [25-27]. The most effective strategy is re-localization Ilv2, Ilv5, and Ilv3 into the cytosol in endogenous *ILV2*-deficient strains resulting in increase in isobutanol titers up to 630 mg/L. To further improve isobutanol production, transhydrogenase-like shunt was constructed to solve cofactor imbalances between NADH occurred via glycolysis and NADPH required by Ilv5. In this system, pyruvate is converted cyclically to oxaloacetate, malate and back to pyruvate, simultaneously converting NADH to NADPH [28]. Previous studies on isobutanol production in *S. cerevisiae* are summarized in Table 2.5.

2.2. Branched-chain amino acid biosynthesis in *S. cerevisiae*

2.2.1. Valine and leucine biosynthesis in *S. cerevisiae*

The branched chain amino acids (BCAAs), L-valine, L-leucine, and L-isoleucine have been usually manufactured by bacterial fermentation, employing mutant strains of *C. glutamicum* and *E. coli*. The amounts of annual production are about 400 tons of L-isoleucine, 500 tons of L-leucine, and 500 tons of L-valine [29]. Recently, various uses of the BCAAs have been suggested such as components of cosmetics and pharmaceuticals, animal feed additives, addictives in infusion solutions and dietary products and precursors in the chemical synthesis of herbicides [30,31].

Table 2.3 Isobutanol production in *S. cerevisiae*

Reference Strain	Pathway localization	Substrates (g/L)	Isobutanol		Description	References
			Titer (mg/L)	Yield (mg/g C-source)		
CEN.PK2-1C	Mitochondrial Ilv235 and cytosolic Ehrlich pathway	Glucose (40)	-	3.86	Batch, overexpression of *ILV2, ILV3, ILV5*	[22]
D452-2	Cytosolic pathway with parallel mitochondrial Ilv235 branch	Glucose (40)	151	3.78	Batch, overexpression of *ILV2NΔ55, ILV3NΔ20, ILVN5Δ34, kivD (L. lactis)*	[27]
YPH499	Mitochondrial Ilv235 and cytosolic Ehrlich pathway	Glucose (20)	143	6.6	*Batch, pdc1Δ, overexpression of ILV2, kivD (L. lactis), ADH6*	[32]
YPH499	Cytosolic pathway with parallel mitochondrial Ilv235 branch	Glucose (20)	63	2.1	Batch, overexpression of *ILV2, ILV2NΔ54, ILVN3Δ41, ILV5NΔ47, kivD (L. lactis), ADH6*	[26]
CEN.PK2-1C	Cytosolic pathway	Glucose (40)	630	14.18	Batch, *ilv2Δ*, overexpression of *ILV2NΔ54, ILV3NΔ19, ILV5NΔ48*	[25]
BY4741 x Y3929 (diploid)	Mitochondrial pathway with parallel cytosolic Ehrlich pathway	Glucose (100)	635	6.4	Batch, overexpression of *ILV2, ILV3, ILV5, ARO10 (MTS), adhA (MTS, L. lactis)*	[23]
YPH499	Cytosolic pathway with parallel mitochondrial Ilv235 branch	Glucose (100)	1620	16	Batch, *lpd1Δ*, overexpression of *ILV2, ILV2NΔ54, ILV3NΔ41, ILV5NΔ47, kivD (L. lactis), ADH6, MAE1*	[28]
CEN.PK2-1C	Mitochondrial Ilv235 and cytosolic Ehrlich pathway	Glucose (20)	146.9	7.3	Batch, *bat1Δald6Δ*, overexpression of *ILV2, ILV5, ILV3, ARO10, ADH2, LEU3Δ601*	This study (Chapter 4)

Table 2.2 Isobutanol production in *S. cerevisiae (Continued)*

Reference Strain	Pathway localization	Substrates (g/L)	Isobutanol		Description	References
			Titer (mg/L)	Yield (mg/g C-source)		
CEN.PK2-1C	Mitochondrial pathway with parallel cytosolic Ehrlich pathway	Glucose (20)	435.2	21.76	Batch, *bat1Δald6Δlpd1Δ*, overexpression of *ILV2, ILV5, ILV3, ARO10(MTS), ADH2 (MTS), LEU3Δ601, MPC1, MPC3, NFS1, ISD11*	This study (Chapter 5)
CEN.PK2-1C	Cytosolic pathway with parallel mitochondrial Ilv235 branch	Glucose (20)	586.3	14.7	Batch, *bat1Δald6Δ*, overexpression of *alsS (B. subtilis), ILV3NΔ19, ILV5NΔ48, kivD(L.lactis), ADH2*	This study (Chapter 6)

Especially, isoleucine,e leucine and valine are part of the essential amino acid in human diet. During the evolutionary track, mammals lost the ability of synthetizing the BCAAs, while plants, bacteria, and fungi can produce them. In this organisms, the BCAA is synthesized via BCAAs biosynthesis pathway tightly-regulated by the end products and pathway intermediates. BCAAs biosynthetic pathway has been deeply investigated in microbiology, not only due to the production of the BCAAs, but also for the production of chemicals that can be produced from this pathway, such as the branched-chain alcohols branched-chain acids even acetoin and 2,3-butanediol [33,34].

In *S. cerevisiae*, BCAAs synthesis pathway is separated into two cellular compartments, mitochondria and cytoplasm (Fig. 2.4). The biosynthesis of valine is completely conducted in mitochondria (Fig. 2.4). The first reaction is carried out by the acetolactate synthase (ALS) that condenses two molecules of pyruvate to α-acetolactate, while releasing CO_2. In yeast, the acetolactate synthase was encoded in Ilv2 and it is regulated by a regulatory subunit, Ilv6. Ilv6 controls the activity of Ilv2 depending on presence of BCAAs (predominantly valine). Under BCAAs-rich conditions, Ilv6 inhibit Ilv2 activity, and oppositely, the activity of Ilv2 is enhanced by Ilv6 in the absence of the BCAAs to synthesis of BCAAs [35].

The second reaction of the valine biosynthesis is the isomerization of α-acetolactate to 2,3-dihydroxy isovalerate (DIV) by the ketol-acid reductoisomerase (Ilv5), which needed of NAPDH and a magnesium ion for the enzyme reaction (Fig. 2.4). And then, dihydroxyacid dehydratase encoding *ILV3* catalyzes third step in this

pathway leading to biosynthesis of 2-KIV by the dehydration of DIV. Especially Ilv3 is iron-sulfur (Fe-S) dependent protein [36].

The final step of the valine biosynthesis is the amination of KIV to valine by branched-chain amino acid aminotransferase, Bat1 and Bat2 in yeast (Fig. 2.4). Bat1 is mitochondrial BCAA aminotransferase highly expressed during exponential phase and repressed during stationary phase [37]. Therefore, Bat1 is believed to be involved in BCAAs biosynthesis. On the other hand, Bat2, paralog of Bat1, is cytosolic BCAA aminotransferase and is expressed during stationary phase, and is thereby involved in BCAA catabolism [38]. Nevertheless, both BCAA transaminases can catalyze the reaction in both directions.

In case of isoleucine biosynthesis, the enzymes employed in this pathway are the same as those of the valine biosynthesis, with the difference that the isoleucine production starts from threonine (Fig. 2.4). Threonine is synthetized from aspartate, either in cytosol or in mitochondria, but the its deamination to 2-keto-butyrate occurs only in the mitochondria by threonine deaminase, Ilv1 [39]. The further steps of the isoleucine biosynthesis occur in parallel to the valine biosynthesis with the difference in intermediate.

The leucine biosynthesis is directly linked with the valine biosynthesis through KIV (Fig. 2.4). KIV receiving an acetyl group from acetyl-CoA, is converted to 2-isopropyl- malate (2-IPM) by the 2-isopropylmalate synthases, Leu4 and Leu9. Leu9 is the mitochondrial minor isozyme, whereas Leu4 mediates the catalytic reaction in both mitochondria and cytoplasm. Leu4 is the major expressed 2-isopropylmalate

synthase isoform and controls gene expression related to BCAAs synthetic pathway via feedback inhibition of leucine [40].

In the next, the leucine biosynthesis is the isomerization of 2-IPM to 3-isopropylmalate (3-IPM) by isopropylmalate isomerase (Leu1), another Fe-S dependent enzyme, in cytosol [41]. Afterwards, 3-IPM is converted to 2-keto-isocaproate (2-KIC) by the isopropylmalate dehydrogenase (Leu2) and then 2-KIC is aminated to leucine [42].

Most of enzymes in BCAAs synthetic pathway are transcriptionally regulated by Leu3, which is an important transcription factor. It was already known to regulate the expression of *LEU1, LEU2, LEU4, ILV2, ILV5,* and *BAT2* genes (Fig. 2.4) [43].

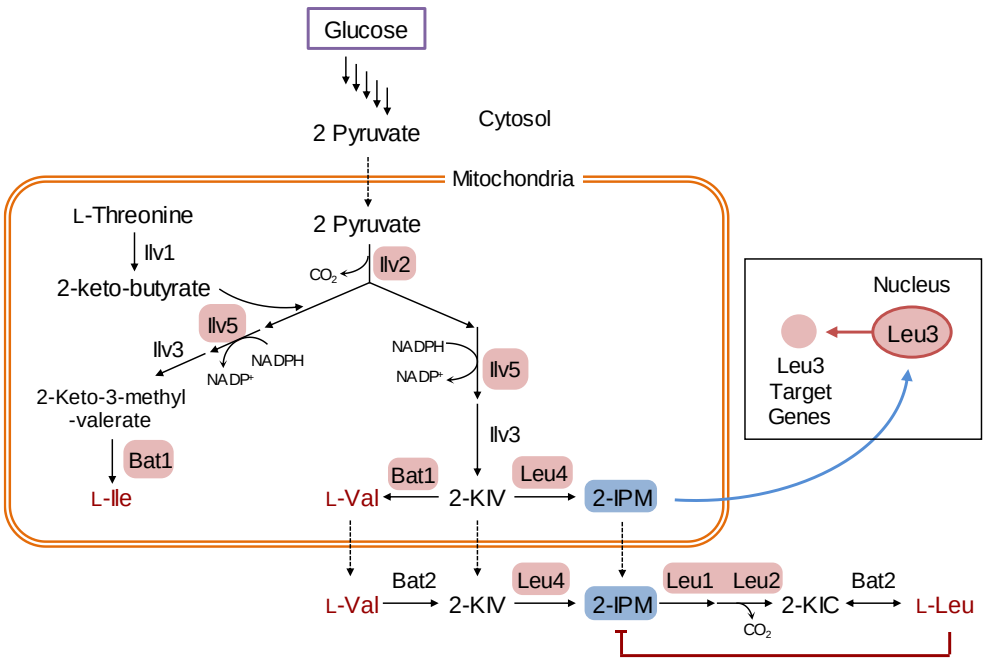

Figure 2.4 Schematic illustration of the branched-chain amino acids (BCAAs) biosynthetic pathways in *S. cerevisiae*

BCAAs are composed of valine, leucine, and isolucine. ILV genes (*ILV1, ILV2, ILV3*, and *ILV5*) is involved in valine and isoleucine biosynthesis and additionally, LEU genes (*LEU4, LEU1*, and *LEU2*) is required for the production of leucine.

2.2.2. Transfcriptional factor Leu3

The Leu3 of *S. cerevisiae* is a transcription factor that regulates the transcription of genes encoding genes involved in BCAAs synthesis. Several genes whose expression is regulated by Leu3p have been identified, including *LEU1*, *LEU2*, *LEU4*, *ILV2*, *ILV5*, and *BAT2* (Fig. 2.4) [42,43]. Leu3 is a member of the zinc cluster protein family, containing six conserved cysteines that bind two zinc ions in a binuclear cluster ($Zn(II)_2Cys_6$) [44]. The Leu3 is composed of 886 amino acids and homodimeric DNA binding protein [45]. The Leu3 protein consists of five domains, which is the DNA binding region of Leu3p near the N-terminus with zinc cluster DNA binding domain from amino acids 37 to 67, linker region, alpha-helix domain from amino acids 85 to 102 involved in dimerization, middle region that is involved in the regulation of Leu3p, and acidic activation domain from amino acids 856 to 886 [46-49]. In order for Leu3 to act as a transcriptional activator, it is required that binding to a specific DNA sequence, dimerization and operation of transcription activation and thus each of the domains in Leu3 is responsible for this function.

Leu3p binds to cognate promoters at upstream activating sequences (UAS) with a exerted repeat 5′-CCG-N_4CGG-3′ via zinc cluster DNA binding domain [45]. The activity of Leu3p as transcriptional activator positively controlled by inducer 2-isopropylmalate (2-IPM), the product of the first step in leucine biosynthesis (Fig. 2.4) [50]. Under absence of 2-IPM condition, interaction occurs between the Leu3p activation domain and the middle region, resulting in the masking of the Leu3p activation domain [47]. Through this self-masking, Leu3 acts as a repressor to inhibit

the expression of target genes. Also, 2-IPM synthesis is feedback inhibited by leucine and thus, Leu3 activity is controlled additionally by leucine because the level of 2-IPM are directly related to the level of leucine [42]. Under leucine-rich condition, 2-IPM synthases Leu4p enzyme activity is inactivated by the leucine [51]. On the other hand, Leu3 acts as a activator in the presence of 2-IPM resulting in the induction of expression of target genes such as *LEU1* and *LEU2* by a Leu3p-2-IPM complex [52].

Based on the regulation mechanism of Leu3, it has been reported to constitutively active Leu3 mutants, regardless of presence or absence of metabolites. Largely internal truncated Leu3 mutant (deletion of 601 amino acids) was an effective transcriptional activator when 2-IPM synthesis was repressed by leucine [53].

2.2.3. Iron-sulfur cluster assembly machinery in *S. cerevisiae*

The iron-sulfur cluster (Fe-S) are prosthetic factor in many prokaryote and eukaryote enzymes with redox, catalytic, and regulatory functions [54]. This cluster is assembled by the iron-sulfur cluster assembly system (ISC), which has been extensively studied and is known to be involved in the incorporation of the Fe-S into apoproteins in both bacteria and eukaryotes [55]. In eukaryotes, two main machinery of Fe-S-protein biogenesis have been illustrated, the mitochondrial iron-sulfur cluster assembly (ISC) and cytosolic iron-sulfur protein assembly (CIA) machineries

(Fig. 2.5) [56,57]. The Fe-S cluster is initially generated via the mitochondrial ISC assembly machinery and it is concerned in maturation of all cellular Fe-S dependent-proteins (mitochondrial, cytosolic, and nuclear). Therefore, functionally, the CIA machinery depends on the mitochondrial ISC machinery (Fig. 2.5).

S. cerevisiae has been more extensively studied about ISC biogenesis as eukaryotic model organism. Also, there are some Fe-S protein carrying out vital metabolic reactions such as Ilv3 and Leu1 enzyme requiring iron-sulfur cluster (ISC) for enzyme activity in valine and leucine biosynthesis in yeast. In the mitochondrial ISC machinery of *S. cerevisiae*, the following proteins are involved: Arh1, Yah1, Yfh1, Isu1, Isu2, Isa1, Isa2, Nfu1, Nfs1, Isd11, Mge1, Ssq1, Jac1, Atm1 and Grx5 (Table 2.4). The current research suggests that Isu1, Isu2, Isa1, Isa2 and Nfu1 are the scaffolds where the ISC is initially assembled before being transferred to the ISC dependent apoproteins. In mitochondria, the ISC assembly is initiated by cysteine desulfurase (Nfs1), which brings a sulfur group from a cysteine and transfers it to the scaffold proteins Isu1 and its homologue Isu2 protein, assisted by Yah1 (Fig 2.5) [58-60]. Cysteine desulfurase activator, Isd11, is fundamental for Nfs1 to fulfill its role. It is unclear how Isd11 facilitates the functions of Nfs1 [61]. In bacteria, some cysteine desulfurases need assistant protein that facilitates the transfer of sulfur to the clusters via formation of and S-S bond [62]. However, Isd11 does not have cysteine residues, which precludes such a mechanism for its enzyme reaction. Yeast mitochondria possess a less chaperone system that is expected to be specifically dedicated to the Nsf1 action, although their exact role is unclear. The Ssq1 chaperone

and the Jac1 J-protein (co-chaperone) function together to assist in the biogenesis of ISC of Fe-S dependent proteins [63]. ATPase activity in the Ssq1chaperone is stimulated by the J-type co-chaperone Jac1, during the interaction with the scaffold protein Isu1 or Isu2. On the other hand, iron is offered to the scaffold proteins by frataxin (Yfh1), which acts as an iron donor (Fig. 2.5) [64]. During ISC biogenesis in mitochondria, iron handling must be tightly controlled to avoid a deleterious increase in the concentration of free iron by Aft1 transcription factor [65].

Transference of the ISC generated to apoproteins is assisted by glutaredoxin (Grx5) [66]. Atm1, one of ABC transporter, is likely to participate in the exporting of the ISC clusters from the mitochondrial matrix to the cytoplasm although the exact substrate of Atm1 is unknown (Fig. 2.5) [67]. Fe-S exported from mitochondrial to cytoplasm by Atm1 transporter is reassembled for cytosolic Fe-S dependent protein via cytosolic iron-sulfur protein assembly (CIA) machineries (Fig. 2.5). Many enzymes involved in CIA system have been identified, but the mechanism is still unclear [68].

2.3. Multi-copy integration in *S. cerevisiae*

Metabolic pathway engineering in the *S. cerevisiae* leads to improved production of a wide range of compounds, ranging from ethanol (from biomass) to natural products such as sesquiterpenes that yeast does not naturally produce by introduce heterologous metabolic pathways synthesis [69,70]. To the introduction

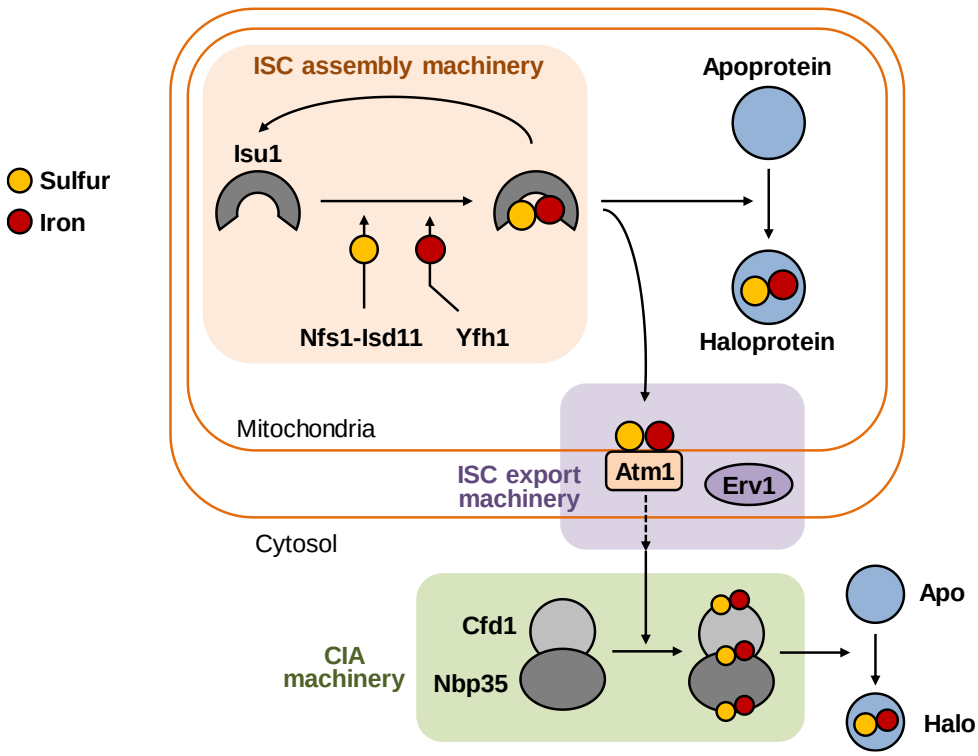

Figure 2.5 Schematic illustration of the Fe-S protein biogenesis in *S. cerevisiae*

In *S. cerevisiae* Iron-Sulfur Cluster (ISC) assembly occurs in mitochondria, which involves an iron donor, a sulfur donor, and a scaffold. The iron is delivered by Yfh1 (iron chaperone) and the sulfur is donated by Nfs1 (cysteine desulfurase) and Isd11 (Nfs1 activator) onto the scaffold protein Isu1.

Table 2.4 Proteins involved in ISC assembly in *S. cerevisiae*

Proteins	Protein Function	Suggested Function In ISC Assembly
Arh1	Ferredoxin reductase	Reduces Yah1/Provides electrons for ISC assembly/transfer/repair
Yah1	Ferredoxin	Provides electrons for ISC assembly/transfer/repair
Yfh1	Frataxin	Stores/Provides Fe directly to ISC assembly and Heme synthesis
Grx5	Glutaredoxin	Regulates glutathionylation state of protein cysteinyl residues
Isa1	Scaffold	Dimer scaffolds initial ISC assembly and then transfers it to apo-proteins
Isa2	Scaffold	Dimer scaffolds initial ISC assembly and then transfers it to apo-proteins
Isu1	Scaffold	Dimer scaffolds initial ISC assembly and then transfers it to apo-proteins
Isu2	Scaffold	Dimer scaffolds initial ISC assembly and then transfers it to apo-proteins
Nfu1	Scaffold	Dimer scaffolds initial ISC assembly and then transfers it to apo-proteins
Ssq1	Hsp70 chaperone	Assists in proper folding of ISC biosynthetic proteins namely Yfh1 and Isa-Isu proteins/Assists in maintaining ISC assembled in scaffold dimer for proper transfer
Jac1	Hsp40 co-chaperone	Assists Ssq1 in interacting with Isu/Isa proteins
Mge1	Cochaperone/Nucleotide exchange factor	Assists Ssq1
Nfs1	Cysteine desulfurase	Provides sulphur for ISC assembly in scaffold dimers or in situ ISC assembly/repair
Atm1	ABC transporter	Involved in ISC export for cytoplasm and nuclear proteins
Isd11	unknown	Fundamental for Nfs1 action

of multi-enzyme pathways requires multi-genes expression system and optimization of pathway by control of gene number and promoter strength, which are two critical control points. In *S. cerevisiae*, both plasmid vectors and chromosomal integration are widely used to introduce genes and control copy number. The plasmid vectors are extremely useful for gene expression, however, plasmids offer limited control of copy number segregational stability and compulsion of selective medium. On the other hand, integration of genes into the genome offers an alternative mechanism for gene introduction, since homologous recombination is very efficient in *S. cerevisiae*. Chromosomal integration also allows the insertion of precise numbers and stability of gene maintenance. Therefore, the method of inserting the gene into the genome is a very effective for manipulating the pathway by metabolic engineering but since a metabolic pathway is made by many genes a method of simultaneously introducing a large amount of genes is necessary.

2.3.4. Multi-copy delta-integration

In *S. cerevisiae*, delta elements have been chosen as the target site for multi-copy genes integration methods and successfully applied for pathway engineering. Delta element, one of transposon in *S. cerevisiae*, are DNA sequences that move from one chromosomal site to another via an RNA intermediate. There are approximately 50 retrotransposons in the yeast genome comprising 5 types (Ty1-5). All five types of Ty elements share the same basic structure flanked by long

terminal repeats (LTRs) and also scattered about the genome as single LTRs [71]. Among them, delta sequences (Ty1 and Ty2) are by far the most abundant at nearly 300 [72]. Therefore, by performing gene integration using these delta sites a large number of genes can be rapidly and randomly introduced into the yeast chromosome, which is called delta integration [73].

By using this method, 'cocktail δ-integration' was used to create strains for the surface expression of β-glucosidase endoglucanase and cellobiohydrolase [74]. Also novel approach for rapid construction of large biochemical pathways into delta site in yeast genome by combination with antibiotic selection G418 or phleomycin selection have led to a high efficiency of multi-copy delta integration in a single transformation [24]. Recently, new delta integration platform was developed by combining CRISPR-Cas9 system (Di-CRISPR) (delta integration CRISPR-Cas9) platform was developed and with newly developed Di-CRISPR platform highly efficient and markerless integration of large biochemical pathways was attained [75].

2.3.5. rDNA-mediated integration

Another multi-copy gene integration system is rDNA-mediated integration in *S. cerevisiae*. The ribosomal DNA (rDNA) of *S. cerevisiae* is encoded by the *RDN1* locus an approximately 1-2 Mb region consisting of 100-200 tandem copies of a 9.1 kb repeat on chromosome XII [76]. Each repeat contains the genes for rRNAs and three types of spacer regions internal transcribed spacers (ITS1 and ITS2)

external transcribed spacers (5' ETS and 3' ETS) and nontranscribed spacers (NTS1 and NTS2). The rDNA-mediated integration used this NTS site and this strategy can increase the copy number of a target gene integrated in the chromosome by homologous recombination [77,78].

However, according to previous study, using rDNA-mediated integration usually occurred a decreased enzyme production and a target gene loss in the yeast chromosome as the cells were passaged which limit stable expression of target gene in *S. cerevisiae* [79]. Therefore, to use rDNA sequence as ideal sites for the target gene integrated, DNA fragment is smaller than the rDNA fragment (9.1 kb), because the stability of exogenous genes mainly depends on the size of integrated fragment.

Recently, there are several studies using rDNA-mediate integration have been reported to improvement of production of proteins [80,81].

2.4. Microbial production of shinorine

2.4.6. Mycosporine-like amino acids

Ultraviolet (UV) ray is the part of the solar electromagnetic spectrum with a wavelength ranging from 200 to 400 nm. Based on its physical properties and biological activity, UV ray is sorted into three types: UV-A (320–400 nm), UV-B (280–320 nm), and UV-C (200–280 nm). Nevertheless, only a small portion of

the entire UV ray emitted by the sun reaches the Earth's surface and is mainly composed of UV-A with a small UV-B component up to 10%. The remaining short-wavelength part, UV-B spectrum (90%) and the entire UV-C spectrum, usually do not penetrate the Earth's stratosphere since they are shielded by the ozone layer [82]. Since the late 1970s, the progressive depletion of the ozone layer has have contributed to increasing permeability of UV-B reaching the Earth's surface [83]. The UV-A and UV-B rays can be damage to a wide variety of biological systems because of its short waves with extreme energy. Both UV rays can induce biomolecules such as DNA and protein by generating reactive oxygen species (ROS), being harmful to living organism including human [84]. Therefore, it is considered necessary to apply sunscreen to reduce the risk of sun exposure. Recently, there is growing demand for the sunscreen material because of its applicability as additive in various cosmetics. Sunscreen comprising physical or chemical materials filter out a broad spectrum of UV rays and prevent the UV-induced damages to humans by applied to the skin. But there are multiple negative effects of these artificial UV filters on marine ecosystems and then gradually shifted the trends of customers toward the use of more environmentally compatible and highly efficient natural UV-absorbing compounds [85].

Recently, mycosporine-like amino acids (MAAs) have attracted attention as a substitute for chemical and physical sunscreen materials. MAAs are small secondary metabolites produced by organisms that live in environments with high volumes of sunlight, such as marine and freshwater environments to protect against solar

radiation [86]. MAAs are widespread in the microbial world and have been reported in many microorganisms including bacteria, cyanobacteria, microalgae, fungi, as well as some multicellular organisms such as macroalgae and marine animals. All MAAs absorb UV light that can be destructive to biological molecules and also they are considered to be multi-functional secondary metabolites that have many cellular functions. MAAs are effective antioxidant molecules and are able to stabilize free radicals within their ring structure. In addition, MAAs are able to boost cellular tolerance to desiccation, salt stress, and heat stress.

So far, over 30 MAAs were found but the exact number of natural compounds within MAAs family is yet determined, since they have recently been discovered and novel molecular species are constantly being discovered. All MAAs absorb ultraviolet wavelengths, typically between 310 and 362 nm covering spectrum of UV-A and UV-B [87]. Therefore, they are considered to be the strongest natural absorbers of UV radiation and are allowed to protect cells from the harmful UV-A and UV-B rays.

MAAs are small molecules (<400 Da) with characteristics of colourless, uncharged, and water-soluble ampholytes, and they share the same chemical structure composed of a cyclohexenone or cyclohexenimine chromophore and a wide variety of substitutions with the nitrogen substituent. The ring structure is thought to absorb UV light and accommodate free radicals. Depending on the type of chromophore, there are two types of MAAs; aminocyclohexenone derivatives possessing a cyclohexenone conjugated with an amino acid and

aminocyclohexenimines derivatives possessing a cyclohexenimine conjugated with an amino acid (Fig. 2.6) [88-90]. Aminocyclohexenone derivatives includes mycosporine-glycine, mycosporine-taurine, mycosporine-alanine, mycosporine-serine collemin A, etc (Fig. 2.7) [91,92]. Aminocyclohexenimines are represented by shinorine porphyra-334, usujirene, asterina-330, palythine, palythinol, palythene, mycosporine-2-glycine, 13-O-β-galactosyl-porphyra-334, etc (Fig. 2.7) [93]. Typically, each cyclohexenimine ring backbone contains the glycine attached to the 3rd carbon atom and an additional amino acid or amino alcohol or enaminone chromophore to the 1st carbon atom (Fig. 2.6).

Differences in the structure of these compounds determine their specific absorption spectra. The aminocyclohexenone derivatives exhibit absorption maxima in the UV-B region, while aminocyclohexenimines derivatives have absorption maxima in the UV-A region. MAAs quickly convert the absorbed energy from UV ray to heat without the generation of free oxygen species, resulting in making them as biodegradable sunscreen [94].

2.4.7. Biosynthetic pathways of mycosporine-like amino acids

The biosynthetic pathways of MAAs has been well elucidated in many organisms. These biosynthetic pathways often share common enzymes and metabolic intermediates with pathways of the primary metabolism. In this pathway, it is believed that 4-deoxygadusol (4-DG) is a common intermediate, synthesized

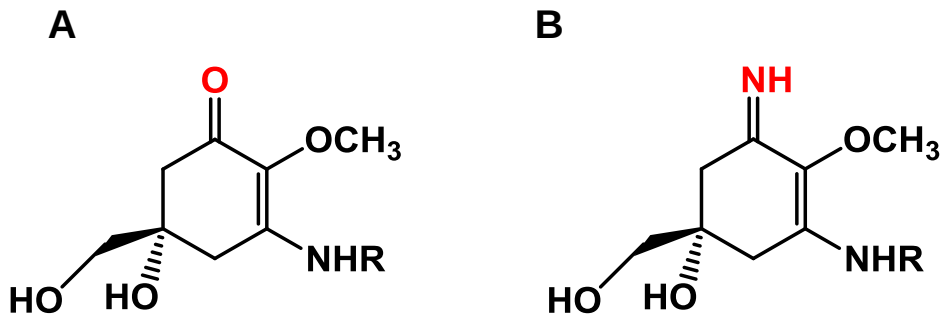

Figure 2.6 Structural chromophore of mycosporine-like amino acids

(A) Aminocyclohexenone and (B) aminocyclohexeniminone rings.

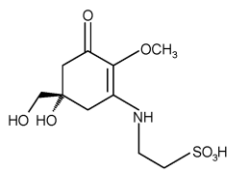

Mycosporine-taurine
λ_{max} = 309 nm

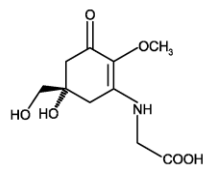

Mycosporine-glycine
λ_{max} = 310 nm

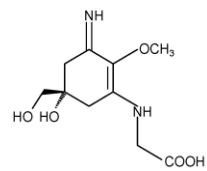

Palythine
λ_{max} = 320 nm

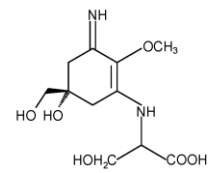

Palythine-serine
λ_{max} = 320 nm

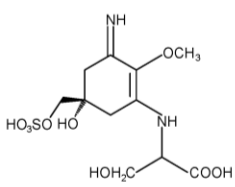

Palythine-serine-sulphate
λ_{max} = 320 nm

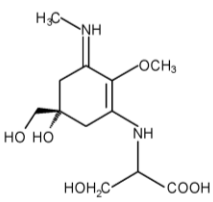

Mycosporine-methylamine serine
λ_{max} = 327 nm

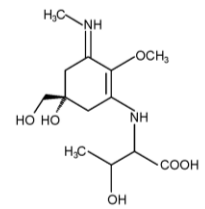

Mycosporine-methylamine threonine
λ_{max} = 327 nm

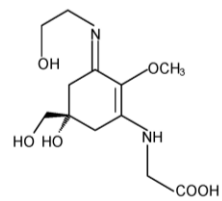

Asterina-330
λ_{max} = 330 nm

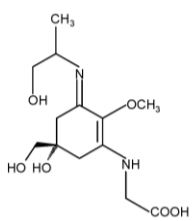

Palythinol
λ_{max} = 332 nm

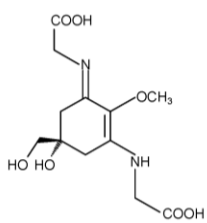

Mycosporine-2-glycine
λ_{max} = 334 nm

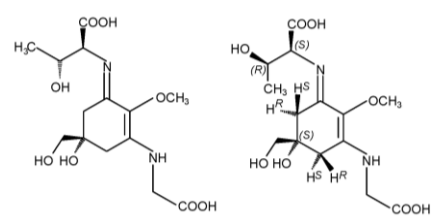

Porphyra-334
λ_{max} = 334 nm

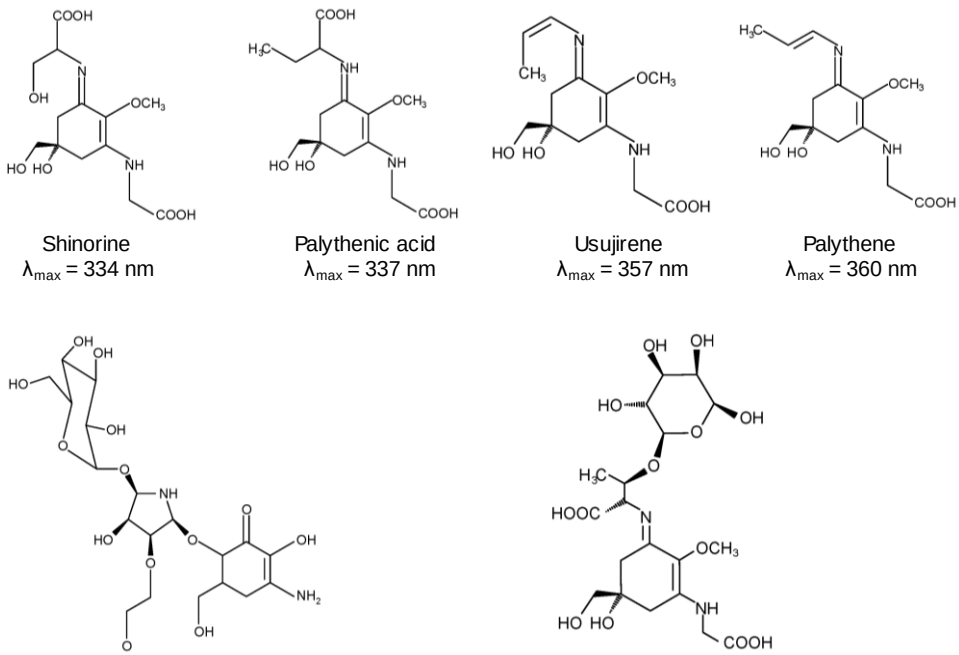

Figure 2.7 Structure of selected MAAs with their absorption maxima (λ_{max}).

through the shikimate pathway and pentose phosphate pathway (PPP), which is then converted into mycosporine glycine (MG) (Fig. 2.8) [95]. Most MAAs are made by combining various amino acids with MG.

At first, it is believed that that MAAs biosynthesis takes place through the shikimate pathway because two genes involved in the shikimate pathway were found (Fig. 2.8) [96,97]. In order to this assumption, the core of MAAs derived from 3-dehydroquinate (3-DHQ) by Ava3858 encoding the dehydroquinate synthase (DHQS) homolog and Ava3857 is encoding the *O*-methyltransferase (*O*-MT), converted to 4-DG, the main immediate precursor of MAAs, and then converted to MAAs in the cyanobacteria *Anabaena variabilis* ATCC 29413 [87]. Therefore, the shikimate pathway believed the major 4-DG synthesis pathway in this hypothesis. On the contrary, the assumption that MAAs are generated by the shikimate pathway has been challenged because it has been found that disruption of 2-epi-5-epi-valiolone (EV) synthase (EVS) involved in synthesis of EV from sedoheptulose 7-phosphate (S7P) which is the different enzymatic reaction with shikimate pathway consisting of DHQS, causes deficiency of production of shinorine, one of MAAs derived from mycosporine-glycine, in the same cyanobacteria. Previously, EVS and DDGS could not be clearly distinguished, but recently, it was found that only DDGS is involved in MAAs production, although DDGS and EVS are very similar [98]. Therefore, the production of MAAs was not produced from EV as an intermediate (Fig. 2.8). This finding suggest that MAAs are synthesized from S7P as precursor derived via the pentose-phosphate pathway [99].

In case of production of shinorine, some cyanobacteria *Nostoc punctiforme* and *Anabaena variabilis*, produce shinorine from S7P, an intermediate of pentose phosphate (PP) pathway by sequential 4-step enzymatic reactions (Fig. 2.8) [100]. S7P is converted to 4-DG by 2-demethyl 4-deoxygadusol synthase (DDGS) and O-MT. Then glycine is conjugated to 4-DG to synthesis mycosporine-glycine (MG) by ATP-grasp ligase. In the last non-ribosomal peptides synthetase (NRPS)-like enzyme or D-ala-D-ala ligase conjugates serine to MG to generate shinorine (Fig. 2.9).

2.4.8. Shinorine production in microorganisms

Shinorine, one of the MAAs is generally produced in cyanobacteria and algae. The physiological role of shinorine as sunscreen chemical to protect against UV radiation is well established in the many native shinorine producer. Especially, the generally used shinorine is extracted from the red algae *Porphyra umbilicalis*, which produces 3.27 mg/gDCW shinorine [101]. In case of cyanobacterial producers, *Fischerella and A. variabilis* ATCC 29413 produced shinorine with 0.76 mg/gDCW and 0.97 mg/gDCW, respectively [102,103]. Also engineered cyanobacteria *Synechocystis* sp. PCC6803 produced 0.71 mg/L shinorine with 2.37 mg/gDCW by introducing shinorine biosynthesis genes from *Fischerella* via multiple promoters [103]. So far, although several efforts have been made to produce shinorine in cyanobacteria and algae, it remains at the level of discovering and expressing gene [101,103,104].

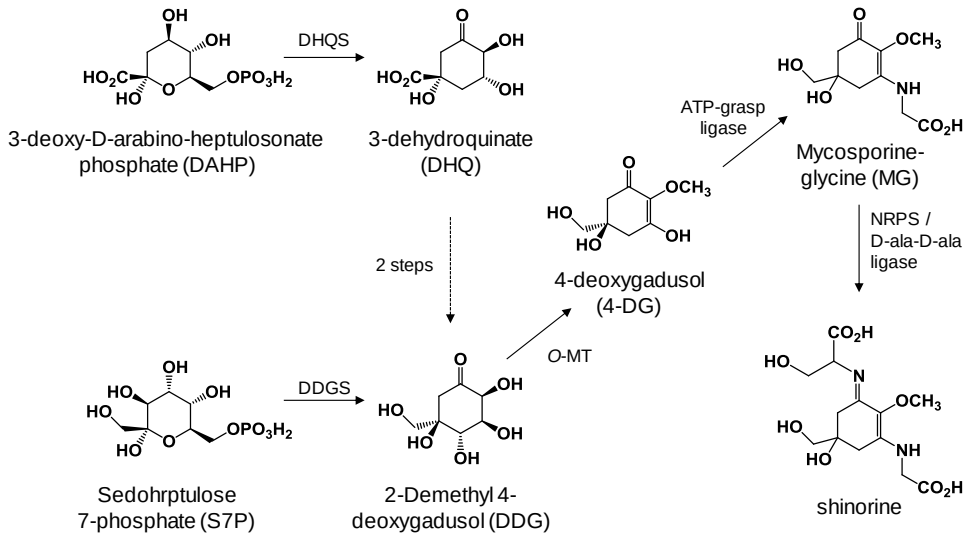

Figure 2.8 Biosynthesis of shinorine in cyanobacteria

In cyanobacteria, it is assumed that shinorine is produced from the shikimate pathway or the pentose phosphate pathway. The 4-DG is a key intermediate of shinorine biosynthesis.

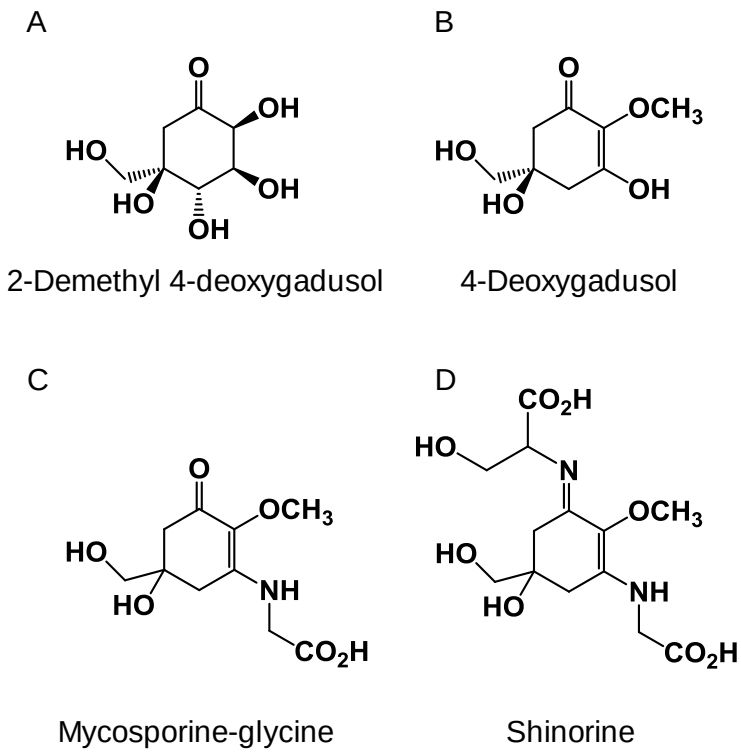

Figure 2.9 Structure of mycosporines and mycosporine-like amino acids

(A) DDG, (B) 4-DG, (C) MG, and (D) shinorine.

Because shinorine is accumulated in cyanobacteria and algae cells, a large amount of cell accumulation is required to mass-production of shinorine. However, theses microorganisms are not suitable strains because cell culture is difficult and takes a long time and is difficult to genetically manipulate [105]. Some bacteria was engineered to produce shinorine. In *E. coli* which is used as a strain to successfully produce various chemicals by using metabolic engineering method, only the overexpression effect of shinorine production-related gene from *A. variabilis* was confirmed [99]. However, the enzymes catalytic reaction of the related genes was examined in this study. Recently, engineered *C. glutamicum* produced 19.1 mg/L shinorine by introducing shinorine biosynthetic genes from *Actinosynnema mirus* DSM43827 and using D-gluconate as carbon source [106]. Also, in *Streptomyces avermitilis*, overexpression of same genes with introduction in *C. glutamicum* mentioned above, significantly, increase the shinorine production to 154.1 mg/L with 11.4 mg/gDCW content using 10-L fermentor operation [107]. Previous studies on shinorine production in microorganisms are summarized in Table 2.5.

2.4.9. Xylose assimilation in *S. cerevisiae*

With rising cost of petroleum fuel and environmental pollution, looking for alternative energy sources replacing conventional non-renewable fossil fuels is essential. Microbial conversion of renewable biomass into biofuels and valuable chemicals is possible option to substitute petroleum refineries in a sustainable

Table 2.5 Production of shinorine in previous studies using microorganisms

Strain	Origin of shinorine gene cluster	Shinorine		Description	References
		Content (mg/gDCW)	Titer (mg/L)		
Escherichia coli	*Anabaena variabilis* ATCC 29413	-	0.15	Culture in LB medium for 20 h at 20°C 500mM IPTG induction	[99]
Streptomyces avermitilis	*Actinosynnema mirus* DSM43827	11.4	154.1	10-liter fermentor culture in vegetative medium containing 60 g/L glucose and 400 mM NH_4Cl at 28°C for 7 days	[107]
Corynebacterium. glutamicum	*Actinosynnema mirus* DSM43827	-	19.1	Fed-batch cuture in brain heart infusion (BHI) medium containing 40 g/L sodium D-gluconate and 0.5 % $CaCO_3$ for 72 h	[106]
Porphyra umbilicalis	*Porphyra umbilicalis*	3.27	-	*P. umbilicalis* culture and anlaysis	[101]
Anabaena variabilis PCC 7937	*Anabaena variabilis* PCC 7937	0.97	-	Culture in BG_{11} medium at 20°C and continuous fluorescence lamp illumination for 72 h	[102]
Fischerella sp. PCC9339	*Fischerella* sp. PCC9339	0.76	0.29	*Fischerella* culture in 300-600 mL BG11 medium at 26°C for 21 days	[103]
Synechocystis sp. PCC6803 (Sh-Pori)	*Fischerella* sp. PCC9339	0.23	0.07	Culture in 300 mL BG_{11} medium at 26°C for 21 days	[103]
Synechocystis sp. PCC6803 (Sh-TP560)	*Fischerella* sp. PCC9339	2.37	0.71	Culture in 300 mL BG_{11} medium cotaining 0.5mM serine at 26°C for 21 days for 13 days	[103]
Saccharomyces cerevisiae	*Nostoc punctiforme* ATCC 29133 *Anabaena variabilis* ATCC 29413	14.3	64.2	Fed-batch cuture in SC-His containing 24 g/L xylose and 3.5 g/L glucose for 10 days at 30°C	This study (Chapter 7)

development, known as biorefinery. To develop economic and sustainable conversion processes at an industrial scale, substrates of the microbial conversion have to be reasonable and eco-friendly without competing food supply to avoid cost of in the production of biofuels. Therefore, microbial strains capable efficient xylose-fermenting are imperative for construction of economically feasible bioconversion processes using the lignocellulosic biomass.

Although there are many microorganisms capable of naturally utilizing xylose such as specially yeasts *Candida*, *Kluyveromyces*, and *Pichia* [108], *S. cerevisiae* non-native producer of xylose, is attractive host with advantages over the native xylose consumer regarding robustness against various stresses in industrial environments, such as low pH, high osmotic pressure, high alcohol concentration, and even phage contamination [109,110]. Therefore, using *S. cerevisiae* to consume xylose has been deeply studied.

To xylose assimilation in *S. cerevisiae*, xylose imported to cell is required to isomerization into xylulose and subsequently xylulose is phosphorylate into xylulose-5-phosphate (X5P) which is an inlet metabolite to pentose phosphate pathway (PPP) (Fig. 2.10). There are two alternatively distinct pathways composed of the oxidoreductase pathway and the isomerase pathway, to conversion of xylose into xylulose in xylose-fermenting microorganisms. Xylose-fermenting yeasts engage the oxidoreductase pathway consisting of two enzymatic reactions of xylose reductase (XR) and xylitol dehydrogenase (XDH), which convert xylose to xylulose via xylitol. In oxidoreductase pathway, redox conversion of xylose is accompanied

by using NADPH and NADH with XR while using only NAD^+ with XDH (Fig. 2.10). Therefore, the cofactor imbalance created by XR is the first limitation of this pathway, not only because NAD^+ is the cofactor required in XR reaction, but also because NADH is the main produced cofactor during glycolysis.

On the other hand, the isomerase pathway involves one enzymatic reaction of xylose isomerase (XI), catalyzing various sugar interconversions of aldose and ketose including xylose and xylulose without cofactor requirement (Fig. 2.10). Although most XIs have been identified from bacterial genome, some anaerobic fungi such as *Piromyces* and *Orpinomyces* can assimilate xylose via XI [111,112].

Xylulose generated via oxidoreductase pathway or the isomerase pathway is converted to X5P via phosphorylation by xylulokinase (XK) and then, the X5P flows into PPP (Fig. 2.10). The PPP is a universal metabolic pathway divided into two distinct pathways, an oxidative route and a non-oxidative route. In *S. cerevisiae*, X5P is metabolized through the non-oxidative pentose phosphate pathway to form various phosphorylated sugars of three, four, five, six, and seven carbons which serve as intermediates of glycolysis or precursors of nucleotides and amino acids. The oxidative pentose phosphate pathway is a major route for generating NADPH which functions as a driving force for the XR activity and a protection mechanism against oxidative stresses [113]. Both pathways are closely interconnected by sharing various intermediates. In particular, E4P obtained via PPP is introduced into the shikimate pathway, which is an aromatic amino acid production pathway, and S7P which is an intermediate of several secondary metabolites, is produced through this

pathway (Fig. 2.10) [113].

Many studies have been conducted to use xylose as a carbon source using *S. cerevisiae*. The XI encoding genes are generally spread over bacterial genomes but it is difficult to express XI with maintaining function in yeast [114,115]. On the other hand, introducing XR-XDH pathway can offer high metabolic flux compared with introducing the XI pathway in *S. cerevisiae*. There have been many studies to effectively utilize xylose in *S. cerevisiae*, but most have been directed to ethanol production from xylose. Previous studies on ethanol production from xylose in *S. cerevisiae* are summarized in Table 2.6.

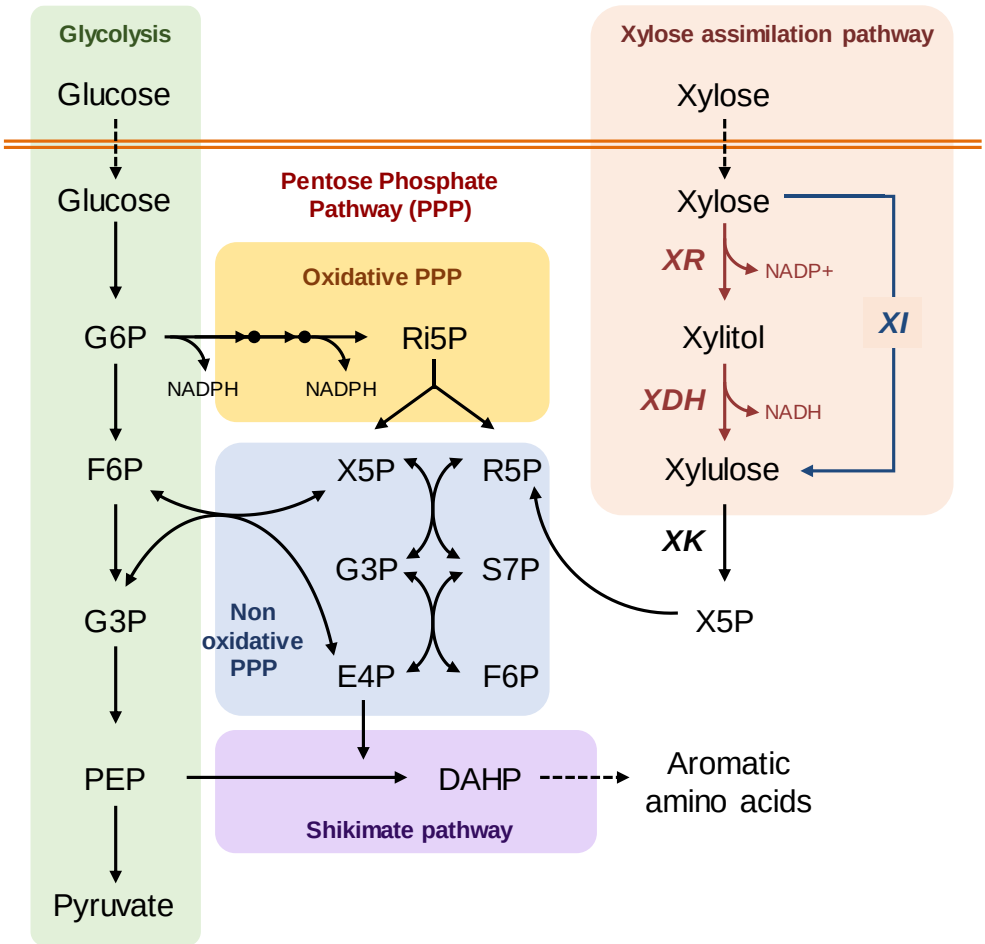

Figure 2.10 Schematic illustration of the xylose assimilation pathways in yeast

Xylose assimilation requires the conversion of xylose into xylulose and xylulose-5-phosphate which is inlet molecule to PP pathway. There are two kinds of xylose assimilation pathway in xylose-fermenting microbes. Most of xylose-fermenting yeasts engage oxidoreductase pathway consisting of xylose reductase (XR), and xylitol dehydrogenase (XDH). On the other hand, xylose is assimilate by xylose isomerase (XI). XI encoding genes are generally spread over bacterial genomes but it is difficult to express XI with maintaining function in yeast.

Table 2.6 Ethanol production from xylose in representative xylose-fermenting engineered *S. cerevisiae*

Reference Strain	Strain Description	Xylose Consumption Rate	Ethanol		Culture Conditions	References
			Production Rate	Yield (g/g xylose)		
H131-A3-AL^{CS}	XI system [*Piromyces XYLA*] *XYL3* (*Sc. stipiti*), *TAL1* (*Sc. stipiti*), *TKL1*, *RPE1*, *RKI1*	1.866 g/(g·h)	0.765 g/(g·h)	0.410	Anaerobic batch, 2×YNB containing 40 g/L xylose	[116]
SXA-R2P-E	XI (mutant *Piromyces XYLA*), *TAL1* (*Sc. stipiti*), *gre3Δpho13Δ*	0.077 g/(OD·h)	0.033 g/(OD·h)	0.453	Anaerobic batch, YNB containing 40 g/L xylose	[117]
SR8	XR–XDH system [*XYL1* (*Sc. stipiti*), *XYL2* (*Sc. stipiti*)] *XYL3* (*Sc. stipiti*), *ald6Δ*, null mutant of *PHO13*	0.129 g/(OD·h)	0.046 g/(OD·h)	0.378	Anaerobic batch, YNB containing 40 g/L xylose	[118]
TMB 3422	XR–XDH system [mutant *XYL1* and *XYL2* (*Sc. stipiti*)] *XKS1*, *TAL1*, *TKL1*, *RPE1*, *RKI1*, *gre3Δ*	0.580 g/(g·h)	0.180 g/(g·h)	0.340	Anaerobic batch, 2× YNB containing 50 g/L xylose	[119]
TMB 3504	XR–XDH system [*XYL1* and *XYL2* (*Sp. passalidarum*), *XYL2* (*Sc. stipiti*)] *XKS1*, *TAL1*, *TKL1*, *RPE1*, *RKI1*, *gre3Δ*	0.760 g/(g·h)	0.330 g/(g·h)	0.400	Anaerobic batch, 2× YNB containing 50 g/L xylose	[120]

Chapter 3.

Materials and methods

3.1. Strains and media

All strains used in this study are listed in Table 3.1. *E. coli* strain DH5α [F^- Φ80d*lacZ*ΔM15 Δ(*lacZYA-argF*)U169 *recA1 endA1 hsdR17* (r_K^-, m_K^+) *phoA supE44* λ^- *th*i-*1 gyrA96 relA1*] was used for genetic manipulations. *E. coli* was cultured in Luria-Bertani (LB) medium (10 g/L tryptone, 5 g/L yeast extract, and 10 g/L NaCl) supplemented with 50 μg/mL ampicillin.

S. cerevisiae strain CEN.PK2-1C (*MATa ura3-52 trp1-289 leu2-3,112 his3Δ1 MAL2-8C SUC2*) were obtained from EUROSCARF and was used as parental strain of all engineered strain. The plasmids and integration DNA fragment was introduced following previously described procedure using lithium acetate (LiOAc).

The *BAT1*, *ALD6*, *LEU4*, and *LPD1* disruption mutants were constructed by using the Cre/*loxP* recombination system [121]. The gene deletion cassette was obtained by PCR amplification from pUG72 as template using a gene-specific primer pair of d_ORF F and d_ORF R. After confirmation of the correct integration of the cassette at the target gene locus through PCR analysis using the confirmation primers (c_ORF F and c_ORF R) the *URA3* marker gene was rescued by transformation of Cre recombinase-expression vector pSH62 [122]. To generate multiple genes deletion strain same procedure was sequentially conducted.

The *TAL1* gene disruption mutant was constructed by using CRISPR/Cas9 mediated genome editing system. The gene-specific deletion cassette was obtained

by PCR amplification using *TAL1* specific primer pair, d_TAL1 F and d_TAL1 R without template and introduced with coex413-Cas9-TAL1gRNA plasmid, consisting of Cas9 gene and guide RNA targeted to *TAL1* gene. After confirmation of deleting *TAL1* gene via PCR analysis using the confirmation primers (c_TAL1 F and c_TAL1 R), coex413-Cas9-TAL1gRNA plasmid was removed by culturing in YPD overnight. Primers used for gene deletion are listed in Table 3.2.

Yeast cells were cultured in YP medium (10 g/L yeast extract and 20 g/L bacto-peptone) supplemented with 20 g/L glucose (YPD) or 20 g/L xylose (YPX) or in synthetic complete (SC) medium (6.7 g/L yeast nitrogen base without amino acids and 1.4 g/L amino acids dropout mixture lacking His, Trp, Leu, and Ura) supplemented with auxotrophic amino acids as needed and the required amount of glucose and xylose.

3.2. Plasmids

Plasmids and primers used in this study are listed in Table 3.3 and Table 3.4, respectively.

3.2.1. Metabolic engineering of *S. cerevisiae* for the production of isobutanol and 3-methyl-1-butanol

All expression plasmids are derived from pRS vector series and genes were expressed under the control of *TEF1* or *TDH3* promoter and the *CYC1* terminator

Table 3.1 Strains used in this study

Strain	Genotype	Reference
E. coli		
DH5α	F- Φ80d*lacZ*ΔM15 Δ(*lacZYA-argF*)U169 *recA1 endA1 hsdR17* (r_K^-, m_K^+) *phoA supE44* λ⁻ *th*i-*1 gyrA96 relA1*	
S. cerevisiae		
CEN.PK2-1C	*MATa ura3-52 trp1-289 leu2-3,112 his3Δ1 MAL2-8C SUC2*	EUROSCARF
WT-1	CEN.PK2-1C (pRS413TEF)	This study
WT-3	CEN.PK2-1C (pRS413TEF, pRS424GPD, pRS426GPD)	This study
WT-4	CEN.PK2-1C (pRS413TEF, pRS424GPD, pRS426GPD, pRS425GPD)	This study
JHY41	CEN.PK2-1C *bat1Δ::loxP*	This study
JHY42	CEN.PK2-1C *ald6Δ::loxP*	This study
JHY43	CEN.PK2-1C *ald6Δ::loxP bat1Δ::loxP*	This study
JHY41-1	JHY41 (pRS413TEF)	This study
JHY42-1	JHY42 (pRS413TEF)	This study
JHY43-1	JHY43 (pRS413TEF)	This study
JHY44	CEN.PK2-1C (pRS413TEF-*LEU3*)	This study
JHY45	CEN.PK2-1C (pRS413TEF-*LEU3Δ601*)	This study
JHY43-3	JHY43 (pRS413TEF, pRS424GPD, pRS426GPD)	This study
JHY431	JHY43 (pRS424GPD-*ILV235*, pRS413TEF, pRS426GPD)	This study
JHY432	JHY43 (pRS424GPD-*ILV235*, pRS413TEF-*LEU3Δ601*, pRS426GPD)	This study
JHY433	JHY43 (pRS424GPD-*ILV235*, pRS413TEF-*LEU3Δ601*, pRSp426GPD-*ARO10 ADH2*)	This study

Table 3.1 Strains used in this study (*Continued*)

Strain	Genotype	Reference
JHY434	JHY43 (pRS424GPD-*ILV235*, pRS413TEF-*LEU3Δ601*, pRS426GPD-*ARO10 ADH2*, pRS425GPD)	This study
JHY435	JHY43 (pRS424GPD-*ILV235*, pRS413TEF-*LEU3Δ601*, pRS426GPD-*ARO10 ADH2*, pRS425GPD-*LEU4*)	This study
JHY436	JHY43 (RSp424GPD-*ILV235*, pRS413TEF-*LEU3Δ601*, pRS426GPD-*ARO10 ADH2*, pRS425GPD-$LEU4^{D578Y}$)	This study
JHY437	JHY43 (pRS424GPD-*ILV235*, pRS413TEF-*LEU3Δ601*, pRS426GPD-*ARO10 ADH2*, pRS425GPD- $LEU4^{D578Y}$ *LEU1*)	This study
JHY46	CEN.PK2-1C *ald6Δ::loxP bat1Δ::loxP lpd1Δ::loxP*	This study
JHY47	CEN.PK2-1C *ald6Δ::loxP bat1Δ::loxP leu4Δ::loxP*	This study
JHY48	CEN.PK2-1C 1C *ald6Δ::loxP bat1Δ::loxP lpd1Δ::loxP leu4Δ::loxP*	This study
JHY46-1	JHY46 harboring p413TEF	This study
JHY461	JHY46 harboring pJIB1	This study
JHY462	JHY46 harboring pJIB2	This study
JHY463	JHY46 harboring pJIB3	This study
JHY464	JHY46 harboring pJIB4	This study
JHY465	JHY46 harboring pJIB5	This study
JHY4301	JHY43 harboring p413GPD-ILV2N54, p414GPD-ILV5N48, and p416GPD-ILV3ΔN19	This study
JHY4302	JHY43 harboring p413ADH-alsS(B), p414GPD-ILV5N48, and p416GPD-ILV3ΔN19	This study
JHY4303	JHY43 harboring p413GPD-alsS(L), p414GPD-ILV5N48, and p416GPD-ILV3ΔN19	This study
JHY4303	JHY43 harboring p413GPD-alsS(L), p414GPD-ILV5N48, and p416GPD-ILV3ΔN19	This study

Table 3.1 Strains used in this study (*Continued*)

Strain	Genotype	Reference
JHY4304	JHY43 harboring p413GPD-alsS(L), p414GPD-ILV5N48(K), and p416GPD-ILV3ΔN19	This study
JHY4305	JHY43 harboring p413GPD-alsS(L), p414GPD-ILV5N48, and p416GPD-ILV3ΔN19(K)	This study
JHY4306	JHY43 harboring p413GPD-alsS(L), p414GPD-ILV5N48(K), and p416GPD-ILV3ΔN19(K)	This study
JHY4307	JHY43 harboring p413CUP1-alsS(B), p414GPD-ILV5N48(K), and p416GPD-ILV3ΔN19(K)	This study
JHY43DC	CEN.PK2-1C *ald6Δ::loxP bat1Δ::loxP URA3::* P_{CUP1}-alsS (*B. subtilis*)-T_{CYC1}	This study
JHY43D1	Selected strain from randomly delta-integrated JHY43 (P_{CUP1}-*alsS* (*B. subtilis*)-T_{CYC1})	This study
JHY43D2	Selected strain from randomly delta-integrated JHY43 (P_{CUP1}-*alsS* (*B. subtilis*)-T_{CYC1})	This study
JHY43D3	Selected strain from randomly delta-integrated JHY43 (P_{CUP1}-*alsS* (*B. subtilis*)-T_{CYC1})	This study
JHY43D1-1	JHY43D1 harboring p413GPD, p414GPD-ILV5N48(K), and p416GPD-ILV3ΔN19(K)	This study
JHY43D2-1	JHY43D2 harboring p413GPD, p414GPD-ILV5N48(K), and p416GPD-ILV3ΔN19(K)	This study
JHY43D2-C	JHY43D2 harboring p413GPD, p414GPD, and p416GPD	This study
JHY43D3-1	JHY43D3 harboring p413GPD, p414GPD-ILV5N48(K), and p416GPD-ILV3ΔN19(K)	This study
JHY43D21	Selected strain from randomly NTS-integrated JHY43D2 (P_{TDH3}- *Kozak sequence-ILV5N48*-T_{CYC1}, P_{TDH3}- *Kozak sequence-ILV3N19*-T_{CYC1})	This study
JHY43D22	Selected strain from randomly NTS-integrated JHY43D2 (P_{TDH3}- *Kozak sequence-ILV5N48*-T_{CYC1}, P_{TDH3}- *Kozak sequence-ILV3N19*-T_{CYC1})	This study

Table 3.1 Strains used in this study (*Continued*)

Strain	Genotype	Reference
JHYS13-1	JHYS13 harboring p416GPD	This study
JHYS13-2	JHYS13 harboring coex416-XYL	This study
JHYS14	Selected strain from randomly NTS-integrated JHYS13 (P_{TDH3}-*XYL1*-T_{CYC1}, P_{TEF1}-*XYL2*-T_{GPM1}, P_{TPI1}-*XYL3*-T_{TPI1})	This study
JHYS15	Selected strain from randomly NTS-integrated JHYS13 (P_{TDH3}-*XYL1*-T_{CYC1}, P_{TEF1}-*XYL2*-T_{GPM1}, P_{TPI1}-*XYL3*-T_{TPI1})	This study
JHYS16	Selected strain from randomly NTS-integrated JHYS13 (P_{TDH3}-*XYL1*-T_{CYC1}, P_{TEF1}-*XYL2*-T_{GPM1}, P_{TPI1}-*XYL3*-T_{TPI1})	This study
JHYS17	Selected strain from randomly NTS-integrated JHYS13 (P_{TDH3}-*XYL1*-T_{CYC1}, P_{TEF1}-*XYL2*-T_{GPM1}, P_{TPI1}-*XYL3*-T_{TPI1})	This study
JHYS18	Selected strain from randomly NTS-integrated JHYS13 (P_{TDH3}-*XYL1*-T_{CYC1}, P_{TEF1}-*XYL2*-T_{GPM1}, P_{TPI1}-*XYL3*-T_{TPI1})	This study
JHYS17-1	JHYS17 harboring p413GPD	This study
JHYS17-2	JHYS17 harboring p414GPD-Ava3858	This study
JHYS19	JHYS17 deleted TAL1	This study
JHYS19-1	JHYS19 harboring p413GPD	This study
JHYS19-2	JHYS19 harboring p413GPD-Ava3858	This study
JHYS19-3	JHYS19 harboring p414GPD	This study
JHYS19-4	JHYS19 harboring p414ADH-STB5	This study
JHYS19-5	JHYS19 harboring p414GPD-TKL1	This study
JHYS19-6	JHYS19 harboring coex414GPD-STB5-TKL1	This study

Table 3.1 Strains used in this study (*Continued*)

Strain	Genotype	Reference
JHY43D23	Selected strain from randomly NTS-integrated JHY43D2 (P_{TDH3}- *Kozak sequence-ILV5N48*-T_{CYC1}, P_{TDH3}- *Kozak sequence-ILV3N19*-T_{CYC1})	This study
JHY43D24	Selected strain from randomly NTS-integrated JHY43D2 (P_{TDH3}- *Kozak sequence-ILV5N48*-T_{CYC1}, P_{TDH3}- *Kozak sequence-ILV3N19*-T_{CYC1})	This study
JHY43D25	Selected strain from randomly NTS-integrated JHY43D2 (P_{TDH3}- *Kozak sequence-ILV5N48*-T_{CYC1}, P_{TDH3}- *Kozak sequence-ILV3N19*-T_{CYC1})	This study
JHY43D24-1	JHY43D24 harboring p413GPD	This study
JHY43D24-2	JHY43D24 harboring pJIB35	This study
JHY43D24-3	JHY43D24 harboring pJIB35KA	This study
JHY43D24-4	JHY43D24 harboring pJIB35AA	This study
JHYS10	CEN. PK2-1C harboring coex413-NpR4	This study
JHYS1-1	CEN. PK2-1C harboring p413GPD-NpR5600, p414GPD-NpR5599, p415GPD-NpR5598, and p416GPD-NpR5597	This study
JHYS1-2	CEN. PK2-1C harboring p413GPD-Ava3858, p414GPD-Ava3857, p415GPD-NpR5598, and p416GPD-NpR5597	This study
JHYS1-3	CEN. PK2-1C harboring p413GPD-Ava3858, p414GPD-NpR5599, p415GPD-NpR5598, and p416GPD-NpR5597	This study
JHYS11	CEN. PK2-1C *HIS3*:: P_{TDH3}-*NpR5600*-T_{CYC1}, P_{TEF1}-*NpR5598*-T_{GPM1}, P_{TDH3}-*NpR5599*-T_{CYC1}, P_{TEF1}-*NpR5597*-T_{GPM1}	This study
JHYS12	Selected strain from randomly delta-integrated WT (P_{TDH3}-*NpR5600*-T_{CYC1}, P_{TEF1}-*NpR5598*-T_{GPM1}, PT_{DH3}-*NpR5599*-T_{CYC1}, P_{TEF1}-*NpR5597*-T_{GPM1})	This study
JHYS13	Selected strain from randomly delta-integrated WT (P_{TDH3}-*NpR5600*-T_{CYC1}, P_{TEF1}-*NpR5598*-T_{GPM1}, P_{TDH3}-*NpR5599*-$_{TCYC1}$, P_{TEF1}-*NpR5597*-T_{GPM1})	This study

Table 3.2 Primers used for strain construction (gene deletion)

Primers	Sequence (5'-3')
d_LPD1 F	ATGTTAAGAATCAGATCACTCCTAAATAATAAGCGGCGGCCGC CAGCTGAAGC
d_LPD1 R	TCAACAATGAATAGCTTTATCATAGGCAGCCATGT GCATAGGCCACTAGTGGATCTG
d_LEU4 F	GACTCAGTTCTTTCAAAGGGTATTTTTTGAAGAAAAAAAAGGA TT CAGCTGAAGCTTCGTACGC
d_LEU4 R	TGCTTCTAGTAATTATATGGTTAAAAAAAAAGGAAAGGAAGTA AAGCATAGGCCACTAGTGGATCTG
d_TAL1 F	TAGTACGATAGTAAAATACTTCTCGAACTCGTCACATATACGT GTACATAGGAAGTATCT
d_TAL1 R	AGAAACGTGCATAAGGACATGGCCTAAATTAATATTTCCGAGA TACTTCCTATGTACACG
c_LPD1 F (-200)	TTGGCGAGAAGTCTCCGC
c_LPD1 R (+200)	CAGGAAGACAAAGCATGCGAG
c_LEU4 F (-300)	ATGTATGTGCGTGCATGTATGTGTGTATGT
c_LEU4 R (+300)	ATTGTCCTTTATGCCTAGTTTTCCAGTTAA
c_TAL1 F (-319)	CGGGAATAAAGCGGAACT
c_TAL1 R (+287)	GGTGGTTCCGGATGTTTT

[123]. *LEU3Δ601* mutant was generated by truncating internal coding region (from 173 to 773 amino acid residues) using overlap extension PCR. The *LEU4* mutant, $LEU4^{D578Y}$, having a G-to-T mutation at nucleotide position 1732 of *LEU4* ORF was created by using overlap extension PCR. To generate pRS424GPD-*ILV235*, pRS426GPD-*ARO10 ADH2*, and p425GPD-$LEU4^{D578Y}$ *LEU1*, where each of the ORFs is flanked by the *TDH3* promoter and the *CYC1* terminator, each ORF was first cloned into pRS424GPD, pRS425GPD, or pRS426GPD vector, and then PCR-amplified DNA fragments containing each ORF and the *TDH3* promoter and/or the *CYC1* terminator were serially cloned into a single plasmid vector.

3.2.2. Improvement of isobutanol production in *S. cerevisiae* by increasing mitochondrial import of pyruvate through mitochondrial pyruvate carrier

To construct p426-MLS plasmid, mitochondrial localization signal (MLS) fragment was generated by annealing complementary oligomers corresponding to the N-terminal 25 residues of *COX4* gene and was inserted between *Spe*I and *Bam*HI sites of p426GPD plasmid [123]. All genes were amplified from *S. cerevisiae* CEN.PK2-1C genomic DNA using target-specific primer pairs. To generate single-gene-expression plasmids for other genes PCR-amplified ORFs were cloned into p413GPD, p414GPD, p416GPD, p423GPD, p425GPD, or p426GPD plasmid under the control of *TDH3* promoter and *CYC1* terminator [123] resulting in p413GPD-*ILV2*, p414GPD-*ILV5*, p416GPD-*ILV3*, p425GPD-*ARO10*, p426GPD-*ADH2*, p426-

MLS-*ARO10*, p426-MLS-*ADH2*, p423GPD-*MPC1*, p423GPD-*MPC2*, and p423GPD-*MPC3*.

To construct multigene-expression plasmids for isobutanol biosynthetic pathway, multiple cloning system was used as previously described with minor modifications [124]. To generate p413-L, *LEU3Δ601* expression cassette (P_{TEF1}-*LEU3Δ601*-T_{CYC1}) flanked by *Sac*I and *Kpn*I was amplified by PCR from p413TEF-*LEU3Δ601* and cloned between *Sac*I and *Kpn*I sites of p413-D plasmid, replacing *alsD* expression cassette [124]. *ILV2* expression cassette (P_{TDH3}-*ILV2*-T_{CYC1}) flanked by *Mau*BI and *Not*I sites was amplified by PCR using a universal primer pair, Univ F2 containing *Mau*BI site and Univ R (containing *Not*I and *Asc*I sites) and sequentially cloned into *Asc*I and *Not*I sites of the p413-L plasmid. Other gene expression cassettes flanked by *Mau*BI and *Not*I sites were also obtained from the single-gene-expression vectors using the same universal primers, and sequentially cloned into *Asc*I and *Not*I sites, resulting in pJIB1, pJIB2, pJIB3, pJIB4, and pJIB5.

3.2.3. Development of multi-copy genome integration system with overexpressing α-acetolactate synthase-inducible phenotypic screening for isobutanol production in *S. cerevisiae*

The N-terminally truncated ILV genes (*ILV2, ILV5*, and *ILV3*) were obtained by PCR amplification using specific primer pairs (ORF F and ORF R), generating *ILV2N54*, *ILV5N48*, and *ILV3ΔN19* with *Bam*HI and *Xho*I at each end using *S. cerevisiae* genomic DNA and cloned into p413GPD, p414GPD, and p416GPD,

respectively resulting in p413GPD-*ILV2*N54, p414GPD-*ILV5*N48, and p416GPD-*ILV3ΔN19* plasmid. The ORF DNA fragments of *alsS* (B) from *B. subtilis*, *alsS* (L) and *kivd* from *L. lactis*, and *ARO10* and *ADH2* from *S. cerevisiae*, were amplified by PCR using each genomic DNA and target-specific primer pairs (ORF F and ORF R). To generate single-gene-expression plasmids, PCR-amplified products were cloned into p413GPD, p414GPD, p416GPD, p414FBA, or p414ADH plasmids, resulting in p413GPD-alsS(L), p413ADH-alsS(B), p414GPD-ARO10, and p414FBA1-ADH2. In p414GPD-*ILV5*N48, and p416GPD-*ILV3ΔN19* plasmid, *ILV5ΔN48* and *ILV3ΔN19* were replaced with the kozak sequence-*ILV5ΔN48* and kozak sequence-*ILV3ΔN19* fragments obtained by PCR amplification with primer pairs (ORF_K F and ORF R), respectively, generating p414GPD-*ILV5ΔN48*(K) and p416GPD-*ILV3ΔN19*(K) plasmids. Also, in p413ADH-alsS(B), P_{ADH1} part was changed to $P_{CUP1,}$ generated by PCR with CUP1p F and CUP1p R primers, with *Sac*I and *Bam*HI and then p413CUP1-alsS(B) was constructed. To construction multigene-expression plasmid, multiple cloning system was used the as previously described with minor modifications [124]. To generate pJIB3 plasmid, *ILV5ΔN48* expression cassette (P_{TDH3}-kozak sequence-*ILV5N48*-T_{CYC1}) flanked by *SacI* and *KpnI* obtained by PCR from p414GPD-*ILV5ΔN48* and cloned between *SacI* and *KpnI* site of p413-D plasmid replacing *alsD* expression cassette. And then *ILV3ΔN19* expression cassette (P_{TDH3}-kozak sequence-*ILV3ΔN19*-T_{CYC1}) flanked by *MauBI* and *NotI* site obtained by PCR using universal primer pair (Univ F2 and Univ R) sequentially cloned into *AscI* and *NotI* sites of the pJIB3 plasmid. Additional gene expression cassettes

sequentially were cloned into pJIB35 using same procedure, resulting in pJIB35KA and pJIB35AA.

To construction of delta-integration DNA fragment, Delta6M-alsS plasmid was constructed. Delta4-1 (167 bp fragment1) and delta4-2 (170 bp fragment2) were obtained from delta4 gene in *S. cerevisiae* genome by PCR amplification using Delta1 R (containing *NotI* site) and Delta1 F and Delta2 R and Delta2 F (containing *NheI* site) primers, respectively. AmpR-expression cassette (fragment3) was obtained in p413GPD using primers, Amp-Ori F and Amp-Ori R. Overlapping PCR product obtained by PCR amplification using the three PCR products (fragment1, 2, and 3) as templates and primer pair (Delta R and Delta2 F) was cloned between *NheI* and *NotI* sites of pUG6MCS, resulting in Delta6M. Genes-expression cassettes, P_{CUP1}-*alsS (B)*-T_{CYC1}, obtained by PCR using primers (Promoter up F and Univ R) were cloned between *NheI* and *NotI* sites of Delta6M, resulting in Delta6M-alsS.

To construction of NTS66M-53 plasmid, two half DNA fragments of NTS1-2, NTS1-2a (400 bp) and NTS1-2b (400 bp), were amplified from genomic DNA of CEN.PK2-1C using primer pairs (NTS1-2a F and NTS1-2a R and NTS1-2b F and NTS1-2b R, respectively). With third PCR product that contains Amp^R expression cassette obtained by PCR using Amp-Ori F and Amp-Ori R primers and fourth PCR product that contains *bleOR* obtained by PCR using TEF prom F and NTS term R primers, overlap PCR was conducted by PCR using NTS1-2a R (containing *Nhe*I site) and NTS term R (containing *Not*I site) and then fused with *ILV5N48*-expression cassette (P_{TDH3}-kozak sequence-*ILV5ΔN48*-T_{CYC1}) obtained by PCR using Promoter

up F and Univ R primers, resulting in NTS66M-5 plasmid. *ILV3ΔN19*-expression cassette (P_{TDH3}-*kozak sequence-ILV3ΔN19*-T_{CYC1}) flanked by *MauBI* and and *NotI* sites were cloned into *AscI* and *NotI* site of the NTS66M-3, resulting in NTS66M-35 plasmid.

3.2.4. Metabolic engineering of *S. cerevisiae* for the production of shinorine a sunblock material from xylose

The NpR genes (*NpR5600, NpR5599, NpR5598*, and *NpR5597*) from *N. punctiforme* ATCC 29133, Ava genes (*Ava3858, Ava3857, Ava3856*, and *Ava3855*) from *A. variabilis* ATCC 29413, and *STB5* and *TKL1* from *S. cerevisiae,* XYL genes (*XYL1*, *XYL2*, and *XYL3*) from pSR306-X123 plasmid were amplified by PCR using each genomic DNA and target-specific primer pairs (ORF F and ORF R). To generate single-gene-expression plasmids, PCR-amplified products were cloned into p413GPD, p414GPD, p415GPD, or p416GPD, or p414ADH plasmids, resulting in p413GPD-NpR5600, p414GPD-NpR5599, p415GPD-NpR5598, p416GPD-NpR5597, p413GPD-Ava3858, p414GPD-Ava3857, p414ADH-STB5, p414GPD-TKL1, p416GPD-*XYL1*, p416GPD-*XYL2*, and p-416*XYL3*. To construction of coex413-NpR4, coex416-XYL, and coex414-STB5-TKL1, the multiple cloning system was used as previously described with minor modifications [124]. The gene-expression cassette (promoter-OFR-terminator) flanked by *MauBI* and and *NotI* sites was obtained by PCR in single-gene-expression vectors using the primers, Univ F2 and Univ R, and then cloned into *AscI* and *NotI* sites of coexpression plasmids.

Additional gene expression cassettes flanked by *MauBI* and *NotI* sites sequentially cloned into *AscI* and *NotI* site of the previously produced plasmids.

To construction of Delta6M, I cloned overlapping PCR product into pUG6MCS . Delta4-1 (167 bp) and delta4-2 (170 bp) were obtained from delta4 gene in *S. cerevisiae* genome by PCR using Delta1 R (containing *NotI* site) and Delta1 F and Delta2 R and Delta2 F (containing *NheI* site) primers, respectively. AmpR-expression cassette was obtained in p413GPD using primers, Amp-Ori F and Amp-Ori R. Overlapping PCR product obtained by PCR using the three PCR products as templates and primer pair (Delta R and Delta2 F) was cloned between *NheI* and *NotI* sites of pUG6MCS, resulting in Delta6M. Genes-expression cassettes (P_{TEF1}-*NpR5597*-T_{GPM1}-P_{TDH3}-NpR*5600*-T_{CYC1} and P_{TEF1}-*NpR5598*-T_{GPM1}-P_{TDH3}-*NpR5599*-T_{CYC1}) obtained by PCR using primers (Promoter up F and Univ R) were cloned between *NheI* and *NotI* sites of Delta6M, resulting in Delta6M-NPR1 and Delta6M-NPR2, respectively.

For NTS site-integration, NTS66M-XYL plasmid was constructed. Two half DNA fragments, NTS1-2a and NTS1-2b, (400 bp and 400 bp) of NTS1-2, were amplified from genomic DNA of CEN.PK2-1C using primer pairs (NTS1-2a F and NTS1-2a R and NTS1-2b F and NTS1-2b R). With third PCR fragment that contains Amp^R and pUG ori obtained by PCR using Amp-Ori F and Amp-Ori R primers and fourth PCR fragment that contains *bleOR* obtained by PCR using TEF prom F and NTS term R primers, overlap PCR was conducted by PCR using NTS1-2a R (containing *NheI* site) and NTS term R (containing *NotI* site) and then cloned with

XYL1-expression cassette (P_{TDH3}-*XYL1*-T_{CYC1}) obtained by PCR using Promoter up F and Univ R primers, resulting in construction of NTS66M-*XYL1* plasmid. *XYL2*-expression cassette (P_{TEF1}-*XYL2*-T_{GPM1}) and *XYL3*-expression cassette (P_{TPI1}-*XYL3*-T_{TPI1}) flanked by MauBI and and NotI sites were cloned into *AscI* and *NotI* site of the NTS66M-*XYL1*, resulting in constructing NTS66M-XYL plasmid.

To *TAL1* deletion using CRISPR/Cas9 system, I constructed plasmids, consisting of Cas9 gene and *TAL1*-specific guide RNA. Gene of Cas9 and guide RNA fragment (P_{SNR52}-structural component-T_{SUP4}) were cloned into p413TEF plasmid resulting in construction coex413-Cas9-gRNA plasmid. *TAL1*-specific target sequence for construction of guide RNA was designed by Yeastiction v0.1 (http://yeastriction.tnw.tudelft.nl). The coex413-Cas9-TAL1gRNA plasmid was construced by DpnI-mediated site directed mutagenesis based on PCR amplification using TAL1 gRNA F and TAL1 gRNA R primers and coex413-Cas9-gRNA plasmid as PCR-template.

3.3. Culture conditions

3.3.5. Metabolic engineering of *S. cerevisiae* for the production of isobutanol and 3-methyl-1-butanol

Yeast cells were pre-cultured in selective SC medium and then inoculated to an A_{600} 0.2 for fermentation. Cells were grown in a 50 mL closed tube with 9 mL culture volume at 30°C with constant shaking at 170 rpm.

3.3.6. Improvement of isobutanol production in *S. cerevisiae* by increasing mitochondrial import of pyruvate through mitochondrial pyruvate carrier

Yeast cells harboring proper plasmid were pre-cultured in selective SC-His medium containing 20 g/L glucose and then inoculated to A_{600} of 0.2 in the same medium with 6.5 mL culture volume in a 50 mL conical tube. Cells were grown at 30°C with constant shaking at 170 rpm.

3.3.7. Development of multi-copy genome integration system with overexpressing α-acetolactate synthase-inducible phenotypic screening for isobutanol production in *S. cerevisiae*

For fermentation in 50mL conical tube yeast cells harboring proper plasmids were pre-cultured in 4 mL selective SC medium containing 20 g/L glucose, inoculated to OD_{600} of 0.2 or 0.5 in the same medium with 6.5 mL in 50 mL conical tube, and then cultured at 30°C with constant shaking at 170 rpm.

For the fermentation with copper induction, overnight culture cells were diluted to OD_{600} of 0.2 or 0.5 incubated for 7 h or 12 h in SC medium containing 20 g/L glucose, and then induced with appropriate concentration of $CuSO_4$.

Table 3.3 Plasmids used in this study

Plasmid	Description	Reference
p413GPD	CEN/ARS, *HIS3*, P_{TDH3}, T_{CYC1}	[119]
p413ADH	CEN/ARS, *HIS3,* P_{ADH1}, T_{CYC1}	[119]
p413TEF	CEN/ARS, *HIS3,* P_{TEF1}, T_{CYC1}	[119]
P414GPD	CEN/ARS, *TRP1*, P_{TDH3}, T_{CYC1}	[119]
p414ADH	CEN/ARS, *TRP1,* P_{ADH1}, T_{CYC1}	[119]
p414TEF	CEN/ARS, *TRP1,* P_{TEF1}, T_{CYC1}	[119]
p415GPD	CEN/ARS, *LEU2*, P_{TDH3}, T_{CYC1}	[119]
p416GPD	CEN/ARS, *URA3,* P_{TDH3}, T_{CYC1}	[119]
p424GPD	2 µ, *TRP1*, P_{TDH3}, T_{CYC1}	[119]
p425GPD	2 µ, *LEU2*, P_{TDH3}, T_{CYC1}	[119]
p426GPD	2 µ, *URA3*, P_{TDH3}, T_{CYC1}	[119]
pUG72	Plasmid containing *loxP-Kl.URA3-loxP* deletion cassette	EUROSCARF
pSH62	CEN/ARS, *HIS3*, P_{GAL1}-*cre*-T_{CYC1}	EUROSCARF
pSH63	CEN/ARS, *TRP1*, P_{GAL1}-*cre*-T_{CYC1}	EUROSCARF
pRS413TEF-*LEU3*	CEN/ARS, *HIS3,* P_{TEF1}-*LEU3*-T_{CYC1}	This study
pRS413TEF-*LEU3Δ601*	CEN/ARS, *HIS3,* P_{TEF1}-*LEU3Δ601*-T_{CYC1}	This study
pRS424GPD-*ILV235*	2 µ, *TRP1*, P_{TDH3}-*ILV2*-T_{CYC1}, P_{TDH3}-*ILV3*-T_{CYC1}, P_{TDH3}-*ILV5*-T_{CYC1}	This study
pRS426GPD-*ARO10 ADH2*	2 µ, *URA3*, P_{TDH3}-*ARO10*-T_{CYC1}, P_{TDH3}-*ADH2*-T_{CYC1}	This study
pRS425GPD-*LEU4*	2 µ, *LEU2*, P_{TDH3}-*LEU4*-T_{CYC1}	This study
pRS425GPD-$LEU4^{D578Y}$	2 µ, *LEU2*, P_{TDH3}-$LEU4^{D578Y}$-T_{CYC1}	This study
pRS425GPD-$LEU4^{D578Y}$ *LEU1*	2 µ, *LEU2*, P_{TDH3}-$LEU4^{D578Y}$-T_{CYC1}, P_{TDH3}-*LEU1*-T_{CYC1}	This study

Table 3.3 Plasmids used in this study (*Continued*)

Plasmid	Description	Reference
p426-MLS	p426GPD containing N-terminal mitochondrial localization signal (MLS) from *COX4*	This study
pJIB1	CEN/ARS, *HIS3*, P_{TEF1}-*LEU3Δ601*-T_{CYC1}, P_{TDH3}-*ILV2*-T_{CYC1}, P_{TDH3}-*ILV5*-T_{CYC1}, P_{TDH3}-*ILV3*-T_{CYC1}, P_{TDH3}-*ARO10*-T_{CYC1}, P_{TDH3}-*ADH2*-T_{CYC1}	This study
pJIB2	CEN/ARS, *HIS3*, P_{TEF1}-*LEU3Δ601*-T_{CYC1}, P_{TDH3}-*ILV2*-T_{CYC1}, P_{TDH3}-*ILV5*-T_{CYC1}, P_{TDH3}-*ILV3*-T_{CYC1}, P_{TDH3}-MLS-*ARO10*-T_{CYC1}, P_{TDH3}-MLS-*ADH2*-T_{CYC1}	This study
pJIB3	CEN/ARS, *HIS3*, P_{TEF1}-*LEU3Δ601*-T_{CYC1}, P_{TDH3}-*ILV2*-T_{CYC1}, P_{TDH3}-*ILV5*-T_{CYC1}, P_{TDH3}-*ILV3*-T_{CYC1}, P_{TDH3}-MLS-*ARO10*-T_{CYC1}, P_{TDH3}-MLS-*ADH2*-T_{CYC1}, P_{TDH3}-*MPC1*-T_{CYC1}	This study
pJIB4	CEN/ARS, *HIS3*, P_{TEF1}-*LEU3Δ601*-T_{CYC1}, P_{TDH3}-*ILV2*-T_{CYC1}, P_{TDH3}-*ILV5*-T_{CYC1}, P_{TDH3}-*ILV3*-T_{CYC1}, P_{TDH3}-MLS-*ARO10*-T_{CYC1}, P_{TDH3}-MLS-*ADH2*-T_{CYC1}, P_{TDH3}-*MPC1*-T_{CYC1}, P_{TDH3}-*MPC2*-T_{CYC1}	This study
pJIB5	CEN/ARS, *HIS3*, P_{TEF1}-*LEU3Δ601*-T_{CYC1}, P_{TDH3}-*ILV2*-T_{CYC1}, P_{TDH3}-*ILV5*-T_{CYC1}, P_{TDH3}-*ILV3*-T_{CYC1}, P_{TDH3}-MLS-*ARO10*-T_{CYC1}, P_{TDH3}-MLS-*ADH2*-T_{CYC1}, P_{TDH3}-*MPC1*-T_{CYC1}, P_{TDH3}-*MPC3*-T_{CYC1}	This study
p413GPD-ILV2ΔN54	CEN/ARS plasmid, *HIS3,* P_{TDH3}-*ILV2ΔN54*-T_{CYC1}	This study
p414GPD-ILV5ΔN48	CEN/ARS plasmid, *TRP1,* P_{TDH3}-*ILV5ΔN48*-T_{CYC1}	This study
p416GPD-ILV3ΔN19	CEN/ARS plasmid, *URA3,* P_{TDH3}-*ILV3ΔN19*-T_{CYC1}	This study
p413GPD-ILV2ΔN54	CEN/ARS plasmid, *HIS3,* P_{TDH3}-*ILV2ΔN54*-T_{CYC1}	This study
p413ADH-alsS(B)	CEN/ARS plasmid, *HIS3,* P_{ADH1}-*alsS* (from *B. subtilis*)-T_{CYC1}	This study
p413GPD-alsS(L)	CEN/ARS plasmid, *HIS3,* P_{TDH3}-*alsS* (from *L. lactis*)-T_{CYC1}	This study

Table 3.3 Plasmids used in this study (*Continued*)

Plasmid	Description	Reference
p414GPD-ILV5ΔN48(K)	CEN/ARS plasmid, *TRP1,* P_{TDH3}-Kozak sequence-*ILV5ΔN48*-T_{CYC1}	This study
p416GPD-ILV3ΔN19(K)	CEN/ARS plasmid, *URA3,* P_{TDH3}- Kozak sequence-*ILV3ΔN19*-T_{CYC1}	This study
p413CUP1-alsS(B)	CEN/ARS plasmid, *HIS3,* P_{CUP1}-*alsS* (from *B. subtilis*)-T_{CYC1}	This study
pJIB35	CEN/ARS plasmid, *HIS3*, P_{TDH3}-*kozak sequence-ILV5ΔN48*-T_{CYC1}, P_{TDH3}-*kozak sequence-ILV3ΔN19*-T_{CYC1}	This study
pJIB35KA	CEN/ARS plasmid, *HIS3*, P_{TDH3}-*kozak sequence-ILV5ΔN48*-T_{CYC1}, P_{TDH3}-*kozak sequence-ILV3ΔN19*-T_{CYC1}, P_{TDH3}-*kivd*-T_{CYC1}, P_{FBA1}-*ADH2*-T_{FBA1}	This study
pJIB35AA	CEN/ARS plasmid, *HIS3*, P_{TDH3}-*kozak sequence-ILV5ΔN48*-T_{CYC1}, P_{TDH3}-*kozak sequence-ILV3ΔN19*-T_{CYC1}, P_{TDH3}-*ARO10*-T_{CYC1}, P_{FBA1}-*ADH2*-T_{FBA1}	This study
Delta6M	Plasmid containing *loxP-KanMX-loxP* and flanked with YARCdelta4-1 and YARCdelta4-2	This study
Delta6M-alsS	Delta6M plasmid, P_{CUP1}-*alsS* (*B. subtilis*)-T_{CYC1}	This study
NTS66M-5	Plasmid containing *bleOR* and flanked with NTS1-2a and NTS1-2b, P_{TDH3}-*kozak sequence-ILV5ΔN48*-T_{CYC1},	This study
NTS66M-53	Plasmid containing *bleOR* and flanked with NTS1-2a and NTS1-2b, P_{TDH3}-*kozak sequence-ILV5ΔN48*-T_{CYC1}, P_{TDH3}-*kozak sequence-ILV3ΔN19*-T_{CYC1}	This study
p413GPD-NpR5600	CEN/ARS plasmid, *HIS3*, P_{TDH3}-*NpR5600*-T_{CYC1}	This study
p414GPD-NpR5599	CEN/ARS plasmid, *TRP1*, P_{TDH3}-*NpR5600*-T_{CYC1}	This study
p415GPD-NpR5598	CEN/ARS plasmid, *LEU2*, P_{TDH3}-*NpR5600*-T_{CYC1}	This study

Table 3.3 Plasmids used in this study (*Continued*)

Plasmid	Description	Reference
p416GPD-NpR5597	CEN/ARS plasmid, *URA3,* P_{TDH3}-*NpR5600*-T_{CYC1}	This study
p413GPD-Ava3858	CEN/ARS plasmid, *HIS3,* P_{TDH3}-*Ava3858*-T_{CYC1}	This study
p414GPD-Ava3857	CEN/ARS plasmid, *HIS3,* P_{TDH3}-*Ava3857*-T_{CYC1}	This study
coex413-NpR4	CEN/ARS plasmid, *HIS3,* P_{TEF1}-*NpR5597*-T_{GPM1}, P_{TDH3}-*NpR5600*-T_{CYC1}, P_{TDH3}-*NpR5599*-T_{CYC1}, P_{TEF1}-*NpR5598*-T_{GPM1}	This study
coex416-XYL	CEN/ARS plasmid, *URA3,* P_{TDH3}-*XYL1*-T_{CYC1}, P_{TDH3}-*XYL2*-T_{CYC1}, P_{TDH3}-*XYL3*-$T_{CYC1\ 1}$	This study
p414ADH-STB5	CEN/ARS plasmid, *TRP1,* P_{ADH1}-*STB5*-T_{CYC1}	This study
p414GPD-TKL1	CEN/ARS plasmid, *TRP1,* P_{TDH3}-*TKL1*-T_{CYC1}	This study
coex414-STB5-TKL1	CEN/ARS plasmid, *TRP1,* P_{ADH1}-*STB5*-T_{CYC1}, P_{TDH3}-*TKL1*-T_{CYC1}	This study
pUG6MCS	pUG6 plasmid containing additional restriction enzyme sites	[125]
Delta6M-NPR1	Delta6M plasmid, P_{TEF1}-*NpR5597*-T_{GPM1}, P_{TDH3}-*NpR5600*-T_{CYC1}	This study
Delta6M-NPR2	Delta6M plasmid, P_{TEF1}-*NpR5598*-T_{GPM1}, P_{TDH3}-*NpR5599*-T_{CYC1}	This study
NTS66M-XYL1	Plasmid containing *bleOR* and flanked with NTS1-2a and NTS1-2b, P_{TDH3}-*XYL1*-T_{CYC1}	This study
NTS66M-XYL	NTS66M plasmid, P_{TDH3}-*XYL1*-T_{CYC1}, P_{TEF1}-*XYL2*-T_{GPM1}, P_{TPI1}-*XYL3*-T_{TPI1}	This study
coex413-Cas9-TAL1gRNA	CEN/ARS plasmid, *HIS3,* P_{TDH3}-*CAS9*-T_{TPI1}, P_{SNR52}-*TAL1gRNA*-T_{SUP4}	This study
Delta6M-NPR1	Delta6M plasmid, P_{TEF1}-*NpR5597*-T_{GPM1}, P_{TDH3}-*NpR5600*-T_{CYC1}	This study
Delta6M-NPR2	Delta6M plasmid, P_{TEF1}-*NpR5598*-T_{GPM1}, P_{TDH3}-*NpR5599*-T_{CYC1}	This study
NTS66M-XYL1	Plasmid containing *bleOR* and flanked with NTS1-2a and NTS1-2b, P_{TDH3}-*XYL1*-T_{CYC1}	This study

Table 3.3 Plasmids used in this study (*Continued*)

Plasmid	Description	Reference
NTS66M-XYL	NTS66M plasmid, P_{TDH3}-*XYL1*-T_{CYC1}, P_{TEF1}-*XYL2*-T_{GPM1}, P_{TPI1}-*XYL3*-T_{TPI1}	This study
coex413-Cas9-TAL1gRNA	CEN/ARS plasmid, *HIS3,* P_{TDH3}-*CAS9*-T_{TPI1}, P_{SNR52}-*TAL1gRNA*-T_{SUP4}	This study

Table 3.4 Primers used for gene cloning

Primers	Sequence (5'-3')
LEU3 F	CGCGGATCCATGGAAGGAAGATCAGATTT
LEU3 F	CGCCTCGAGTTAAACCTTGGGATTGAACG
LEU3 OL F	TAACGCTCTTAAGCTCGTCGGAACAACTGAATCATGCAA
LEU4 OL R	TTTGCATGATTCAGTTGTTCCGACGAGCTTAAGAGCGTT
ILV2 F	GCGGCTAGCATGATCAGACAATCTACGCT
ILV2 R	GCGCTCGAGTCAGTGCTTACCGCCTGTAC
IVL5 F	GCGGCTAGCATGTTGAGAACTCAAGCCGC
ILV5 R	GCGGTCGACTTATTGGTTTTCTGGTCTCA
ILV3 F	GCGACTAGTATGGGCTTGTTAACGAAAGT
ILV3 R	GCGGTCGACTCAAGCATCTAAAACACAAC
ARO10 F	GCGCTCGAGCTATTTTTTATTTCTTTTAAGTGC
ARO10 R	GCGCTCGAGTTAGACGAAGATAGGAATCTTGT
ADH2 F	GCGACTAGTATGTCTATTCCAGAAACTCAA
ADH2 R	GCGCTCGAGTTATTTAGAAGTGTCAACAAC
LEU1 F	GCGACTAGTATGGTTTACACTCCATCCAAGGGTCCA
LEU1 R	GCGCTCGAGCTACCAATCCTGGTGGACTTTATCGAAAGT
LEU4 F	GCGCCCGGGATGGTTAAAGAGAGTATTATTGCTC
LEU4 R	GCGCTCGAGTTATGCAGAGCCAGATGCCGCAGCA
MPC1 F	GCGGGATCCATGTCTCAACCGGTTCAACG
MPC1 R	GCGCTCGAGTTACTGTTTACCAGTTTTTT
MPC2 F	GCGGGATCCATGTCTACATCATCCGTACG
MPC2 R	GCGCTCGAGTTATCTGCCCGTAGTAATTT
MPC3 F	GCGGGATCCATGTCAGCATCAGCTTTTAA
MPC3 R	GCGCTCGAGTCAGTGCGTTATTGGCGGAT

Restriction enzyme sites are underlined

Table 3.4 Primers used for gene cloning (*Continued*)

Primers	Sequence (5'-3')
MTS F	CTAGCATGCTTTCACTACGTCAATCTATAAGATTTTTCAAGCCA GCCACAAGAACTTTGTGTAGCTCTAGATATCTGCTTCAGACTAG TG
MTS R	GATCCACTAGTCTGAAGCAGATATCTAGAGCTACACAAAGTTCT TGTGGCTGGCTTGAAAAATCTTATAGATTGACGTAGTGAAAGCA TG
ILV2ΔN54 F	AGCTGGATCCATGCCAGAGCCTGCTCCAAGTT
ILV2ΔN54 R	GCGCTCGAGTCAGTGCTTACCGCCTGTACGCT
ILV5ΔN48 F	CTGAGGATCCATGAAGCAAATCAACTTCGG
ILV5ΔN48 R	GATCCTCGAGTTATTGGTTTTCTGGTCTCAAC
ILV3ΔN19 F	GTACGGATCCATGGCAAAGAAGCTCAACAAGTA
ILV3ΔN19 R	TGCACTCGAGTCAAGCATCTAAAACACAACC
K_ILV5ΔN48 F	GCGGGATCCAAAAAATGAAGCAAATCAACTTCGG
K_ILV3ΔN19 F	GCGCTCGAGTTATGATTTATTTTGTTCAGCA
alsS (B) F	CTGAGGATCCATGACAAAAGCAACAAAAGAAC
alsS (B) R	CTGACTCGAGCTAGAGAGCTTTCGTTTTCA
alsS (L) F	GCGGGATCCATGGCACAATCCCTTCCC
kivd F	GCGGGATCCATGTATACAGTAGGAGATTACC
kivd R	GCGCTCGAGTTATGATTTATTTTGTTCAGCA
CUP1p F	GCGGAGCTCTAAGCCGATCCCATTACCGA
CUP1p R	GCGGGATCCTTTATGTGATGATTGATTGATTGAT
Delta1 R	ATAGCGGCCGCATGTTTATATTCATTGATCCTATTACA
Delta1 F	CACATTTCCCCGAAAAGTGCATTTAAATTGTTGGAATAGAAATC AACTATC
Amp-Ori F	GCACTTTTCGGGGAAATGTG
Amp-Ori R	CTCAACATTCACCCATTTCTCAATTTAAATCGCAGGAAAGAACA TGTGAG

Restriction enzyme sites are underlined

Table 3.4 Primers used for gene cloning (*Continued*)

Primers	Sequence (5'-3')
Delta2 R	TGAGAAATGGGTGAATGTTGAG
Promoter up F	GCGGCTAGCGAGCTCGGAAACAGCTATGACCATGA
NTS term R	GCGGGCGCGCCGCGGCCGCTAAGGGTTCTCGAGAGCTC
TEF prom F	GCCAAAAATTTACTTCGCGCGGCCCGACATGGAGGCCCAGAAT
NTS1-2b F	GCGAAGTAAATTTTTGGCG
NTS1-2b Amp R	TTTCCCCGAAAAGTGCATTTAAATCTAGTTTCTTGGCTTCCTATG
NTS1-2a F	CCGAGCGTGAAAGGATTTGCC
NTS1-2a R	GCGGCTAGCCAACCATTCCATATCTGTTAAG
Univ F	GACTACGCGTGGAACAAAAGCTGGAGCTC
Univ R	GACTACGCGTGCGGCCGCTAATGGCGCGCCATAGGGCGAATTGGG TACC
Promoter up F	GCGGCTAGCGAGCTCGGAAACAGCTATGACCATGA
NTS term R	GCGGGCGCGCCGCGGCCGCTAAGGGTTCTCGAGAGCTC
TEF prom F	GCCAAAAATTTACTTCGCGCGGCCCGACATGGAGGCCCAGAAT
NTS1-2b F	GCGAAGTAAATTTTTGGCG
NTS1-2b Amp R	TTTCCCCGAAAAGTGCATTTAAATCTAGTTTCTTGGCTTCCTATG
NTS1-2a F	CCGAGCGTGAAAGGATTTGCC
NTS1-2a R	GCGGCTAGCCAACCATTCCATATCTGTTAAG
NpR5600 F	GCGGGATCCATGAGTAATGTTCAAGCATCG
NpR5600 R	GCGCTCGAGTCACACTCCCAATAGTTTGG
NpR5599 F	GCGGGATCCATGACCAGTATTTTAGGACG
NpR5599 R	GCGCTCGAGTTATACCAAGCGTCTAATCAG
NpR5598 F	GCGGGATCCATGGCACAATCAATCTCTTTA
NpR5598 R	GCGCTCGAGTAGTCGCCCCCTAATTCC

Restriction enzyme sites are underlined

Table 3.4 Primers used for gene cloning (*Continued*)

Primers	Sequence (5'-3')
NpR5597 F	GCGGGATCCATGCCAGTACTTAATATCCTT
NpR5597 R	GCGCTCGAGTCAATTTTGTAACACCTTTTTATTA
Ava3858 F	GCGGGATCCATGAGTATCGTCCAAGCAAA
Ava3858 R	GCGCTCGAGTTATTTAACACTCCCGATTAATTCT
Ava3857 F	GCGGGATCCATGACAAATGTGATTGTCCAACC
Ava3857 R	GCGCTCGAGTTAAGGTTGTATTCTGCGGAT
Ava3856 F	GCGGGATCCATGGCACAATCCCTTCCC
Ava3856 R	GCGCTCGAGCTAATCTCCCCCCAATTCCA
Ava3855 F	GCGGGATCCATGCAGACTATAGATTTTAATATTCG
Ava3855 R	GCGCTCGAGTTATGAATTATTTTCCAGACAATCTTG
XYL1 F	GCGGGATCCATGCCTTCTATTAAGTTGAACTC
XYL1 R	GCGCTCGAGTTAGACGAAGATAGGAATCTTGT
XYL2 F	GCGGGATCCATGACTGCTAACCCTTCCTT
XYL2 R	GCGCTCGAGTTACTCAGGGCCGTCAATG
XYL3 F	GCGGGATCCATGACCACTACCCCATTTG
XYL3 R	GCGCTCGAGTTAGTGTTTCAATTCACTTTCCATC
STB5 F	GCGGGATCCATGGATGGTCCCAATTTTG
STB5 R	GCGGTCGACTCATACAAGTTTATCAACCCAAG
TKL1 F	GCGGGATCCATGACTCAATTCACTGACA
TKL1 R	GCGCTCGAGTTAGAAAGCTTTTTTCAAAGGAG

Restriction enzyme sites are underlined

3.3.8. Metabolic engineering of *S. cerevisiae* for the production of shinorine a sunblock material from xylose

For shake flask fermentation yeast cells harboring particular plasmid were pre-cultured in selective SC medium containing 20 g/L glucose and inoculated to OD_{600} of 0.2 in 10 mL of selective SC medium containing glucose and xylose mixed the proper proportion in 100 mL flask and then cultured at 30 ºC with shaking at 170 rpm.

Fed-batch fermentation in flask was performed in 25 mL SC-His medium containing 18 g/L xylose and 2 g/L glucose at 30 °C with agitation speed of 170 rpm. JHYS17-2 strain was pre-cultured in SC-His medium containing 20 g/L glucose and inoculated into the fermenter with initial OD_{600} of 1. The feeding solution (600 g/L xylose and 400 g/L glucose) was added to the culture medium when the xylose concentration was lower than 5 g/L.

3.4. RNA preparation and quantitative reverse transcription PCR

The 1 mL of cells was harvested and frozen at -80ºC in 300 µL of lysis buffer [10 mM Tris-HCl (pH 7.4), 10 mM EDTA, 0.5% SDS]. 300 µL of acidic phenol was added to each sample and incubated at 65ºC for 20 min with occasional vortexing. Prior to chloroform extraction, the solution was chilled on ice for 10 min. After centrifugation and ethanol precipitation, the resulting RNA pellets were dissolved in

RNase-free water. The relative amount of mRNA was determined by quantitative reverse transcription PCR (qRT-PCR).

Relative amount of *ILV2*, *ILV5*, and *LEU4* mRNA was determined by qRT-PCR using obtained total RNA. Briefly, 1 µg of total RNA was used for reverse transcription in a 30 µl reaction volume containing 200 unit of myeloblastosis virus reverse transcriptase (Thermo scientific), 2 µg oligo dT (IDT) and 1 µl each of 10 mM dNTPs at 42°C for 1 h. For qRT-PCR analysis, reaction mixture containing 1 µl cDNA, 1 x SYBR Green I master mix (Roche Applied Science), and 5 pmol each of gene-specific primers was used. PCR was performed with 40 cycles of 95°C for 20 s, 60°C for 20 s, and 72°C for 20 s on a LightCycler 480 II System (Roche Applied Science). The *ACT1* housekeeping gene was used as a reference control. The crossing point (Cp) values were processed using LightCycler Software version 1.5 (Roche Applied Science) and expression levels were normalized as target/reference ratios. Primer sequences used for qRT-PCR are shown in Table 3.4.

3.5. Quantitative PCR (qPCR)

The engineered yeast strains were cultured in YPD medium and harvested for the genomic DNA isolation. All genomic DNA were isolated following previously described procedure using a lithium acetate (LiOAc)-SDS solution [126]. To determine the copy numbers of integrated genes into yeast chromosome, qRT PCR was performed using the isolated genomic DNA. For qPCR analysis, reaction

mixture containing 5 μl genomic DNA, 5 pmol each of gene-specific primers, and 1 x SYBR Green I master mix (Roche Applied Science) were used. qPCR was performed with 45 cycles of 95°C for 40 s, 55°C for 20 s, and 72°C for 20 s on a LightCycler 480 II System (Roche Applied Science). The ACT1 housekeeping gene was used as a reference control. The crossing point (Cp) values were processed using LightCycler Software version 1.5 (Roche Applied Science) and expression levels were normalized as target/reference ratios. The qPCR primers used in this study are shown in Table 4.3.

3.6. Analytic methods

Cell growth was determined by the measurement of an optical density at 600 (OD_{600}) with spectrophotometer (Varian Cary® 50 UV-Vis). Isobutanol and 3-methyl-1-butanol concentrations were determined by gas chromatography (GC) equipped with an auto-sampler (CP-8410, Varian, Netherlands), DB-WAX capillary column (length of 30 m, 0.32 mm of an inner diameter, 0.25 μm in strength of stationary phase film; Agilent, Waldbronn, Germany), and a flame ionization detector (FID). Helium was used as carrier gas with a flow rate of 29 ml/min. Analysis method is as follows. 0.8 μl filtered supernatant was injected to the GC in split injection mode

Table 3.5 Primers used for qRT-PCR and qPCR

Primers	Sequence (5'-3')
ILV2 RT F	GGTATGGTTACTCAATGGCAATCCC
ILV2 RT R	CAACTTAGCGTCCAATTCCTCTTGC
ILV5 RT F	CGCCAGAAGAGGTGCTTTGGACTG
ILV5 RT R	GCTTTTCTCTGTAGTCAGGTTGAG A
LEU4 RT F	CGCCCTATCAAACTTGTTGAACGTG
LEU4 RT R	GCCTTTTCGTTGTCGGCATTACGC
alsS (B) qPCR F	CGCACCCTCTTGAAATCGTT
alsS (B) qPCR R	CCGAGTGTTTGCATACCGTT
ILV5ΔN48 qPCR F	CCCTCAGAATGGCAGAGGAA
ILV5ΔN48 qPCR R	GACGCACTGTTTCACCATCA
ILV3ΔN19 qPCR F	CTAGCTGCACCTTTGGAACC
ILV3ΔN19 qPCR R	GAGCGAATCCCAGTCAATCG
NpR5600 qPCR F	ATGGCGAAGAGTTGCTTTCC
NpR5600 qPCR R	GTGTGACCGTAGGCAATGAC
NpR5599 qPCR F	CCCTCAGAATGGCAGAGGAA
NpR5599 qPCR R	GACGCACTGTTTCACCATCA
NpR5598 qPCR F	CTAGCTGCACCTTTGGAACC
NpR5598 qPCR R	GAGCGAATCCCAGTCAATCG
NpR5597 qPCR F	AAACTGACGATGGCGACTTG
NpR5597 qPCR R	ACCAAGGTTGTCCCTTTGGA
XYL1 qPCR F	TTGGTCAAGGCCGGTAAGAT
XYL1 qPCR R	ATGGGTGGTGTTCAACTTGC
XYL2 qPCR F	CCATCCAGATTCTCCGACGA

with a 20:1 ratio and inlet temperate was 250°C. The GC oven temperature was held initially at 35°C for 5 min and increased to 120°C with 6°C/min. It was finally raised to 230°C with 50°C/min and then held for 3min. The temperature of FID was held at 270°C. For data quantification Galaxie chromatography Data system (Varian, Netherlands) was used.

High performance liquid chromatography (HPLC) analysis was performed to quantify the concentrations of glucose, ethanol, glycerol, xylose, isobutanol. 1 mL of culture supernatants were collected and filtered through a 0.22 μm syringe filter, and then analyzed in UltiMate 3000 HPLC system (Thermo fishers scientific) equipped with an Aminex HPX-87H column (300 mm x 7.8 mm, 5μm, Bio-Rad) and a refractive index (RI) detector. The column was eluted with 5 mM H_2SO_4 as a flow rate of 0.6 ml/min at 60ºC and RI detector was kept at 35ºC.

To quantify the concentration of shinorine, 2 sets of 4 mL of culture broth were collected. One was dried in oven to measure the g dry cell weight (gDCW) and the other was centrifuged and filtered supernatants was used for shinorine measurement in medium. Isolated cell broken with chloroform used to measure the amount of shinorine accumulated in the cells. The yeast cells obtained by centrifugation were dissolved in 1 mL of water, added of 1.5 mL of chloroform, and then vortexed for 3 minutes. This was centrifuged again, and only the water layer was separated and filtered to prepare a sample. Standard curve was generated by using shinorine obtained from CJ cheiljedang BIO quantitated by Ultimate3000 HPLC system (Thermo Fisher Scientific) with Agilent Eclipse XDB-C18 column (5 μm, 4.6 x 250

mm). Analysis was performed with adequate solvent (water : acetonitrile = 95 : 5) as a mobile phase at a flow rate of 0.5 mL/min and shinorine was detected with UV-Vis detector at 334 nm. The column temperature was maintained at 40 °C.

Chapter 4.

Metabolic engineering of *S. cerevisiae* for the production of isobutanol and 3-methyl-1-butanol

4.1. Introduction

Higher alcohols have received much attention as next generation transport fuels compatible with current infrastructure because of their higher energy density and lower moisture absorption compared with ethanol [127,128]. Researches have been focused on the microbial production of branched-chain higher alcohols such as isobutanol and 3-methyl-1-butanol, which have higher octane values than their linear-chain counterparts [14,129]. Prokaryotic cells such as *E. coli*, *B. subtilis*, and *C. glutamicum* have been successfully engineered to produce isobutanol by introducing the last two steps of Ehrlich pathway, which allows the conversion of 2-ketoacids, the intermediates in the amino acid biosynthetic pathways, into corresponding alcohols [129]. Although the engineered bacterial strains produced high concentrations of isobutanol with high yields even to a theoretical maximum, isobutanol toxicity is the major bottleneck for their industrial scale applications [128,130,131].

Yeast has been considered as an attractive alternative system to produce isobutanol because of its high tolerance to isobutanol up to 20 g/L and robustness in harsh industrial conditions [132-134]. *S. cerevisiae* naturally produces small amounts of fusel alcohols including isobutanol and 3-methyl-1-butanol from the catabolism of amino acids [5]. In *S. cerevisiae*, production of 2-KIV from pyruvate occurs in the mitochondrial matrix by the consecutive actions of Ilv2 (ALS), Ilv5 (KARI), and Ilv3 (DHAD) (Fig. 4.1) [135]. Valine is also synthesized from 2-KIV

in the mitochondria by Bat1, a mitochondrial isoform of branched-chain amino acid aminotransferase [6,136]. Whereas, degradation of valine to 2-KIV occurs in the cytosol by Bat2, a cytosolic counterpart of Bat1 [6,137]. 2-KIV is further degraded to isobutanol via several KDCs and ADHs in yeast. 2-KIV is also an intermediate for leucine biosynthesis. Conversion of 2-KIV to 2-ketoisocaproate (2-KIC) is catalyzed by three enzymatic steps involving Leu4 (2-isopropylmalate synthase), Leu1 (isopropylmalate isomerase), and Leu2 (3-isopropylmalate dehydrogenase) [138] and 2-KIC can be either converted to leucine by Bat2 or degraded to 3-metyhl-1-butanol via Ehrlich pathway (Fig. 4.1).

So far, several efforts have been made to produce isobutanol in *S. cerevisiae*, which include overexpression of genes involved in valine synthesis (*ILV2, ILV3,* and *ILV5*) and degradation (*BAT2,* KDCs and ADHs. In addition, to locate the two pathways in a same compartment, Ilv2, Ilv3, and Ilv5 were expressed in the cytoplasm [25,27], or KDCs and ADHs were expressed in the mitochondria [23]. The highest isobutanol titers of a strain expressing all the enzymes in the mitochondria were 279 mg/L and 635 mg/L in minimal and complete media, respectively [23]. Recently, enhanced isobutanol production has been reported by deleting *LPD1* encoding pyruvate dehydrogenase which compete for pyruvate availability, and also by overexpressing NADPH-generating malic enzyme (Mae1) to resolve cofactor imbalance. The engineered strain produced 1.62 g/L isobutanol with a yield of 16 mg/g glucose [28].

In this study, I introduced new strategies to increase the production of

isobutanol and 3-methyl-1-butanol in yeast. In addition to overexpressing the enzymes in the biosynthetic pathways by using heterologous promoters as previously reported, the expression of endogenous genes in the valine and leucine biosynthetic pathways was further increased by expressing a constitutively active form of Leu3 transcription factor. In combination with the deletion of two competitive pathways, the resulting isobutanol-production strain produced 376.9 mg/L isobutanol, exhibiting about a 7.1-fold increase compared with wild type. In addition, the strain engineered for 3-methyl-1-butanol production produced 765.7 mg/L 3-methyl-1-butanol which is the highest titer ever reported in yeast.

4.2. Increase in isobutanol production by introducing a constitutively active Leu3 transcription factor

S. cerevisiae CEN.PK2-1C strain used in this chapter has several point mutations in the *LEU2* gene (leu2-3,112) in the leucine biosynthetic pathway, resulting in limited production of not only leucine but also 3-methyl-1-butanol (Fig. 1). Therefore, I first focused on the increase in isobutanol production.

Leu3 is a $Zn(II)_2Cys_6$ family of transcription factor involved in the regulation of branched-chain amino acid biosynthesis [28,44]. 2-Isopropylmalate (2-IPM) an intermediate in the leucine biosynthetic pathway binds to the middle domain of Leu3 leading to its activation [49,138]. In the absence of 2-IPM, Leu3 can act as a repressor. The Leu3 target genes include *ILV2*, *ILV5*, *BAT1*, *LEU4*, *LEU1*, and *LEU2*

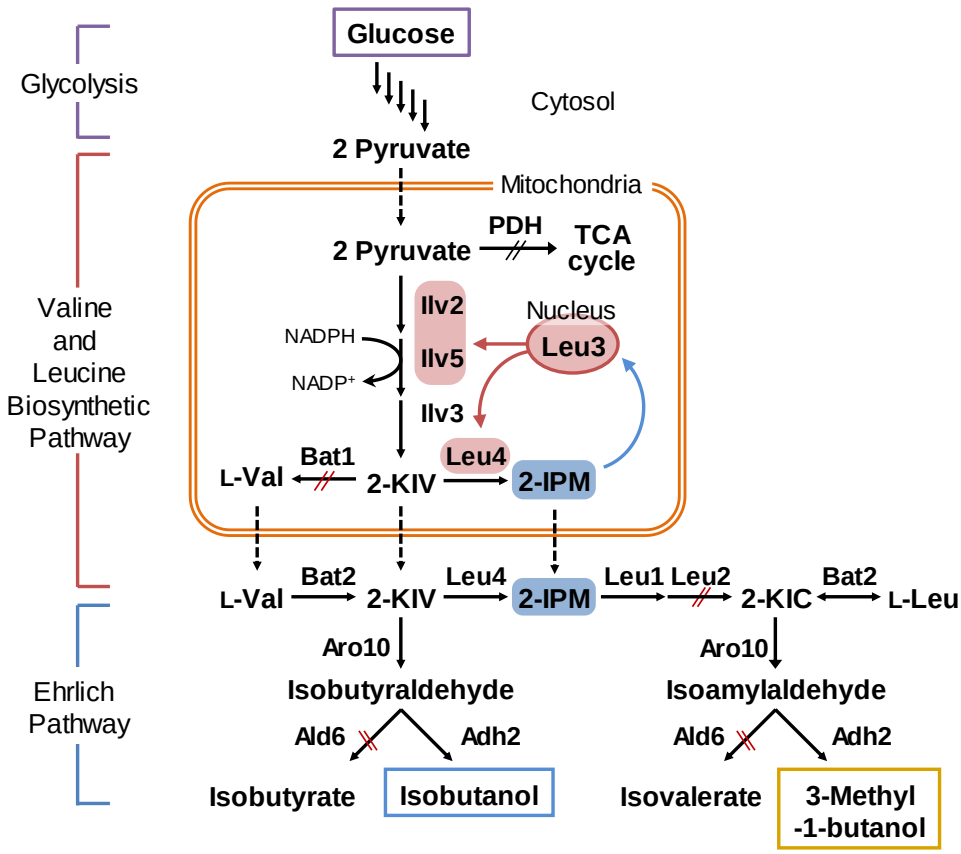
Glycolysis
Valine and Leucine Biosynthetic Pathway
Ehrlich Pathway
Glucose
Cytosol
2 Pyruvate
Mitochondria
2 Pyruvate
PDH
TCA cycle
Ilv2
Ilv5
Nucleus
Leu3
NADPH
NADP+
Ilv3
Leu4
Bat1
L-Val
2-KIV
2-IPM
L-Val
Bat2
2-KIV
Leu4
2-IPM
Leu1 Leu2
2-KIC
Bat2
L-Leu
Aro10
Isobutyraldehyde
Aro10
Isoamylaldehyde
Ald6
Adh2
Ald6
Adh2
Isobutyrate
Isobutanol
Isovalerate
3-Methyl -1-butanol

Figure 4.1 Schematic illustration of the biosynthetic pathways to produce isobutanol and 3-methyl-1-butanol from glucose in *S. cerevisiae*

2 molecules of pyruvate are converted to 2-ketoisovalerate (2-KIV) by sequential actions of three mitochondrial enzymes, Ilv2 (acetolactate synthase), Ilv5 (ketoacid reductoisomerase), and Ilv3 (dihydroxyacid dehydratase). 2-KIV is converted to valine by Bat1, a mitochondrial branched-chain amino acid aminotransferase. On the other hand, valine degradation to 2-KIV is mediated by Bat2 in cytosol. In the leucine biosynthetic pathway, 2-KIV is converted to 2-isopropylmalate (2-IPM) by Leu4 (2-isopropylmalate synthase) both in the mitochondria and cytosol, and then the conversion of 2-IPM to 2-ketoisocaproate (2-KIC) in cytosol is catalyzed by Leu1 (isopropylmalate isomerase) and Leu2 (3-isopropylmalate dehydrogenase). 2-IPM binds to Leu3, activating its function as a transcriptional activator of *ILV2*, *ILV5*, *BAT1*, *LEU1*, *LEU2*, and *LEU4* genes. 2-KIV and 2-KIC are converted into corresponding aldehydes and alcohols by various 2-ketoacid decarboxylases (KDCs) and alcohol dehydrogenases (ADHs), respectively. Isobutyraldehyde and isoamylaldehyde can also be oxidized into corresponding acids by aldehyde dehydrogenases (ALDs).

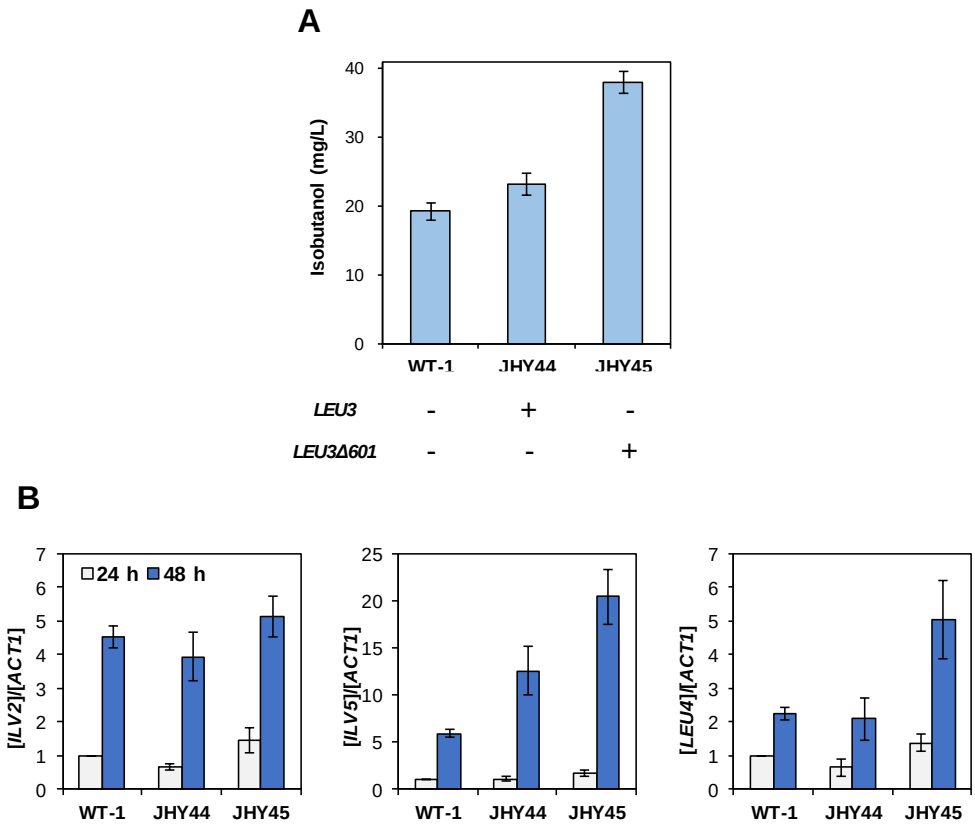

Figure 4.2 Improvement of the isobutanol production by deleting competing pathways and by expressing Leu3Δ601, a constitutively active form of Leu3 transcription factor.

A. Isobutanol production titers of WT-1 and cells overexpressing *LEU3* (JHY44) or *LEU3*Δ601 (JHY45) grown in SC-His medium with 2% glucose for 48 h.

B. Expression levels of *ILV2, ILV5*, and *LEU4* obtained by qRT-PCR. WT-1, JHY44, and JHY45 cells were grown in SC-His medium containing 2% glucose for the indicated times and mRNA levels of *ILV2*, *ILV5*, and *LEU4* were quantified by qRT-PCR and normalized to *ACT1*.

in valine and leucine biosynthetic pathways (Fig. 4.1) and genes involved in amino acid uptake and other functions [42,43,139,140]. It has been known that deletion of the internal region of Leu3 encompassing the 2-IPM binding domain makes Leu3 constitutively active even in the absence of 2-IPM [46].

Therefore, as an effort to increase expression levels of multiple genes involved in branched-chain amino acid biosynthesis, we overexpressed *LEU3* or *LEU3Δ*601, encoding a constitutive active form of Leu3, from the *TEF1* promoter by cloning the gene into a pRS413TEF plasmid. Overexpression of *LEU3* (JHY44) led to a slight increase in isobutanol production (23.2 mg/L) compared with wild type control (Fig. 4.2B). Notably, overexpression of *LEU3Δ601* (JHY45) enhanced isobutanol production approximately by 2 folds (38 mg/L). To confirm the effect of Leu3Δ601 on the transcriptional activation of its target genes, we analyzed mRNA levels of *ILV2*, *ILV5*, and *LEU4* by qRT-PCR in cells overexpressing *LEU3* or *LEU3Δ601* (Fig. 4.2B). As expected, JHY45 strain overexpressing *LEU3Δ601* showed increased mRNA levels of *ILV2*, *ILV5*, and *LEU4* compared with the control strain (Fig. 4.2B). On the contrary, *LEU3*-overexpressing cells (JHY44) showed induction of *ILV5* expression to a lesser extent than that observed in JHY45, while exhibiting a slight repression of *ILV2* and *LEU4* expression (Fig. 4.2B). Such gene-specific effects of *LEU3* overexpression might be related to the fact that Leu3 can act as both activator and repressor depending on conditions. These results suggest that increase in expression levels of *ILV2*, *ILV5*, and potentially other targets by the constitutively active Leu3Δ601 transcription factor might contribute to isobutanol

production, although the transcriptional activation effects of Leu3Δ601 might be variable depending on the promoter structures of the target genes.

Bat1 and Bat2 are branched-chain amino acid aminotransferases localized in mitochondria and cytosol, respectively [136]. In the valine metabolic pathways, Bat1 catalyzes valine synthesis from 2-KIV, whereas Bat2 is mainly responsible for the reverse reaction degrading valine to 2-KIV, which leads to isobutanol production via Ehrlich pathway (Fig. 4.1) [141]. Accordingly, Bat1-mediated valine synthesis might compete with isobutanol production from 2-KIV [142]. In cytosol, 2-KIV is converted to isobutyraldehyde by KDCs (Fig. 4.1). Oxidation of isobutyraldehyde to isobutyrate by aldehyde dehydrogenases (ALDs) competes with the production of isobutanol by ADHs [5]. Among the three cytosolic ALDs (Ald2, Ald3, and Ald6), Ald6 is known to be involved in isobutyrate production [142].

In previous my master's thesis, I deleted *BAT1* and *ALD6* to increase isobutanol production by eliminating competing pathways. Deletion of both *BAT1* and *ALD6* exerted additive effect on isobutanol production achieving 61.2 mg/L isobutanol production in *ald6Δbat1Δ* strain (JHY43-1).

4.3. Enhancing isobutanol production by overexpression of genes in the biosynthetic pathway

Next, to further enhance the metabolic fluxes leading to isobutanol production, we overexpressed all the genes in the isobutanol biosynthetic pathway. *ILV2*, *ILV5*, and

ILV3 genes involved in the biosynthesis of 2-KIV from pyruvate [8] were cloned into a single high copy number plasmid vector (pRS424GPD) and expressed under the control of *TDH3* promoter. Overexpression of *ILV2*, *ILV5*, and *ILV3* genes in *ald6Δbat1Δ* strain (JHY431) led to a 20% increase in isobutanol production (72. 1 mg/L) compared with *ald6Δbat1Δ* containing empty vectors (JHY43-3) (Fig. 4.3). Additional expression of *LEU3Δ601* (JHY432) further increased isobutanol production up to 132. 5 mg/L (Fig. 4.3).

Production of isobutanol from 2-KIV involves two steps mediated by several KDCs and ADHs in *S. cerevisiae*. Among the four KDCs (Pdc1, Pdc5, Pdc6, and Aro10), Aro10 has been shown to have the highest affinity to branched-chain 2-keto acids [143]. On the other hand, among the six ADHs (Adh1, Adh2, Adh3, Adh4, Adh5 or Sfa1), Adh2 was shown to be most effective in isobutanol production [25]. Therefore, we also overexpressed *ARO10* and *ADH2* genes from the *TDH3* promoter by cloning the genes together into a pRS426GPD plasmid vector. The highest level of isobutanol production was achieved by overexpression of *ARO10* and *ADH2* in JHY432 strain (JHY433), resulting in final concentration of 146. 9 mg/L with a yield of 7.3 mg/g glucose at 48 h (Fig. 4.3).

Next, I measured isobutanol production in JHY433 strain in the presence of higher concentrations of glucose. In minimal medium containing 10% glucose, JHY433 strain produced up to 376.9 mg/L isobutanol, whereas wild type control (WT-3) produced only 53.1 mg/L (Fig. 4.4A). During the fermentation with 10% glucose, glucose was mostly consumed after 96 h and the carbons were mainly used

to produce ethanol in both WT-3 and JHY433 strains (Fig. 4.4B), suggesting that reducing ethanol production might be critical to further improve the isobutanol production yield.

4.4. Improvement of 3-methyl-1-butanol production in *S. cerevisiae*

The conversion of 2-KIV to 2-KIC an intermediate for the production of leucine and 3-methyl-1-butanol requires three sequential enzymatic steps involving Leu4, Leu1, and Leu2 (Fig. 4.1) [138]. In CEN.PK2-1C strain I used for isobutanol production, 3-methyl-1-butanol production via leucine biosynthetic pathway is inactivated, although it might not be completely inhibited. However, 3-methyl-1-butanol can be produced by the degradation of exogenous leucine in the minimal medium (83 mg/L) via Ehrlich pathway. Accordingly, JHY433 strain engineered for isobutanol production also showed a 3.6-fold increase in 3-methyl-1-butanol production (80.7 mg/L in minimal medium containing 100 g/L glucose) compared with wild type control (WT-3) (22.5 mg/L) after 96 h cultivation (Fig. 4.5).

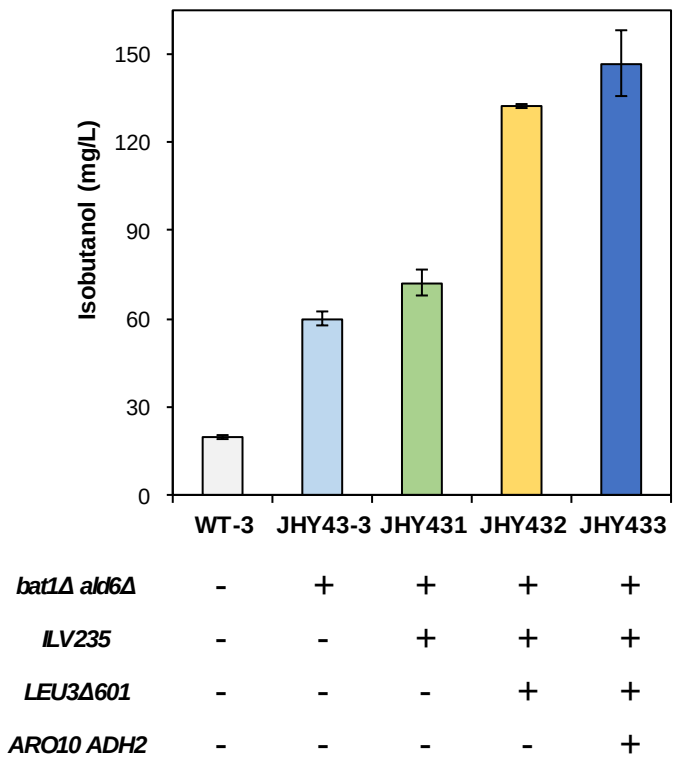

Figure 4.3 Isobutanol production in metabolically engineered yeast strains.

The effects of *bat1Δald6Δ*, and the overexpression of *LEU3Δ601, ILV2*, *ILV3*, *ILV5*, *ARO10*, and *ADH2* on isobutanol production were investigated in the indicated engineered strains. Empty vectors were transformed if necessary to grow all the strains in the same SC-His-Trp-Ura medium with 2% glucose. Isobutanol titers were measured after 48 h cultivation.

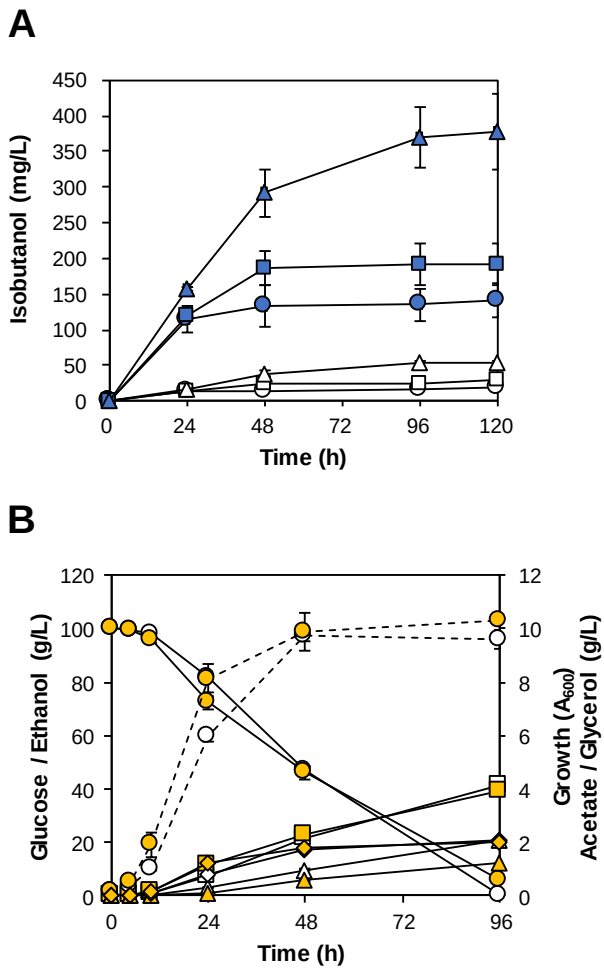

Figure 4.4 Metabolite profiles of JHY433 and WT-3 strains

A. Isobutanol production at various glucose concentrations. WT-3 (open symbol) and JHY433 (closed symbol) cells were grown in SC-His-Trp-Ura medium containing 2% (circle), 4% (square), and 10% (triangle) glucose.

B. Metabolite profiles of WT-3 (open symbol) and JHY433 (closed symbol) cells grown in SC-His-Trp-Ura medium containing 10% glucose. Cell growth (circle and dashed line) and concentrations of glucose (circle), ethanol (square), acetate (triangle), and glycerol (diamond) are shown.

To regenerate leucine biosynthetic pathway in CEN.PK2-1C strain, *LEU2* gene was introduced by transforming the cells with pRS425GPD plasmid containing *LEU2* gene as a selection marker. Although wild type cells containing pRS425GPD plasmid (WT-4) were grown in selective minimal medium lacking leucine (SC-His-Leu-Trp-Ura), 3-methyl-1-butanol titer (52.3 mg/L) was 2.3-fold higher than that of pRS425GPD-deficeint wild type cells (WT-3) grown in medium containing 83 mg/L leucine (SC-His-Trp-Ura). These data indicate that 3-methyl-1-butanol production via Leu biosynthetic pathway becomes functional in WT-4. Introduction of *LEU2* gene into JHY433 strain (JHY434) dramatically increased 3-methyl-1-butanol concentration up to 514.4 mg/L (Fig. 4.5). However, even with the increase in 3-methyl-1-butanol synthesis from 80.7 mg/L to 514.4 mg/L, JHY434 still produced similar level of isobutanol (386.0 mg/L) compared with JHY433 strain.

2-KIV is a common substrate for KDCs leading to isobutanol production and for Leu4 leading to 3-methyl-1-butanol production (Fig. 4.1). To induce the 2-KIV flux to 3-methyl-1-butanol production, genes involved in 2-KIC synthesis were overexpressed. Overexpressing *LEU4* in the JHY434 background (JHY435) increased 3-methyl-1-butanol titer to 577.0 mg/L, while reduced isobutanol titer to 331.5 mg/L, suggesting that the increase in Leu4 activity can compete with KDCs to increase the availability of 2-KIV for 3-methyl-1-butanol production (Fig. 4.5). Leu4 activity is regulated by free leucine, the final product of the biosynthetic pathway, through feedback inhibition [138]. It has been known that mutation of the key regulatory residue, Asp578, to Tyr makes Leu4 insensitive to the feedback inhibition

[144]. JHY436 strain overexpressing *LEU4*^{D578Y} instead of *LEU4* was more effective for 3-methyl-1-butanol production, exhibiting increased 3-methyl-1-butanol titer up to 765.7 mg/L with further decreased isobutanol production (294.5 mg/L) (Fig. 4.5). Since additional overexpression of *LEU1* exhibited a negative effect on 3-methyl-1-butanol production (Fig. 4.5), JHY436 showed the best performance for 3-methyl-1-butanol production among my engineered strains.

4.5. Conclusions

In this chapter, both strategies to increase the production of isobutanol and 3-mehtyl-1-butanol were used in *S. cerevisiae* via enhancing innate isobutanol and 3-methyl-1-butanol biosynthetic pathways. The transcription of endogenous genes in the valine and leucine biosynthetic pathways was increased by expressing Leu3Δ601, a constitutively active form of Leu3 transcriptional activator. For the production of isobutanol, JHY433 strain produced 376.9 mg/L isobutanol production from 100 g/L glucose by additionally overexpressing genes involved in isobutanol production (*ILV2*, *ILV3*, *ILV5*, *ARO10*, and *ADH2*) in *ald6Δbat1Δ* strain (JHY43) expressing *LEU3Δ601*. Since 2-KIV is a common intermediate for the production of isobutanol and 3-methyl-1-butanol, I tried to shift the flux of 2-KIV to 3-methyl-1-butanol production in the isobutanol-production strain by additional overexpression of genes involved in 2-KIC synthesis. The final JHY436 strain engineered for 3-methyl-1-

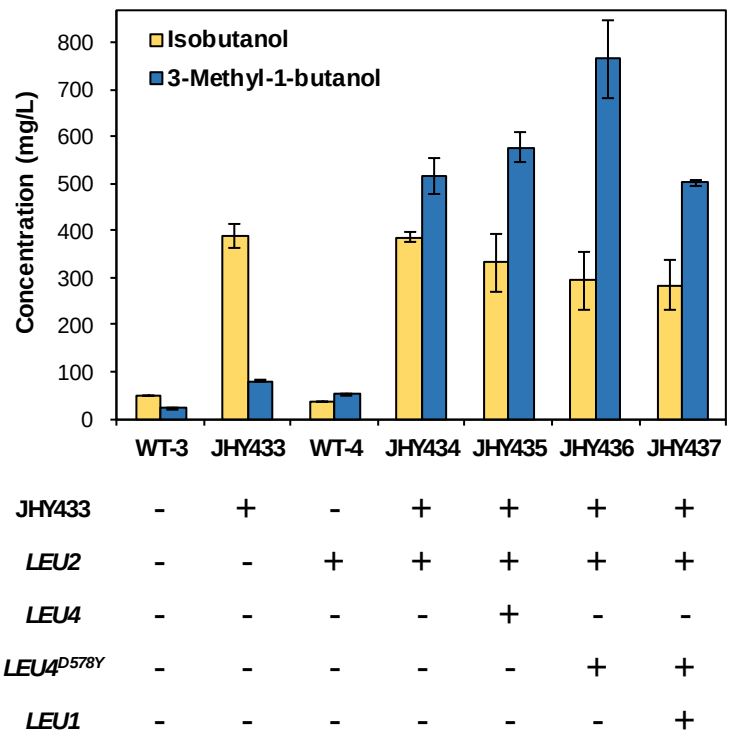

Figure 4.5 Improvement of 3-methyl-1-butanol production by overexpressing enzymes in leucine biosynthetic pathway

The effects of *LEU2, LEU4, LEU4*^{D578}*Y*, and *LEU1* overexpression on isobutanol and 3-methyl-1-butanol productions were detected in JHY433 background. WT-3 and JHY433 were grown in SC-His-Trp-Ura and other strains were grown in SC-His-Leu-Trp- Ura medium with 10% glucose for 96 h.

butanol production showed dramatic increase in 3-methyl-1-butanol titer (765.7 mg/L) compared with the starting wild type strain having *LEU2* mutation (WT-3) or wild type strain with reintroduced functional *LEU2* gene (WT-4).

Chapter 5.

Improvement of isobutanol production in *S. cerevisiae* by increasing mitochondrial import of pyruvate through mitochondrial pyruvate carrier

5.1. Introduction

S. cerevisiae can naturally produce small amounts of isobutanol from glucose [5]. Although several metabolic engineering efforts have been made to produce isobutanol in *S. cerevisiae*, the reported production levels are still low compared with those produced in bacteria [22,23,25,27,32,145,146]. Because isobutanol production pathway is subdivided by subcellular compartmentalization in *S. cerevisiae*, it is essential to transport intermediates across the membranes, which could be one of the bottlenecks in isobutanol production [23].

In *S. cerevisiae* cytosolic pyruvate generated by glycolysis is imported into the mitochondrial matrix by mitochondrial pyruvate carrier (MPC) (Fig. 5.1) [147,148] . Two molecules of pyruvate are converted into a 2-KIV by consecutive actions of Ilv2 (ALS), Ilv5 (KARI), and Ilv3 (DHAD) in the mitochondria, and 2-KIV is further converted into isobutanol in the cytoplasm by endogenous KDCs and ADHs in yeast (Fig. 5.1) [5]. 2-KIV is also used for the production of branched-chain amino acids including valine and leucine. Valine is generated from 2-KIV by mitochondrial branched-chain amino acid transferase (Bat1) (Fig. 5.1) [6,136]. On the other hands, 2-KIV is first converted to 2-isopropylmalate (2-IPM) by 2-isopropylmalate synthase (Leu4), followed by three enzymatic steps mediated by Leu1, Leu2, and Bat2 to produce leucine (Fig. 5.1) [138]. To overcome the limitations resulting from subcellular compartmentalization of isobutanol pathway enzymes in yeast, the whole biosynthetic pathway was relocated either to the cytoplasm by expressing

mitochondrial enzymes (Ilv2, Ilv3, and Ilv5) in the cytoplasm [25,27], or to the mitochondria by expressing cytosolic enzymes (KDCs and ADHs) in the mitochondria [23]. In a study comparing the effects of the two approaches, the mitochondrial pathway led to higher isobutanol production level than the cytosolic pathway [23].

In this chapter, isobutanol-production strain was further improved by deleting *LPD1*, encoding a subunit of pyruvate dehydrogenase (PDH) and by mitochondrial compartmentalization of the biosynthetic pathway based on previous studies [28]. The mitochondrial isobutanol production was further improved by increasing the transport of pyruvate from cytoplasm to the mitochondrial matrix by overexpressing MPC. Furthermore, isobutanol production was additionally improved by overexpressing genes related to iron-sulfur cluster assembly to increase in Ilv3 activity.

5.2. Disruption of competing pathways to increase isobutanol production

In my previous master's thesis, I improved isobutanol production by deleting *ALD6* encoding aldehyde dehydrogenase and *BAT1* encoding branched-chain amino acid aminotransferase, which are involved in oxidation of isobutyraldehyde and valine synthesis respectively competing with isobutanol production [149]. To further

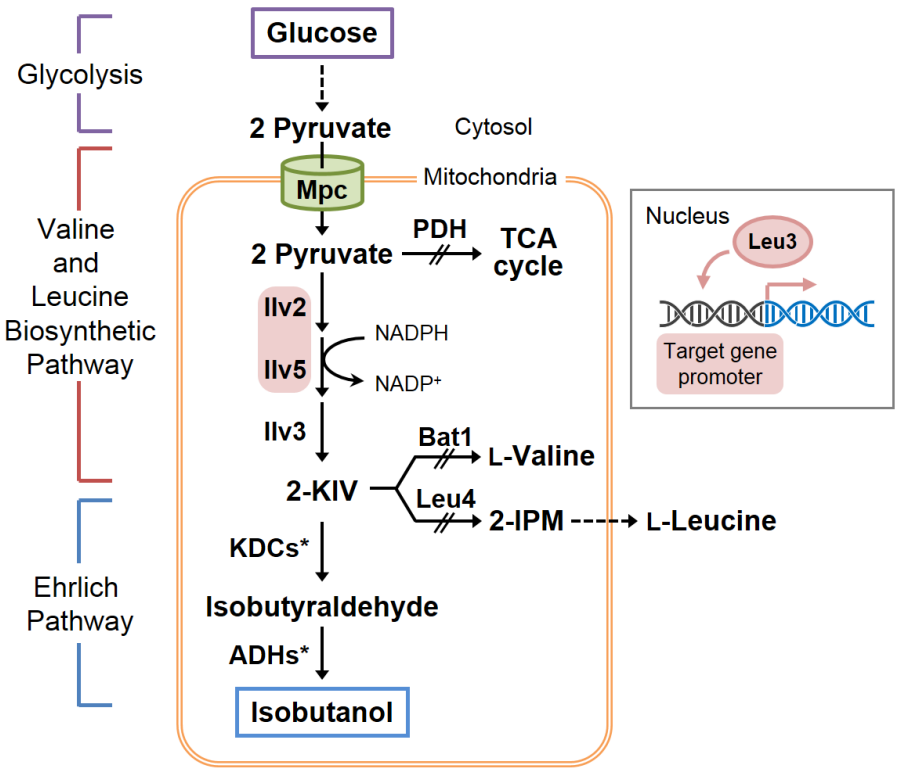

Figure 5.1 Biosynthetic pathways for isobutanol production from glucose in *S. cerevisiae* using in this chapter

Cytosolic pyruvate, produced by glycolysis, is imported into the mitochondria through mitochondrial pyruvate carrier (MPC) complex. Two molecules of mitochondrial pyruvate are converted to one molecule of isobutanol via 2-ketoisovalerate (2-KIV) and isobutyraldehyde by sequential actions of Ilv2 (acetolactate synthase), Ilv5 (ketol acid reductoisomerase), Ilv3 (dihydroxyacid dehydratase), 2-ketoacid decarboxylases (KDCs), and alcohol dehydrogenases (ADHs). Leu3 is a transcriptional activator of *ILV2*, *ILV5*, and *BAT1* genes. * indicates mitochondrial targetting expression. Dashed line indicates multiple enzymatic reactions.

improve isobutanol production in *bat1Δald6Δ* (JHY43) strain, genes involved in other competing pathways were additionally deleted. Pyruvate imported into the mitochondria is converted to acetyl-CoA by PDH complex and then used for production of ATP via TCA cycle (Fig. 5.1) [150]. In *S. cerevisiae*, PDH complex is encoded by five genes *PDB1*, *PDA1*, *LAT1*, *LPD1*, and *PDX1* [150], among which deletion of *LPD1* was shown to be most effective in increasing isobutanol production [28]. Therefore, I additionally deleted *LPD1* in JHY43, generating *bat1Δald6Δlpd1Δ* (JHY46) strain. In agreement with previous studies [149], JHY43 showed an increase in isobutanol production compared with wild type, and isobutanol production increased further in JHY46 even with reduced growth rate (Fig. 5.2). JHY46 produced 112.6 mg/L isobutanol after 48 h, indicating a 7.1- and 3.0- fold increase compared with WT (15.9 mg/L) and JHY43 (37.3 mg/L), respectively (Fig. 5.2).

In addition, the effect of deleting *LEU4* encoding 2-isopropylmalate (2-IPM) synthase, which is the first enzyme in the leucine biosynthetic branch from 2-KIV was tested [138]. The resulting *bat1Δald6Δleu4Δ* (JHY47) strain showed increased isobutanol production up to 53.5 mg/L compared with JHY43, indicating a positive effect of *LEU4* deletion in *bat1Δald6Δ* strain background (Fig. 5.2). Therefore, next *LEU4* and *LPD1* deletion was combined generating *bat1Δald6Δlpd1Δleu4Δ* (JHY48) strain. Although JHY48 produced 1.8-fold higher level of isobutanol than did JHY47, the final production level (95.3 mg/L) was lower than that of JHY46. Consequently, JHY46 showing the highest level of isobutanol production was chosen as a platform

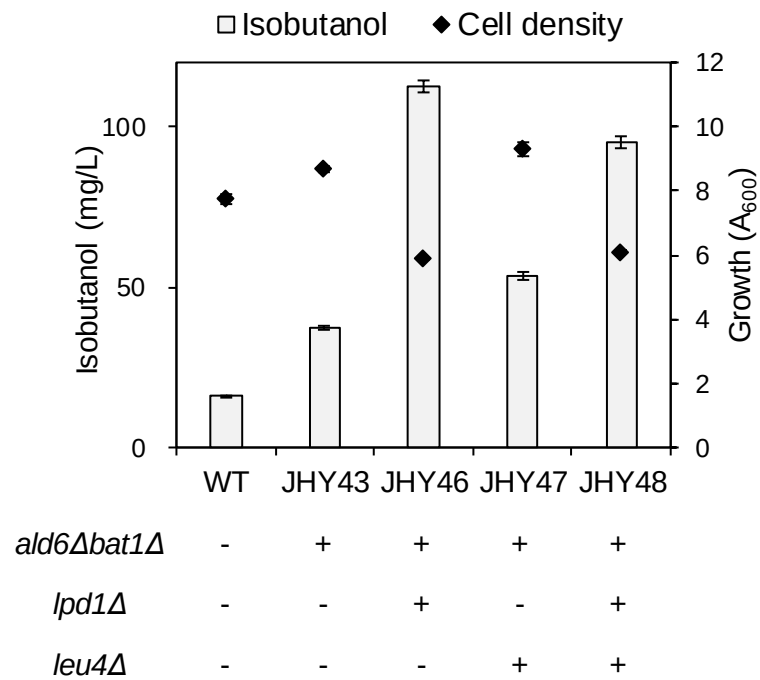

Figure 5.2 Improvement of isobutanol production by deleting genes in competing pathways

WT (CEN.PK2-1C), JHY43 (*ald6Δbat1Δ*), JHY46 (*ald6Δbat1Δlpd1Δ*), JHY47 (*ald6Δbat1Δleu4Δ*), and JHY48 (*ald6Δbat1Δlpd1Δleu4Δ*) cells were grown in SC medium containing 2 % glucose for 48 h. Each value indicates the average ± SD of triplicate experiments.

strain for the following metabolic engineering.

5.3. Overexpression of mitochondrially re-localized isobutanol biosynthetic pathways

To further increase isobutanol production genes involved in isobutanol production were overexpressed in JHY46 (*bat1Δald6Δlpd1Δ*) strain. Isobutanol biosynthesis from pyruvate requires six enzymes Ilv2, Ilv5, Ilv3, KDC, and ADH (Fig. 5.1) [5,8]. Previously, I overexpressed these enzymes in their natural compartments; Ilv2, Ilv5, and Ilv3 in the mitochondria and Aro10 (KDC) and Adh2 (ADH) in the cytoplasm [149]. In addition, *LEU3Δ601*, encoding a constitutively active form of Leu3 transcription factor for *ILV2* and *ILV5* [46], was also expressed to increase endogenous expression levels of Leu3 target genes [149]. By overexpressing these 6 genes in *bat1Δald6Δ* by co-transformation of three plasmids, including two high copy number plasmids 146.9 mg/L isobutanol was produced form 2% glucose [149]. In this study, to ensure more stable gene expression, a single multigene-expression plasmid containing all the required genes by using multiple cloning system was constructed [151]. The CEN/ARS-based low copy number plasmid pJIB1 consists of *ILV2*, *ILV3*, *ILV5*, *ARO10*, *ADH2*, and *LEU3Δ601* controlled by the strong constitutive promoter, P_{TDH3} or P_{TEF1} and terminator, T_{CYC1} (Table 3.3). The JHY46 strain harboring empty p413TEF vector (JHY46-1) produced 127.4 mg/L isobutanol, while JHY46 harboring pJIB plasmid (JHY461) produced up to 155.0 mg/L isobutanol in SC-His medium containing 2% glucose after 48 h (Fig. 5.3), showing

mild effect of gene overexpression. Although overexpressing isobutanol pathway enzymes in their natural compartments improved isobutanol titer this native pathway requires the transport of an intermediate, 2-KIV, from the mitochondria to the cytoplasm. It has been shown previously that construction of mitochondrial pathway by re-localization of cytosolic enzymes KDC and ADH into mitochondria could improve isobutanol production by overcoming such a limitation [23].

Therefore, I also developed mitochondrial pathway by expressing Aro10 and Adh2 in the mitochondria by tagging the proteins with N-terminal mitochondrial localization signal (MLS) of *COX4* [152], as described previously [23]. In pJIB2 plasmid *ARO10* and *ADH2* of pJIB1 were replaced with MLS-*ARO10* and MLS-*ADH2*. JHY46 harboring pJIB2 (JHY462) produced up to 185.7 mg/L isobutanol after 48 h, showing a 1.2-fold higher isobutanol titer than that produced in JHY461 (Fig. 5.3). These results suggest that confining Ehrlich pathway in mitochondria might lead to spatial concentration of intermediates and enzymes involved in isobutanol production, resulting in more efficient isobutanol production as demonstrated previously [23].

5.4. Enhancing mitochondrial pyruvate uptake by overexpressing mitochondrial pyruvate carrier (MPC)

Pyruvate is a critical intermediate for the isobutanol production. Especially, the size of mitochondrial pyruvate pool might be directly related to isobutanol titer produced

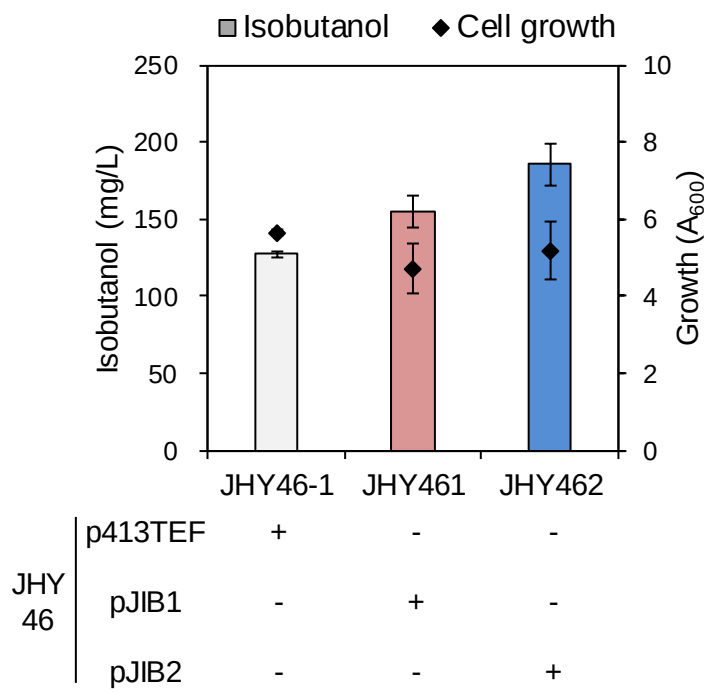

Figure 5.3 Improvement of isobutanol production by overexpressing genes involved in isobutanol biosynthetic pathway

JHY46-1 (*ald6Δbat1Δlpd1Δ* [EV]), JHY461 (*ald6Δbat1Δlpd1Δ* [JIB1]), and JHY462 (*ald6Δbat1Δlpd1Δ* [JIB2]) cells were grown in SC-His medium containing 2 % glucose for 48 h. Each value indicates the average ± SD of triplicate experiments.

via mitochondrial isobutanol biosynthetic pathway. In yeast, cytosolic pyruvate is considered to cross the mitochondrial outer membrane through a kind of porins, the voltage-dependent anion channel (VDAC) [153]. The mitochondrial pyruvate carrier (MPC) in the mitochondrial inner membrane is responsible for the transport of pyruvate into the mitochondrial matrix (Fig. 5.4A) [147,148]. *S. cerevisiae* has three homologous MPC subunit proteins, Mpc1, Mpc2, and Mpc3, which generate two types of hetero-oligomeric complex [147,148]. The low-affinity MPC_{FERM} is composed of Mpc1 and Mpc2, whereas the high-affinity MPC_{OX} is composed Mpc1 and Mpc3 (Fig. 5.4A) [154]. The common subunit Mpc1 is expressed regardless of the carbon source, but Mpc2 and Mpc3 are expressed under fermentative and respiratory conditions, respectively, leading to differential expression levels of MPC_{FERM} and MPC_{OX}, and subsequent differential pyruvate flux to the mitochondria, depending on the carbon metabolic conditions [154].

To further improve isobutanol production in the mitochondria, the effects of overexpressing MPC_{FERM} or MPC_{OX} was investigated in JHY462 strain. *MPC1*, MPC_{FERM} (*MPC1* and *MPC2*) or MPC_{OX} (*MPC1* and *MPC3*) genes were additionally cloned into pJIB2, generating plasmids pJIB3, pJIB4, and pJIB5 respectively (Table 3.3). JHY46 strain harboring pJIB3 (JHY463) showed improved isobutanol production up to 265.5 mg/L compared with JHY462, indicating that overexpression of *MPC1* alone can contribute to isobutanol production in mitochondria (Fig. 5.4B). Overexpression of MPC_{FERM} (JHY464) also improved isobutanol production, but to a lesser extent than the overexpression of *MPC1*. Cells overexpressing MPC_{OX}

(JHY465) showed the highest level of isobutanol production, reaching 330.9 mg/L which is a 1.9-fold higher level than that produced in JHY462. Taken together, mitochondrial isobutanol production could be successfully improved by increasing mitochondrial pyruvate pool via overexpressing MPC, especially in the form of MPC_{OX}.

Compared to wild type control strain harboring empty vector (WT-1), the engineered strain JHY465 showed reduced glucose uptake rate and lower final cell density, whereas producing about 22-fold higher level of isobutanol (Fig. 5.5). Glycerol production also increased up to 1.63 g/L in JHY465 compared to WT-1 (0.38 g/L). Inhibition of TCA cycle pathway by *LPD1* deletion might be mainly responsible for the growth phenotype of JHY465. The consumed glucose was mostly used to produce ethanol in both WT-1 and JHY465 producing similar levels of ethanol suggesting that the overexpressed MPC_{OX} might redirect only minor part of cytosolic pyruvate to the mitochondria (Fig. 5.4A). WT-1 strain consumed glucose faster than JHY465 (Fig. 5.5). The glucose was mainly used to produce ethanol in both WT-1 and JHY465 strains (Fig. 5.5).

5.5. Enhancing isobutanol production in by overexpressing the basic elements of Iron-Sulfur cluster assembly

To further improved mitochondrial isobutanol biosynthetic pathway, genes involved in iron-sulfur cluster assembly were additionally overexpressed.

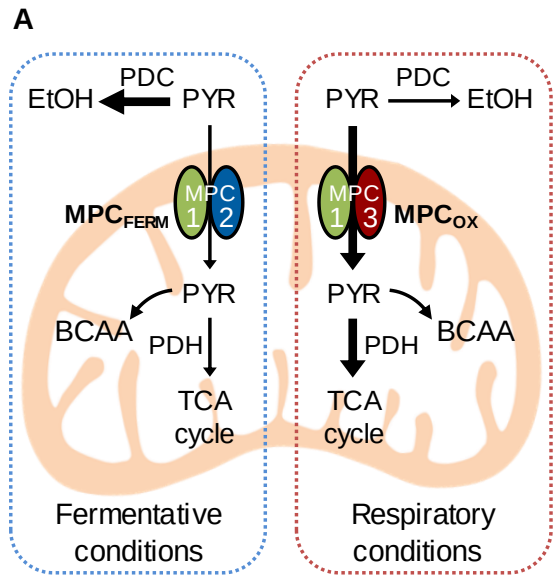
A
PDC
EtOH
PYR
PYR
PDC
EtOH
MPC 1 2
MPC$_{FERM}$
MPC 1 3
MPC$_{OX}$
PYR
PYR
BCAA
PDH
PDH
BCAA
TCA cycle
TCA cycle
Fermentative conditions
Respiratory conditions

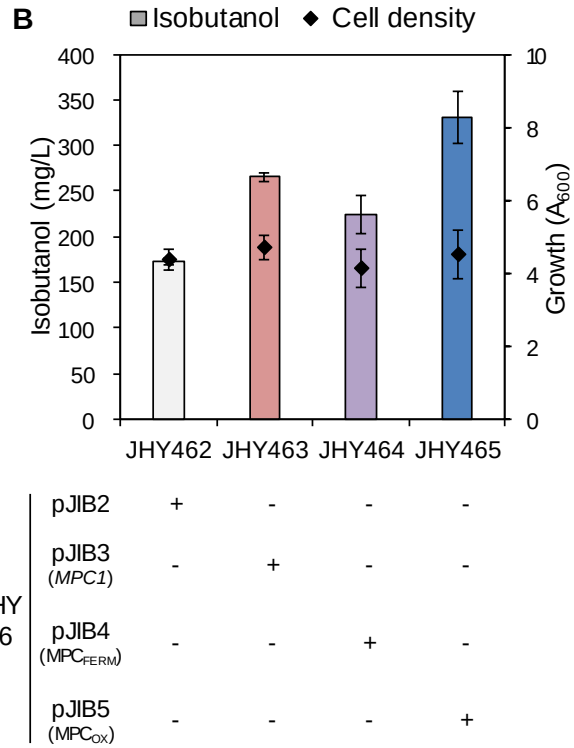
B
Isobutanol
Cell density
Isobutanol (mg/L)
Growth (A_{600})
400
350
300
250
200
150
100
50
0
10
8
6
4
2
0
JHY462 JHY463 JHY464 JHY465
JHY 46
pJIB2 + - - -
pJIB3 (*MPC1*) - + - -
pJIB4 (MPC$_{FERM}$) - - + -
pJIB5 (MPC$_{OX}$) - - - +

Figure 5.4 Effects of overexpressing different forms of MPC complex on isobutanol production

A. Roles of MPC in mitochondrial pyruvate transport. Under fermentative conditions, the low-activity MPC_{FERM}, composed of Mpc1 and Mpc2, is expressed and competing for cytosolic pyruvate with pyruvate decarboxylase (PDC). Most of the pyruvate is left in the cytosol and is finally converted to ethanol by PDC. On the other hand, under respiratory conditions, the high-activity MPC_{OX}, composed of Mpc1 and Mpc3, is expressed, whereas PDC is downregulated. Consequently, pyruvate is efficiently transported to the mitochondrial matrix and then enters the TCA cycle via pyruvate dehydrogenase (PDH). EtOH, ethanol; PYR, pyruvate; BCAA, branched chain amino acid.

B. JHY462 (*ald6Δbat1Δlpd1Δ* [JIB2]), JHY463 (*ald6Δbat1Δlpd1Δ* [JIB3]), JHY464 (*ald6Δbat1Δlpd1Δ* [JIB4]), and JHY465 (*ald6Δbat1Δlpd1Δ* [JIB5]) were grown in SC-His medium containing 2 % glucose for 48 h. Each value indicates the average ± SD of triplicate experiments.

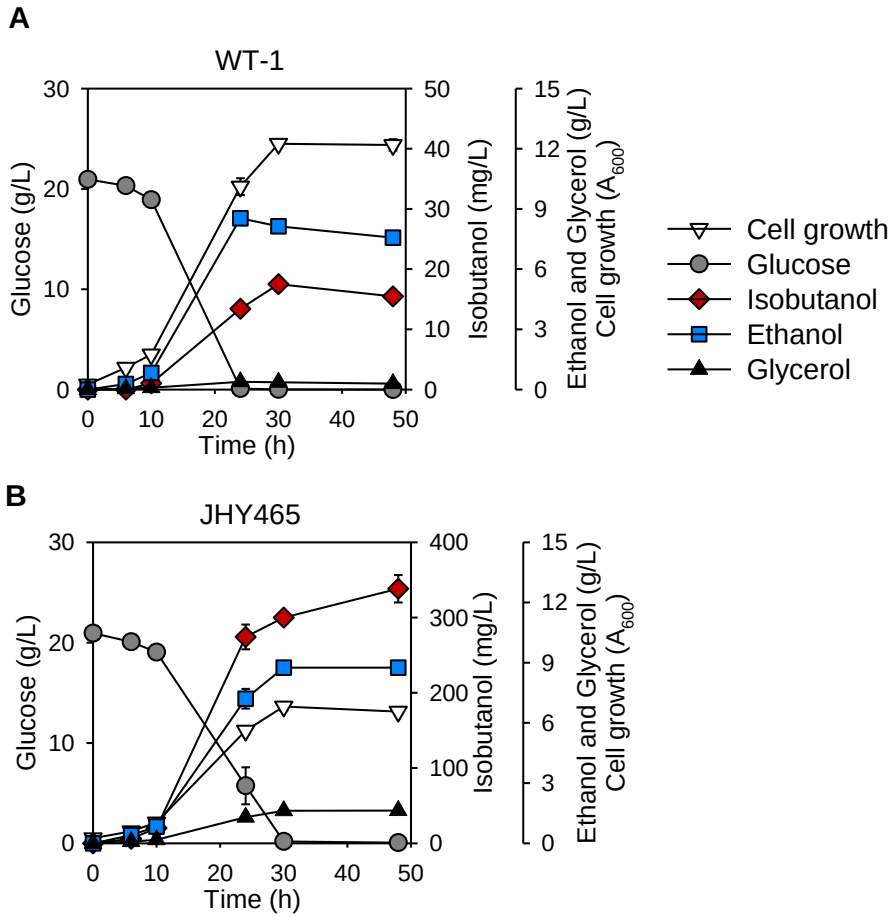

Figure 5.5 Metabolite profiles of JHY465 and WT-1 strains

A. JHY465 (*ald6Δbat1Δlpd1Δ* [JIB5]) was grown in 9 ml of SC-His medium containing 2 % glucose.

B. WT-1 (WT [EV]) was grown in 9 ml of SC-His medium containing 2 % glucose. Each value indicates the average ± SD of triplicate experiments.

Dihyroxyacid dehydratase (*ILV3*) involved in valine catabolism is iron-sulfur (Fe-S) dependent protein that needs Fe-S cluster (ISC) for its activation. In yeast, ISC assembly occurs in mitochondria, which involves an iron donor, a sulfur donor, and a scaffold. The iron is delivered by Yfh1 (iron chaperone) and the sulfur is donated by Nfs1 (cysteine desulfurase) onto the scaffold protein Isu1 [155].

To further improve isobutanol production in the mitochondria, effects of overexpressing genes involved in ISC assembly was investigated the in JHY465 strain. JHY465 strain harboring pJIB5 and pJIBNI (JHY465-2) showed the highest level of isobutanol production up to 435.2 mg/L compared with JHY465-1, indicating that overexpression of *NFS1* and *ISD11* can contribute to isobutanol production via increasing Ilv3 activity (Fig. 5.6). Overexpression of *ISU1* (JHY465-3) also improved isobutanol production, but to a lesser extent than the overexpression of *NFS1* and *ISD11* (Fig. 5.6). On the other hand, additional overexpression of *YFH1* with *NFS1, ISD11,* and *ISU1* (JHY435-5) decrease the isobutanol production (327.4 mg/L) (Fig. 5.6). Therefore, to increase of isobutanol production using mitochondrial pathway sulfur donor pool is important and overexpressing Nfs1 and Isd11 especially, was effective in enhancing Ilv3 activity resulting in increasing isobutanol production.

5.6. Conclusions

In summary, isobutanol production was improved by deleting competing pathway

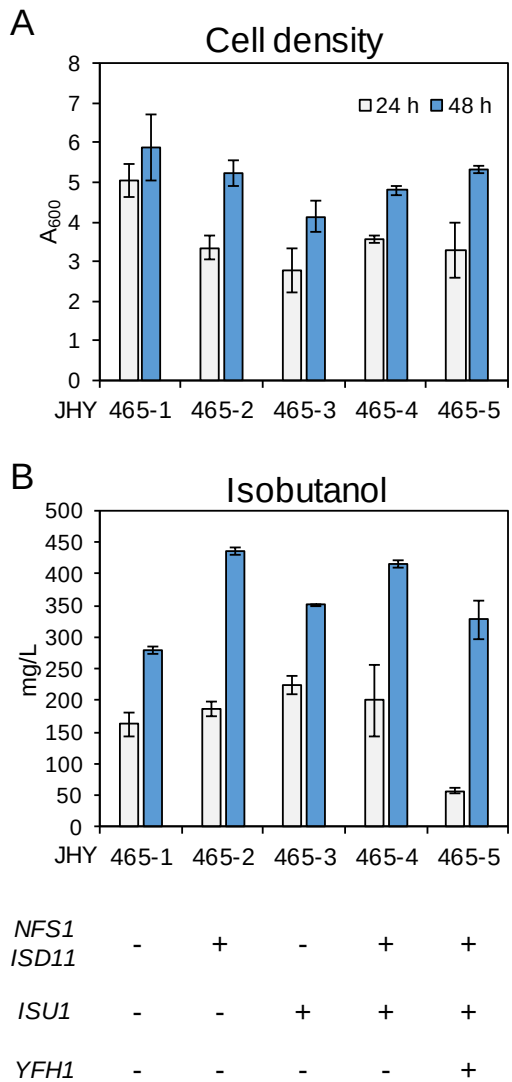

Figure 5.6 Effects of overexpressing genes involved in iron-sulfur cluster assembly machinery on isobutanol production

JHY465-1 (*ald6Δbat1Δlpd1Δ* [JIB5, ev]), JHY465-2 (*ald6Δbat1Δlpd1Δ* [JIB5, JIBNI]), JHY465-3 (*ald6Δbat1Δlpd1Δ* [JIB5, JIBI]), JHY465-4 (*ald6Δbat1Δlpd1Δ* [JIB5, JIBNII]), and JHY465-5 (*ald6Δbat1Δlpd1Δ* [JIB5, JIBISC]), cells were grown in SC-His, Trp medium containing 2 % glucose for 48 h. (A) Cell growth. (B) Isobutanol production. Each value indicates the average ± SD of triplicate experiments.

enzymes (Bat1, Ald6, and Lpd1) overexpressing all biosynthetic enzymes (Ilv2, Ilv5, Ilv3, Aro10, and Adh2) in the mitochondria by re-locating Aro10 and Adh2 into the mitochondria, and overexpressing a constitutively active transcription factor, Leu3Δ601. Also, isobutanol production was more improved via mitochondrial pathway by increasing mitochondrial uptake of pyruvate through MPC. In this chapter the effects of overexpressing Mpc1, MPC_{FERM} (Mpc1 and Mpc2) or MPC_{OX} (Mpc1 and Mpc3) were compared on mitochondrial isobutanol production. Taken together, my final engineered strain JHY465 with improved mitochondrial pyruvate transport showed a significant increase in isobutanol titer (338.3 mg/L). Furthermore, additionally overexpressing genes cysteine desulfurase (Nfs1 and Isd11) related to iron-sulfur cluster assembly to increase in Ilv3 activity improved isobutanol production reaching at 435.2 mg/L, compared with the wild type strain and previous reports [23,28].

Chapter 6.

Development of multi-copy genome integration system with overexpressing α-acetolactate synthase-inducible phenotypic screening for isobutanol production in *S. cerevisiae*

6.1. Introduction

Unlike bacteria, the isobutanol production pathway in yeast is subdivided by mitochondria (Fig. 6.1). In *S. cerevisiae*, cytosolic pyruvate is imported to mitochondria by mitochondrial pyruvate carrier (MPC) complex and then pyruvate is condensed to 2-KIV by sequential catalytic reaction of Ilv2 (ALS), Ilv5 (KARI), and Ilv3 (DHAD) in mitochondrial matrix [5,147,148]. The mitochondrial 2-KIV is exported to cytosol and then finally converted to isobutanol through Ehrlich pathway, involving endogenous KDCs and ADHs. Therefore, in order to increase isobutanol production in *S. cerevisiae,e* subcellular compartmentalization of valine biosynthetic enzymes is one of the limiting factors. To overcome this limitation, isobutanol biosynthetic pathway is reconstructed to two different pathways; relocalization of whole isobutanol biosynthetic pathway to cytoplasm by expressing mitochondrial enzymes (Ilv2, Ilv3, and Ilv5) or to mitochondrial matrix by expressing cytosolic enzymes (KDCs and ADHs) into mitochondria. In the mitochondrial pathway, despite overexpression of the MPC complex to increase mitochondrial pyruvate, a large amount of pyruvate still existed in the cytoplasm and was used for ethanol production. Therefore, transport of cytosolic pyruvate to mitochondria is still a limiting factor in isobutanol production via mitochondrial isobutanol biosynthetic pathway.

In *S. cerevisiae*, based on the knowledge accumulated, various tools have been developed for application to metabolic engineering, such as gene expression system,

promoter and terminator engineering, and multiple copies integration system [110]. Introducing engineered metabolic pathway into *S. cerevisiae* via genes expression based on plasmid is convenient and easy to use, but using multiple copies of yeast replicating or centromeric plasmids can be burden to maintain simultaneously in a single cell and also in order to maintain the plasmids, a specific medium must be used [156,157]. Therefore, integration of the genes into chromosome is needed for securing long-term stability of gene expression. In *S. cerevisiae*, since homologous recombination worked efficiently, genome integration methods using it are well established. In order to effectively introduce the metabolic pathway into the yeast by integration of genes into genome, it is required that easy of gene integration, stability of the insertion, multiple integration, and effective strain selection method. Therefore, it is of great interest to construct novel methods for quickly integrating multi-copy number of genes at once and selecting the desired strain precisely. In *S. cerevisiae*, delta-integration using and rDNA integration using delta or rDNA repeat sites with about 100 copies in yeast, respectively, are one of the methods that enable the multiple copy integration [73,158]. Recently, researches using delta-integration have been carried out for engineering the metabolic pathway by introducing large amounts of genes into the chromosome coupled with the antibiotic selection method or the CRSPR-Cas9 system in yeast [24,75,159].

In this chapter, I developed *S. cerevisiae* strain with enhancing isobutanol production by construct of artificial cytosolic isobutanol biosynthetic pathway via exploiting multi-copy delta- and rDNA-integration of related genes (Fig. 6.1). In

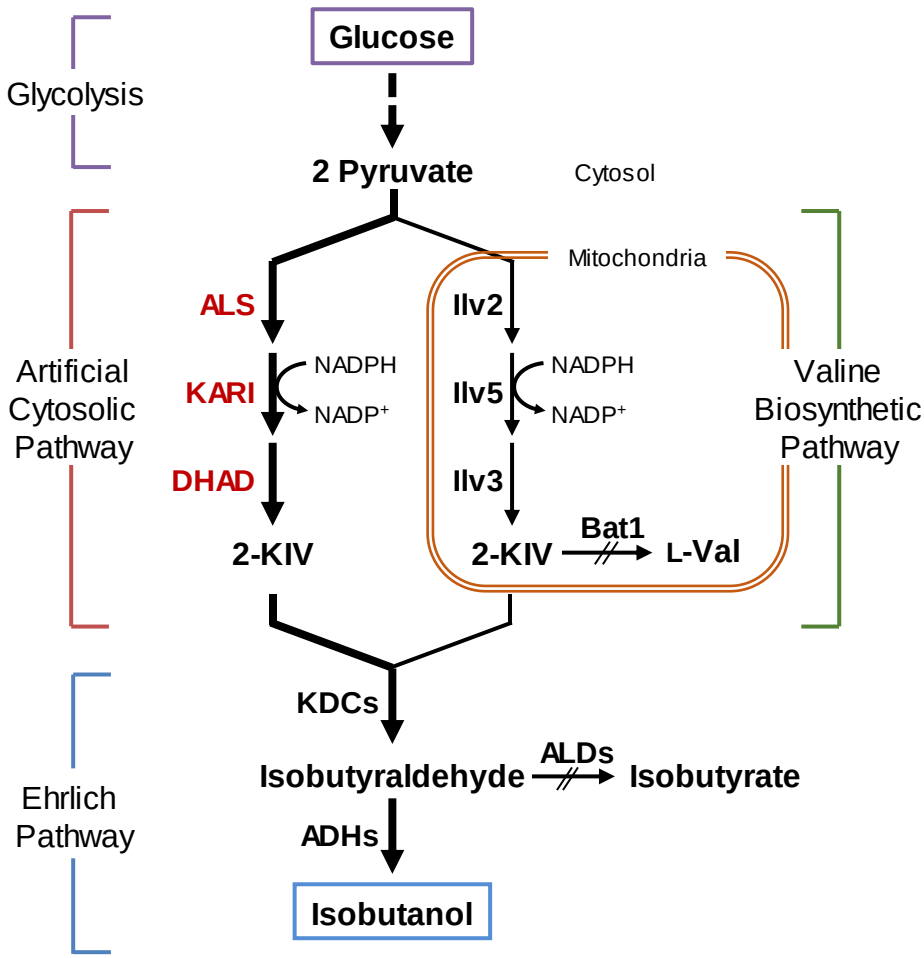

Figure 6.1 Schematic illustration of construction of artificial cytosolic isobutanol biosynthetic pathway.

Pyruvate is converted to 2-ketoisovalerate (2-KIV) by sequential catalytic reaction of α-acetolactate synthase (ALS), ketolacid reductoisomerase (KARI), and dihydroxyacid dehydratase (DHAD), and then 2-KIV can converted to isobutanol by 2-ketoacid decarboxylase (KDCs) and alcohol dehydrogenase (ADH). Deleted gene is indicated by double slash (//) and dashed line indicate multiple enzymatic actions.

yeast library obtained using the two integration methods, to select suitable strain, I constructed a new selection method using the characteristics of alsS from bacteria as well as applying the antibiotic selection method (Fig. 6.2). Moreover, overexpressing cytosolic Ilv5 and Ilv3 with the addition of kozak sequence to the enzymes, KDC (kivd) from *L. lactis*, and ADH (Adh2) further increased the production of isobutanol.

6.2. Construction of cytosolic isobutanol biosynthetic pathway in *S. cerevisiae*

S. cerevisiae naturally produces small amount of the isobutanol via an innate pathway, which is compartmentalized by mitochondria, but the titer is very small (Fig. 6.1). In innate isobutanol synthetic pathway in *S. cerevisiae*, pyruvate synthesized via glycolysis is entered into mitochondria and is converted to 2-KIV by α-acetolactate synthase (ALS), ketolacid reductoisomerase (KARI), and dihydroxyacid dehydratase (DHAD), encoded in *ILV2*, *ILV5*, and *ILV3*, respectively, via the valine biosynthetic pathway (Fig. 6.1). Subsequently, 2-KIV is released into the cytoplasm and is converted to isobutanol along the Ehrlich pathway (Fig. 6.1)[5]. To increase production of isobutanol, sufficient pyruvate should be introduced into the mitochondria, but pyruvate is mainly used to make ethanol from the cytoplasm in most cultured conditions. To overcome this compartmentalization problem in isobutanol production, some attempts have been made to re-locate the valine biosynthesis enzymes Ilv2, Ilv5, and Ilv3 from the mitochondria into the cytoplasm

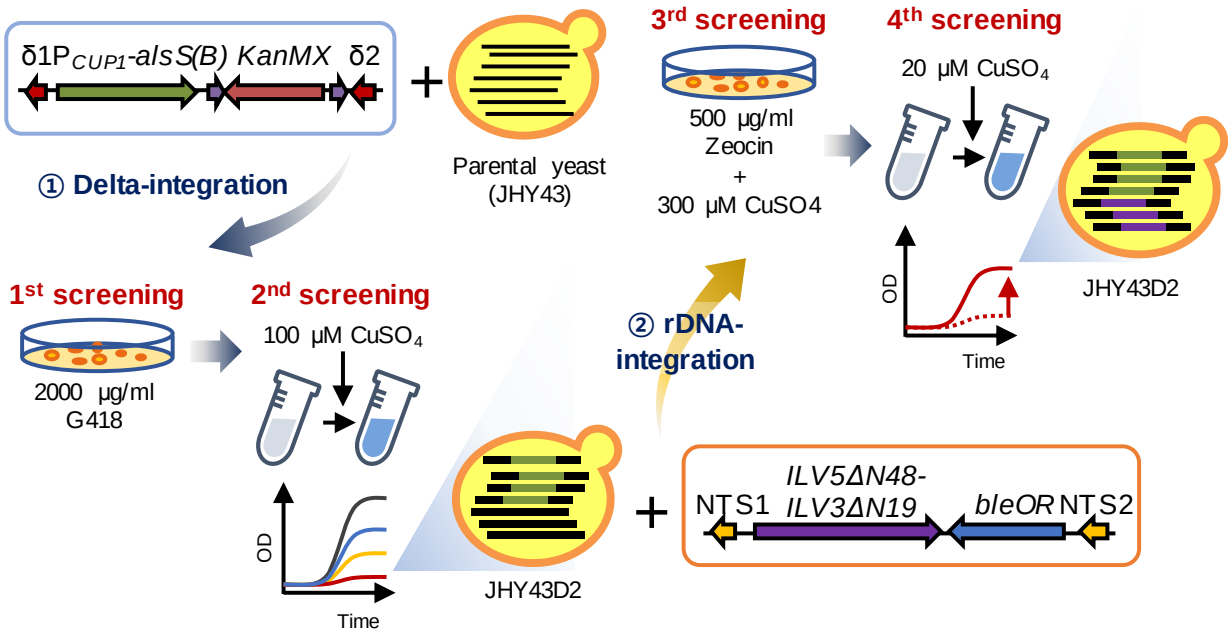

Figure 6.2 Schematic diagram of the overall concept of this chapter

Experimental design to construction of cytosolic isobutanol biosynthetic pathway by assembling multi-copy genes into yeast genome via delta integration and rDNA integration.

by construction of N-terminally truncated Ilv2, Ilv5, and Ilv3 resulting in production of mutant enzymes with lacking of the mitochondrial targeting sequence [25]. This cytosolic pathway has been successfully adopted to produce isobutanol in *S. cerevisiae* in previous studies.

Therefore to introduction of artificial cytosolic isobutanol biosynthetic pathway into *S. cerevisiae,* I also constructed llv2, Ilv5, and Ilv3 N-terminally truncated mutant, *ILV2*ΔN54, *ILV5ΔN48,* and *ILV3ΔN19* following the previous study and cloned into p413GPD, p414GPD, p416GPD plasmid, generating p413GPD-*ILV2*ΔN54 p,414GPD-*ILV5ΔN48*, and p416GPD-ILV6N19 controlled by strong constitutive promoter, P_{TDH3}. Furthermore, the *alsS* genes from *B. subtilis* and *L. lactis* bacteria and *alsS* (*B. subtilis*) and *alsS* (*L. lactis*) were cloned into p413ADH plasmid and p413GPD, resulting in constructing p413ADH-alsS(B) and p413GPD-alsS(L), respectively.

To verify the effect of introducing cytosolic isobutanol pathway into *S. cerevisiae*, *bat1Δald6Δ* strain (JHY43) as parental strain, which was strain with disruption of competing pathways, consisting of branched-chain amino acid aminotransferase (*BAT1*) and aldehyde dehydrogenase (*ALD6*), which is involved in valine biosynthesis from 2-KIV and oxidation of isobutyraldehyde via Ehrlich pathway, respectively, was used and also increased isobutanol production at 61.2 mg/L, in my previous study. Three strains with commonly *ILV5* as KARI and *ILV3* as DHAD were prepared by introducing three different ALS, *ILV2*ΔN54 (*S. cerevisiae*), *alsS* (*B. subtilis*), and *alsS* (*L. lactis*). The *bat1Δald6Δ* strain harboring

p413GPD-*ILV2ΔN54*, p414GPD-*ILV5ΔN48*, and p416GPD-*ILV3ΔN19* plasmids (JHY4306) produced 71.8 mg/L isobutanol resulting in 1.2-fold increasing compared with JHY43 (Figure 2A). JHY4307 strain, *bat1Δald6Δ* strain harboring p413ADH-alsS(B), p414GPD-*ILV5ΔN48*, and p416GPD-*ILV3ΔN19* plasmids, produced 75.5 mg/L isobutanol after 48-cultivation (Figure 2A). On the other hand, JHY43 strain harboring p413GPD-alsS(L), p414GPD-*ILV5ΔN48*, and p416GPD-*ILV3ΔN19* plasmids (JHY4303) showed improved isobutanol production up to 96.6 mg/L, which is about 35 % and 28 % higher level than produced in JHY4301 and JHY4302, respectively (Fig. 6.3).

It is believed that the deficiency of cell growth in JHY4303 strain induced by overexpression of alsS from *L. lactis* under control of strong promoter, P_{TDH3} was associated with the enzyme activity of alsS (Fig. 6.3). In the case of expression of alsS derived from *B. subtilis* using the strong promoter $P_{TDH3,}$ no transformant could be obtained and thus alsS (*B. subtilis*) had to be expressed using a relatively weak promoter, P_{ADH1} compared with P_{TDH3}. This result indicates that alsS (*B. subtilis*) is more active than alsS (*L. lactis*).

6.3. Increase in isobutanol production by introducing a kozak sequence into ketol-acid reductoisomerase and dihydroxy-acid dehydratase.

In order to increase the production of isobutanol, the activity of alsS, the first gene

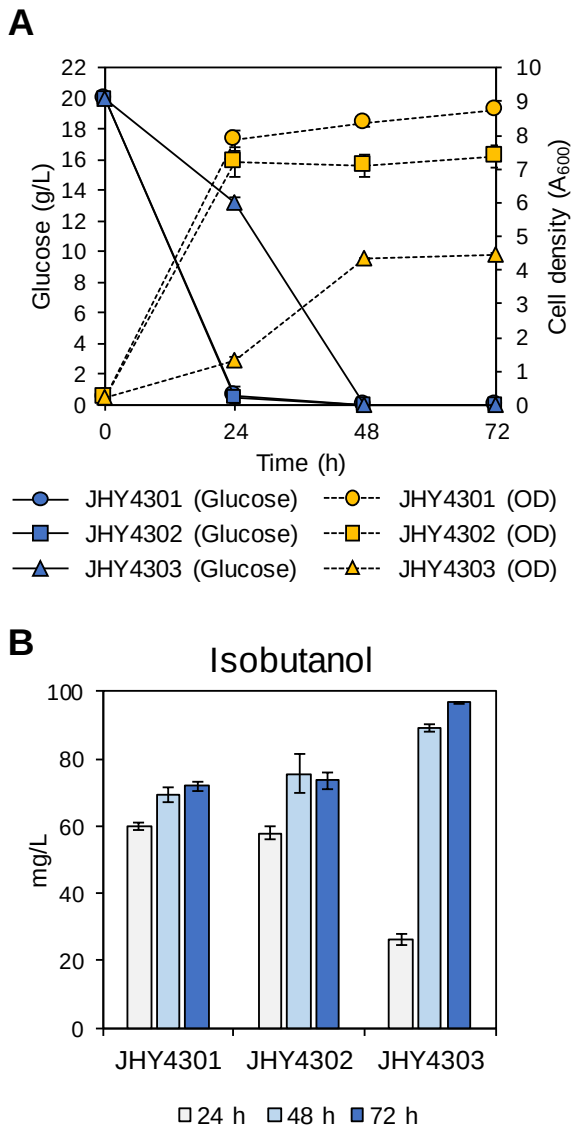

Figure 6.3 Effect of overexpression of a-acetolactate synthases (ALSs) from various microorganisms in *S. cerevisiae*

All cells were grown in SC-His, Trp, Ura medium containing 2 % glucose for 72 h. (A) Cell growth and glucose consumprion. (B) Isobutanol production. Each value indicates the average ± SD of triplicate experiments.

involved in isobutanol biosynthesis, is important factor. Overexpression of *alsS* is indispensable for the increase of isobutanol production, but there is a major drawback that cells overexpressing *alsS* with a strong promoter do not grow well. One of the causes of this inhibition of cell growth inhibition is the insufficient level of expression of the supporting enzymes. In a study in which 2,3-butanndiol was produced by overexpressing the same *alsS* (*B. subtilis*) in yeast, no inhibition of cell growth by *alsS* expression was observed, suggesting that the enzyme activity of α-acetolactate decarboxylase, alsD, which is the enzymes involved in the reactions following the reaction of alsS, is sufficient [124]. Therefore, it was expected that inhibition of cell growth in *alsS* overexpressing strain would be alleviated, and also isobutanol production would be increased by increasing the levels of *ILV5* and *ILV3* enzymes.

Although Ilv3 and Ilv5 as GPD promoters, P_{TDH3} known to be sufficiently strong in *S. cerevisiae*, were expressed it was tried to more increase the level of protein expression by improving translational efficiency. As a method for increasing the efficiency of enzyme translation of both genes, kozak sequence was introduced into upstream of start codon of genes. In eukaryotes including *S. cerevisiae*, 5' untranslated region (5'-UTR) plays an important role in initiation of translation, especially a 5'-UTR rich in adenine, which occupies from start codon to -6 position, is conserved in *S. cerevisiae* and this consensus sequence is called the kozak sequence [160,161]. There are several studies that the level of protein expression is increased by introducing the kozak sequence upstream of the start codon [162-164].

Therefore, five adenine sequences were introduced in front of the start codon (AAAAAATG) to increase the expression level of the *ILV5ΔN48* and *ILV3ΔN19* genes.

The effect was confirmed about introducing kozak sequence into *ILV5ΔN48* and *ILV3ΔN19* for producing isobutanol by transformation of p414GPD-*ILV5ΔN48*(K) and/or p416GPD-*ILV3ΔN19*(K) plasmids into JHY43 strain harboring p413GPD-alsS(L). The strain JHY4304, JHY43 strain harboring p413GPD-alsS(L), p414GPD-*ILV5ΔN48*(K), and p416GPD-*ILV3ΔN19* plasmids, produced 111.2 mg/L of isobutanol which was higher production compared with isobutanol production in JHY4303 with *ILV5ΔN48* and *ILV3ΔN19* without kozak sequences (Fig. 6.4). Also overexpression of alsS (*L. lactis*), *ILV5ΔN48*, and *ILV3ΔN19* with kozak sequence (K-*ILV3ΔN19*) in *bat1Δald6Δ* strain (JHY4305) led to a 2.6 % increase in isobutanol production (99.2 mg/L) compared with JHY4303 strain (Fig. 6.4). Moreover, the JHY4306 strain overexpressing K-*ILV5ΔN48* and K-*ILV3ΔN19* instead of *ILV5ΔN48* and *ILV3ΔN19* was more effective for the production of isobutanol exhibiting increased isobutanol titer up to 133.9 mg/L with further higher final cell density and faster glucose consumption rate compared to JHY4303 strain (Fig. 6.4).

6.4. Enhancing isobutanol production by overexpression of alsS from *B. subtilis* using copper inducible promoter P_{CUP1}

According to previous experimental results it would be expected that *alsS* from *B.*

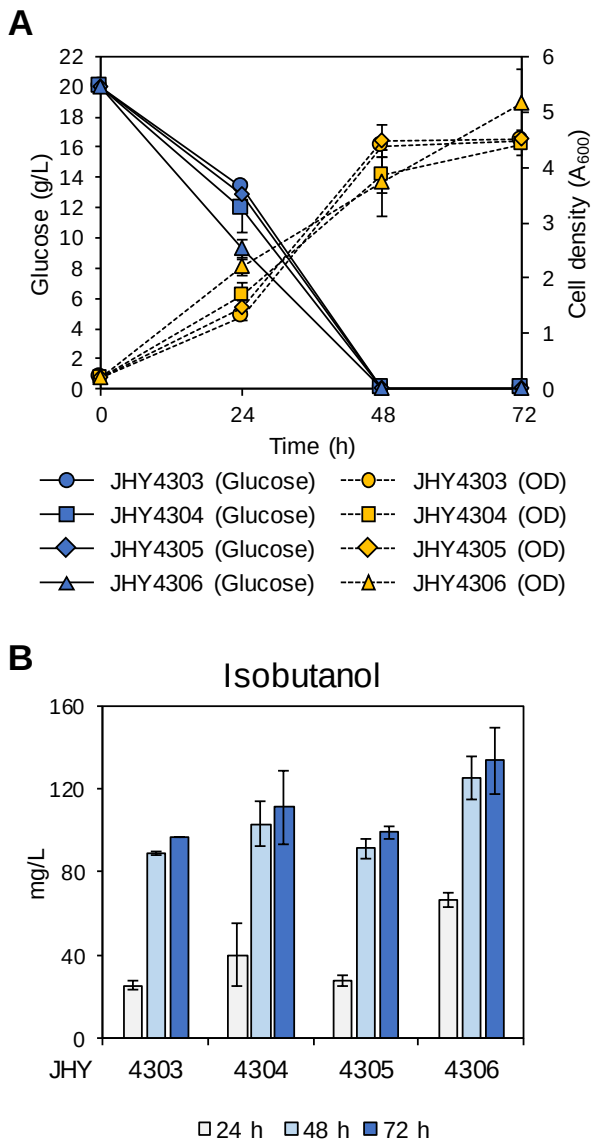

Figure 6.4 Effect of introduction of kozak sequence into KARI and DHAD

All cells were grown in SC-His, Trp, Ura medium containing 2 % glucose for 72 h. (A) Cell growth and glucose consumprion. (B) Isobutanol production. Each value indicates the average ± SD of triplicate experiments.

subtilis (alsS (B)) is more active than alsS from *L. lactis* (alsS (L)). However, *alsS* (B) could not expressed by using a strong promoter because of cell death. Therefore, it was assumed that overexpressing *alsS* (B) controlled by inducible promoter might be possible to increase cell growth and isobutanol production by overexpressing the gene at a specific time point. There are several inducible promoter in *S. cerevisiae* and copper inducible promoter, P_{CUP1}, was chosen to expression of *alsS* (B). The expression of *CUP1* gene encoding metallothionein is induced in presence of copper ions in the cell by the binding of the transcriptional activator Ace1 to the upstream region (promoter) of the *CUP1* gene [165-167]. To construct a plasmid containing the promoter of *CUP1* gene (P_{CUP1}) promoter part, P_{ADH1}, in p413ADH-alsS(B) plasmid was replaced with promoter of *CUP1* gene, P_{CUP1}, resulting in generation of p413CUP1-alsS(B) plasmid.

To prove the effect of expressing *alsS* (B) controlled by P_{CUP1}, I performed transformation of p413GPD-alsS(L) or p413CUP1-alsS(B) plasmids into JHY43 strain harboring p414GPD-*ILV5ΔN48*(K) and p416GPD-*ILV3ΔN19* plasmids. All cells were cultured for 7h and then $CuSO_4$ used as a copper induction chemical was treated into culture medium at a concentration of 100 μM. A JHY4307 strain overexpressing *alsS* (B) under control of P_{CUP1} produced isobutanol at 54.2 mg /L, which is similar to the production of isobutanol in the control strain JHY43 without copper induction (Fig. 6.5). On the other hand, with copper induction JHY4307 strain showed significantly increase in isobutanol production to 205.3 mg/L, which is increased by 3.8-fold and 1.6-fold compared with JHY4307 cultured without

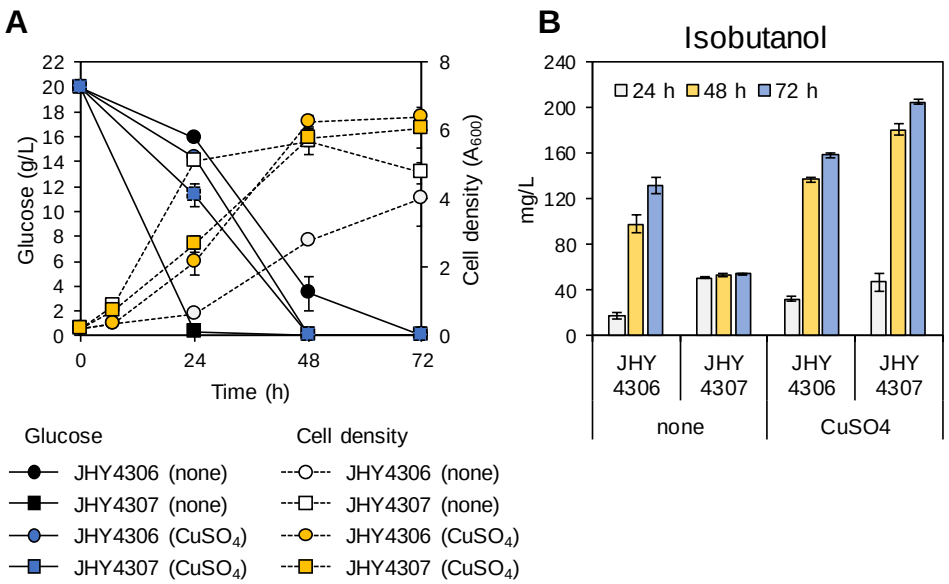

Figure 6.5 The effect of overexpressing *alsS* from *B. subtilis* using copper inducible promoter, P_{CUP1} on isobutanol production.

JHY4306 and JHY4307 were grown in SC-His, Trp, Ura medium containing 2 % glucose for 72 h. The label of none or $CuSO_4$ indicates presence or absence of CuSo4 in medium. After 7 hours of cell culture, $CuSO_4$ was treated at a concentration of 100 μM. (A) Cell growth and glucose consumprion. (B) Isobutanol production. Each value indicates the average ± SD of duplicate experiments.

$CuSO_4$ and JHY4306 cultured with $CuSO_4$, respectively (Fig. 6.5). Surprisingly, even in JHY4306 strain overexpressing *alsS* (L) by P_{TDH3}, isobutanol production was increased due to copper induction (Fig. 6.5B). This result indicates that cell death caused by overexpression of *alsS* (B) using P_{TDH3} can be successfully overcome by expressing using copper inducible promoter. Moreover, it can be confirmed that the activity of *alsS* (B) is stronger than that of *alsS* (L) through the production of isobutanol because the strain expressing *alsS* (B) with P_{CUP1}, generally known to be a weaker promoter than the P_{TDH3} even though P_{CUP1} is induced by copper with high concentration, produced more isobutanol than the strain expressing *alsS* (L) with $_{P}TDH3$ (Fig. 6.5) [168].

6.5. Integration of *alsS* derived from *B. subtilis* into *S. cerevisiae* chromosome via delta-integration and construction of strain screening methods using copper induction system

Next, I tried to integrate *alsS* (B) with P_{CUP1} to yeast chromosome by multi-copy delta-integration (Figure 1B). The delta-integration is a method of introducing a gene into a retrotransposon (Ty) site existing in about 100-copy in the yeast gene [72]. Coupled with an antibiotic selection, a yeast strain in which multi-copy of genes are introduced into a chromosome can be selected quickly [24].

To perform the delta-integration, the Delta6M-alsS plasmid consisting of

delta4-1 sequence, *alsS* gene expression cassette (P_{CUP1}-*alsS* (B)-T_{CYC1}), antibiotic G418 selection cassette (*KanMX*), and delta4-2 sequence was constructed. And then integration donor DNA fragments with delta sites at both ends obtained by treating *Swa*I into this plasmid, were transformed into yeast JHY43, generating *alsS* integrated yeast library. I first screened and selected strains with integration donor DNA fragment introduced in genome using G418 antibiotics (Fig. 6.2). And then based on the characteristics of alsS enzyme which is induces growth-deficiency via overexpressing, I tried to construct a 2nd screening system that selects yeast strain with more *alsS* gene from yeast library (Fig. 6.2). It was assumed that copper induction promotes cell growth inhibition in yeast strains with multi-copy *alsS* genes because of *alsS* under control of P_{CUP1}, and then I can obtained yeast strains introducing a lot of *alsS* genes by selection of the strains with growth deficiency. Thus, 26 yeast strains capable of growing on YPD agar plate containing 2000 μg/ml G418 were cultured for 7 h and then 100 mM $CuSO_4$ was supplemented to culture medium. Through this 2nd screening three strains JHY43D1, JHY43D2, and JHY3D3 strains whose cell growth was significantly slower than control strains (JHY43) were selected from engineered yeast library (Fig. 6.6).

To verify the isobutanol production in selected strains, I additional overexpressed *ILV5ΔN48* and *ILV3ΔN19* genes by transformation of p414GPD-*ILV5ΔN48*(K) and p416GPD-*ILV3ΔN19*(K) plasmids into JHY43D1, JHY43D2, and JHY3D3 strains resulting in generating JHY43D1-1, JHY43D2-1, and JHY43D3-1 strains. The JHY4307 strain was used as control strain with

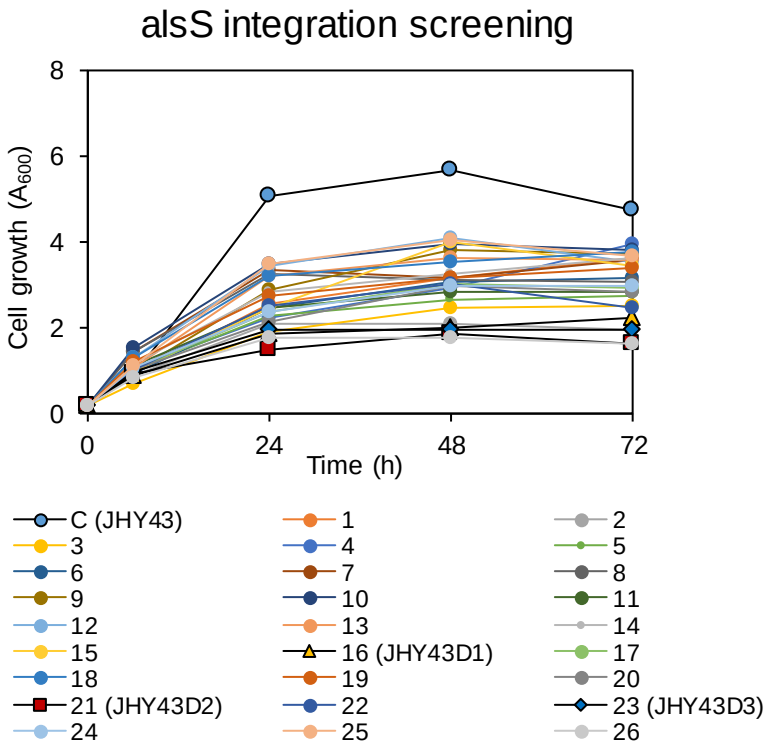

Figure 6.6 Screening of JHY43 strain integrating *alsS* from *B. subtilis* into genome via multi-copy delta-integration.

All yeast cells were inoculated to OD_{600} of 0.2 and were cultured in SC mix mediμM containing of 20 g/L glucose. After 7 hours of cell culture, $CuSO_4$ was treated at a concentration of 100 μM.

overexpressing *alsS* (B), K-*ILV5ΔN48*, and K-*ILV3ΔN19* via plasmids. All cells cultured in SC-His, Trp, Ura medium for 12 h and the $CuSO_4$ was supplemented into culture medium with 20 μM. The JHY4307 strain produced 172.7 mg/L isobutanol (Fig. 6.7C), which is lower than that of same strain in previous study (Fig. 6.5B), because I treated $CuSO_4$ at a lower concentration (20 μM) than in previous studies (100 μM). Among the three selected strain, JHY43D2-1 strain showed the best performance for isobutanol production (290.4 mg/L), indicating a 1.7-fold higher compared with JHY4307, although cell growth rate was slow compared with JHY4307, JHY43D1-1, and JHY43D3-1 strain (Fig. 6.7).

The isobutanol production tendencies were well correlated with a result of qPCR analysis. The copy number of the introduced *alsS* in the chromosomes of JHY43D1, JHY43D2, and JHY43D3 strains was analyzed by qPCR. As a result, JHY43D2 strain, JHY43D2-1 parental strain showed the highest isobutanol production, contains about 4 copies of *alsS* gene compared with control strain JHY43DC, while JHY43D1 genome contains >1 copy of *alsS* and JHY43D3 strain contains one copy of *alsS* (Fig. 6.7D). This results suggest that multiple copies of *alsS* could be introduced into the yeast genome by using delta-integration, and the expression of *alsS* in the chromosome could produce more isobutanol than the plasmid expression. Also, the amount of *alsS* is important for increase in isobutanol production, but induced cell growth-deficiency. Especially, JHY43D-C, JHY43D2 strain harboring empty vectors, p413GPD, p414GPD, and p416GPD significantly showed slow glucose consumption rate and cell growth rate compared with JHY43D2-1 (Fig.

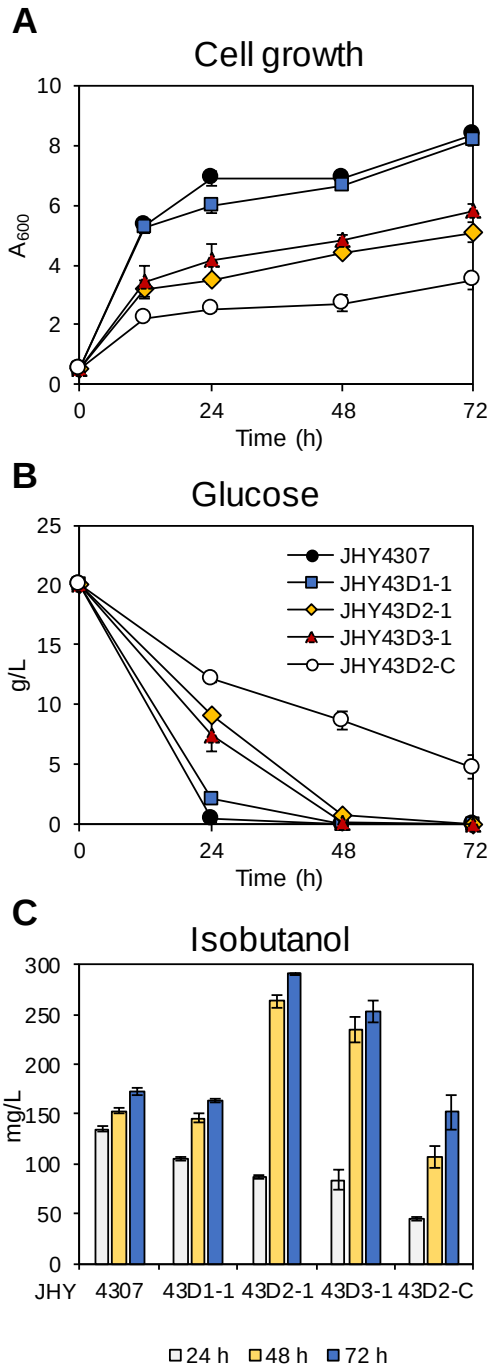
A
Cell growth
10
8
6
4
2
0
A_{600}
0
24
48
72
Time (h)
B
Glucose
25
20
15
10
5
0
g/L
JHY4307
JHY43D1-1
JHY43D2-1
JHY43D3-1
JHY43D2-C
0
24
48
72
Time (h)
C
Isobutanol
300
250
200
150
100
50
0
mg/L
JHY 4307
43D1-1
43D2-1
43D3-1
43D2-C
24 h
48 h
72 h

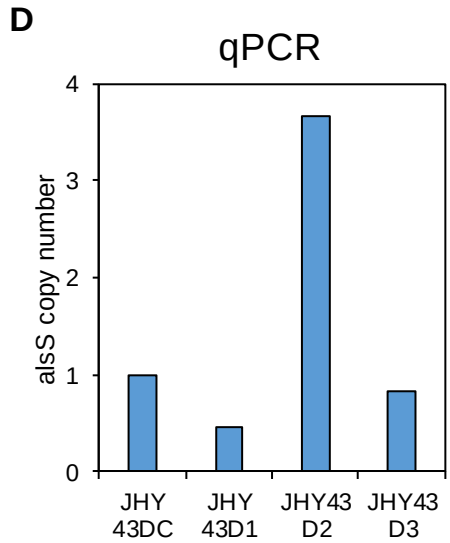

Figure 6.7 Production of isobutanol in yeast strains introducing *alsS* into chromosome by delta-integration.

(A) Cell growth. (B) The amount of glucose remaining in the media. (C) Isobutanol production. All yeast cells were inoculated to OD_{600} of 0.5 and were cultured in SC-His, Trp, Ura medium containing of 20 g/L glucose for 72 h. After 12 hours of cell culture, $CuSO_4$ was treated at a concentration of 20 μM. (D) Quantitative PCR (qPCR) for calculation of copy numbers of integrated *alsS* from *B. subtilis* in JHY43 strain derivatives.

6.7AB). Therefore, overexpression of *ILV5ΔN48* and *ILV3ΔN18* with *alsS* (B) genes can relieve the cell growth inhibition.

6.6. Assembly of cytosolic isobutanol biosynthetic pathway by multi-copy rDNA-integration of *ILV5ΔN48* and *ILV3ΔN19* genes.

In JHY43D2 strain having 4-copy of *alsS* gene in chromosome, the severe impediment of cell growth is observed (Fig. 6.7A), but overexpression of *ILV5ΔN48* and *ILV3ΔN19* involved in the reaction following the alsS enzyme reaction solves this problem and improved isobutanol production (Fig. 6.7). Therefore I introduced *ILV5ΔN48* and *ILV3ΔN19* genes additionally into JHY43D2 strain by integration into rDNA repetitive unit of *S. cerevisiae* genome. Because, in *S. cerevisiae genome*, the ribosomal DNA (rDNA) encoded on chromosome XII, an approximately 1-2 Mb region, is composed of 150 tandem copies of a 9.1 kb repeat unit containing nontranscribed spacers (*NTS1* and *NTS2*), NTS site was used as a homologous recombination site for multiple copies integration of *ILV5ΔN48* and *ILV3ΔN19* genes into yeast [76].

To perform multi-copy rDNA integration of *ILVΔN48* and *ILV3ΔN19* genes, I constructed NTS66-*ILV5*3 plasmid consisting of NTS2-1 sequence, gene expression cassette (P_{TDH3}-kozak sequence-*ILV5ΔN48*-T_{CYC1} and P_{TDH3}-kozak sequence-*ILV3ΔN19*-T_{CYC1}), antibiotic phleomycin selection cassette (*bleOR*), and NTS2-1

sequence. And then integration donor DNA fragments with NTS sites at both ends obtained by treating *Swa*I into this plasmid, were transformed into JHY43D2 strain, resulting in generation of *ILV5ΔN48* and *ILV3ΔN19* genes integrated yeast library (Fig. 6.2). In a similar procedure with the delta integration, to select strain inserted gene expression cassette in yeast genome, antibiotic selection was used by supplementing zeocin into YPD agar plate at 500 μg/mL concentration. Also, in order to improving selectivity of strains having more copy number *ILV5ΔN48* and *ILV3ΔN19* genes, the transformants were grown in YPD plate containing zeocin and additional 500 μM $CuSO_4$ (Fig. 6.2). Since *alsS* is overexpressed by copper in the medium, large amounts of *ILV5ΔN48* and *ILV3ΔN19* should be introduced into JHY43D2 genome and expressed a lot to maintain growth in this medium. Therefore, I obtained a strain capable of growing in YPD medium supplemented with both antibiotics and high concentration of $CuSO_4$, and confirmed the production of isobutanol through cell fermentation (Fig. 6.2).

Selected five engineered strain were cultured in SC medium for 12 h and the treated with 20 μM $CuSO_4$ in culture medium. Among them, the best variant JHY43D24 strain produced 227. 2 mg/L isobutanol with higher final cell density compared with parental strain JHY43D2 (Fig. 6.8A). Furthermore, the JHY43D24 genome contains more 3 copies of *ILV5ΔN48* and *ILV3ΔN19* compare with JHY43D2 resulting from qPCR analysis (Fig. 6.8D). On the other hand, JHY43D22 and JHY43D25 showed higher growth rate than the JHY43D24 but produced less isobutanol, 189.7 mg/L and 165.9 mg/L, respectively (Fig. 6.8C). As a result, I

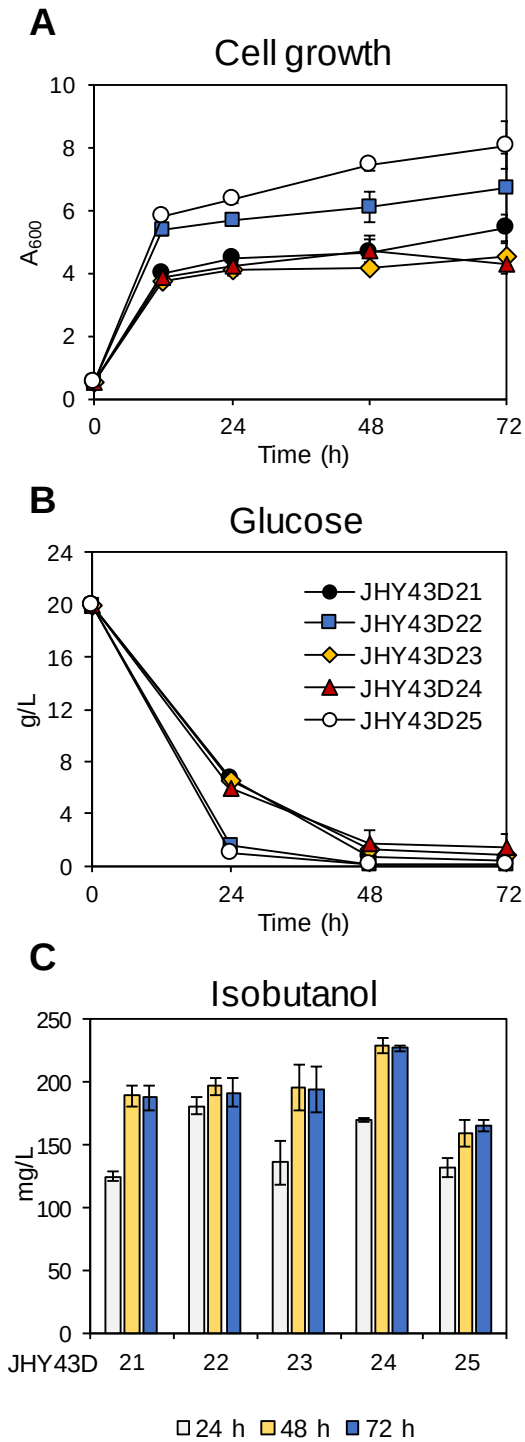
A
Cell growth
10
8
6
4
2
0
A600
0
24
48
72
Time (h)
B
Glucose
24
20
16
12
8
4
0
g/L
JHY43D21
JHY43D22
JHY43D23
JHY43D24
JHY43D25
0
24
48
72
Time (h)
C
Isobutanol
250
200
150
100
50
0
mg/L
JHY43D
21
22
23
24
25
24 h
48 h
72 h

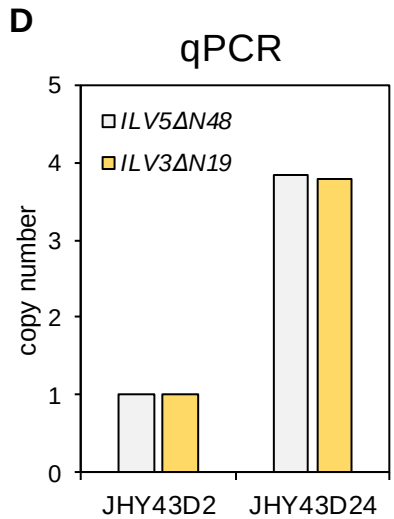

Figure 6.8 The effect of integration of *ILV5ΔN48* and *ILV3ΔN19* using NTS-site integration

The selected strains, JHY43D22, JHY43D23, JHY43D24, JHY43D25 and JHY43D26 were diluted to OD_{600} of 0.5 and cultured in SC mix medium containing 20 g/L glucose for 72 h. After 12 hours of cell culture, $CuSO_4$ was treated at a concentration of 20 μM. (A) Cell growth. (B) The amount of glucose remaining in the media. (C) Isobutanol production. Each value indicates the average ± SD of triplicate experiments. (D) Quantitative PCR (qPCR) for calculation of copy numbers of integrated *ILV5ΔN48* and *ILV3ΔN19* in JHY43D2

successfully alleviate cell growth deficiency occued by *alsS* overexpression via multi-copy integration of *ILV5ΔN48* and *ILV3ΔN19* using rDNA integration.

6.7. Enhancing isobutanol production by overexpression of additional *Ilv5ΔN48* and *Ilv3ΔN19* 2-ketoacid decarboxylase and alcohol dehydrogenase

To further improve isobutanol production, I investigate the effect of additional overexpressing Ilv5ΔN48 and Ilv3ΔN19 using plasmid in JHY43D24. Then I constructed pJIB53 plasmid consisting of kozak sequence-*ILV5ΔN48* and kozak sequence-*ILV3ΔN19* controlled by strong constitutive promoter, P_{TDH3}. JHY43D24 strain harboring pJIB53 (JHY43D24-2) produced upto 240.2 mg/L isobutanol after 72 h, showing a 1.13-fold higher isobutanol titer then that produced in JHY43D24-1 strain, JHY43D24 strain harboring empty vector p413GPD but both strain showed similar cell growth rate (Fig. 6.9). These results suggest that there is still the potential to increase isobutanol production by increasing copy number of *ILV5ΔN48* and *ILV3ΔN19*, although three copies of these genes have been contained in JHY43D24 strain.

In *S. cerevisiae*, isobutanol is produced from 2-KIV via valine catabolic pathway, Ehrlich pathway (Fig. 6.1). Through the Ehrlich pathway, 2-KIV is converted to isobutyraldehyde by KDCs and then converted to isobutyrate or isobutanol by the oxidation reaction associated with aldehyde dehydrogenases

(ALDs) or by reduction reaction associated with ADHs, respectively [5]. In previous my study, the oxidative process, a competitive pathway in isobutanol production, was already blocked by disruption of *ALD6* gene involved this route. Therefore, I tried to enhance the Ehrlich pathway by overexpressing KDC and ADH. To increase isobutanol production, *ARO10* from *S. cerevisiae* and *kivd* from *L. lactis*, which were already found to be effective in the synthesis of isobutanol, as KDC and *ADH2* from *S. cerevisiae* as ADH were overexpressed in yeast. The KDC (*kivd* or *ARO10*) and *ADH2* genes under the control of strong constitutive promoter, P_{TDH3} and P_{FBA1}, respectively, were cloned into pJIB53 plasmid, generating pJIB53KA plasmid, containing *kivd* and *ADH2*, and pJIB53AA plasmid, containing *ARO10* and *ADH2*. The JHY43D24 strain, harboring pJIB53KA plasmid (JHY43D24-3) showed significant improvement in isobutanol production (265.5 mg/L) compared with JHY43D24-2 strain, while cells overexpressing *ARO10* and *ADH2* (JHY43D24-4) exhibited similar levels of isobutanol titer (246.3 mg/L) with JHY43D24-2 strain (Fig. 6.9). This result suggests that kivd derived from *L. lactis* is more effective in isobutanol production in this isobutanol production pathway, although there is a report that Aro10 is more effective than kivd in isobutanol production.

Next, in order to further improve the isobutanol titer, I fermented JHY43D24-3 strain in the presence of higher concentrations of glucose. The fermentation was carried out in SC-His medium containing 40 g/L glucose with initial cell density of OD_{600} of 1 and 20 μM $CuSO_4$ after 7 h. After 96 h culture, the JHY43D24-3 strain produced upto 586.3 mg/L isobutanol (Fig. 6.10).

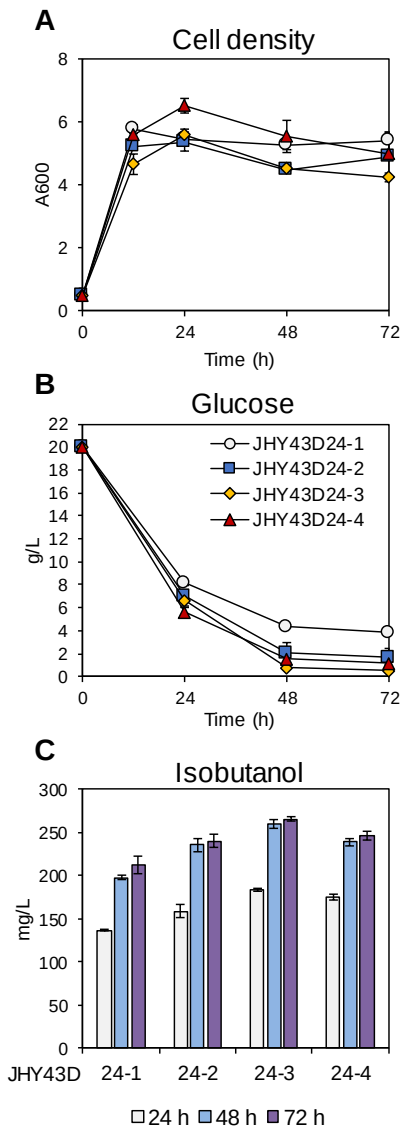

Figure 6.9 The effect of overexpressing additional *ILV5ΔN48* and *ILV3ΔN19* and genes related to Ehrlich pathway

All cells were diluted to OD_{600} of 0.5 and cultured in SC-His medium containing 20 g/L glucose for 72 h. After 12 hours of cell culture, $CuSO_4$ was treated at a concentration of 20 μM. (A) Cell growth. (B) The amount of glucose remaining in the media. (C) Isobutanol production. Each value indicates the average ± SD of triplicate experiments.

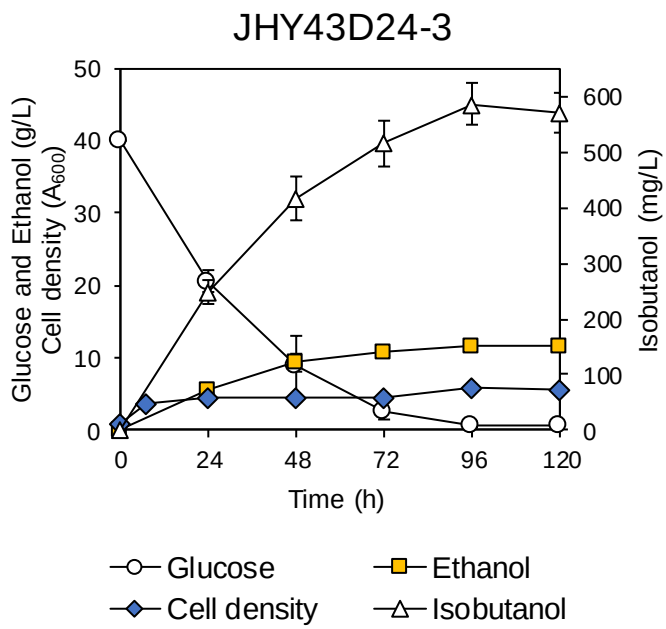

Figure 6.10 Metabolite profiles of JHY43D24-3 strain

JHY43D24-3 was inoculated to OD_{600} of 1 and cultured in SC-His medium containing 40 g/L glucose for 120 h. After 7 hours of cell culture, $CuSO_4$ was treated at a concentration of 10 μM.

6.8. Conclusions

In this chapter, *S. cerevisiae* strain with enhancing isobutanol production was developed by construct of artificial cytosolic isobutanol biosynthetic pathway via exploiting multi-copy delta- and rDNA-integration of related genes. In yeast library obtained using the two integration methods, to select suitable strain, I constructed a new selection method using the characteristics of *alsS* from bacteria as well as applying the antibiotic selection method. Moreover, overexpressing cytosolic Ilv5 and Ilv3 with the addition of kozak sequence to the enzymes, KDC (kivd) from *L. lactis*, and ADH (Adh2) further increased the production of isobutanol.

Chapter 7.

Metabolic engineering of *S. cerevisiae* for the production of shinorine a sunblock material from xylose

7.9. Introduction

Ultraviolet (UV) rays are harmful in many living things. There are three-type of UV rays UV-A, UV-B, and UV-C. The UV-C (100-280 nm) with the highest energy cannot reach the earth's surface because it is shielded by the stratospheric ozone layer. The UV-A (315-400 nm) and UV-B (280-315 nm) are the UV rays reaching the earth' surface, and especially UV-A, the most commonly penetrating type of UV ray mainly affects the ecosystem [82]. It is known that both UV can damage biomolecules including DNA and proteins by inducing reactive oxygen species (ROS), being harmful to living organism including human [84]. Therefore, it is considered necessary to apply sunscreen because continuous depletion of ozone layer leads to increase in UV-A and UV-B exposure on earth [83]. Recently, there is growing demand for the sunscreen material because of its applicability as additive in various cosmetics [169]. Chemical and physical sunscreen materials like oxybenzoate, ZnO, and TiO_2 have already used a lot but they have several disadvantages as cosmetics additives. These materials can induce xeroderma and allergy in humans and cause environmental pollution [85]. Therefore, bio-sunscreen compounds have attracted attention for replacement of chemical and physical sunscreen.

A mycosporine-like amino acids (MAAs), water soluble and colorless materials, are one of the family of UV-absorbing natural products, which are synthesized in some of cyanobacteria, fungi, and microalgae. There are approximately 30 MAAs

and all of them have cyclohexenmine choromophore conjugated with two amino acids or an imino alcohols of which variation cause the difference between absorption spectra of MAAs [86,88-93]. Among MAAs, especially, shinorine, consisting of glycine and serine residues, is the most attractive molecule as sunscreen because it has broad maximal absorbance wavelengths from 310 to 365 nm covering UV-A spectra and high molecular extinction coefficient (ε=44700 $M^{-1}cm^{-1}$) [170].

The shinorine biosynthetic pathway has been identified well in many organisms. There are two alternative pathways for the production of shinorine, route via dehydroquinate (DHQ) or route via sedoheptulose 7-phosphate (S7P) [171]. Some cyanobacteria produce 4-deoxygadusol (4-DG), the first key intermediate from, DHQ using DHQS homologous enzyme. On the other hand, in cyanobacteria *N. punctiforme* and *A. variabilis*, shinorine is produced from S7P an intermediate of pentose phosphate (PP) pathway, by sequential 4-step enzymatic reactions (Fig. 7.1) [99]. S7P is converted to 4-DG by 2-demethyl 4-deoxygadusol synthase (DDGS) and *O*-methyltransferase (*O*-MT). Then glycine is conjugated to 4-DG to synthesis mycosporine-glycine (MG) by ATP-grasp ligase. In the last, non-ribosomal peptides synthetase (NRPS)-like enzyme or D-ala-D-ala ligase conjugates serine to MG to generate shinorine (Fig. 7.2).

So far, although several efforts have been made to produce shinorine in cyanobacteria, it remains at the level of discovering and expressing genes (Table 2.4). Because shinorine is accumulated in cyanobacteria cells, a large amount of cell

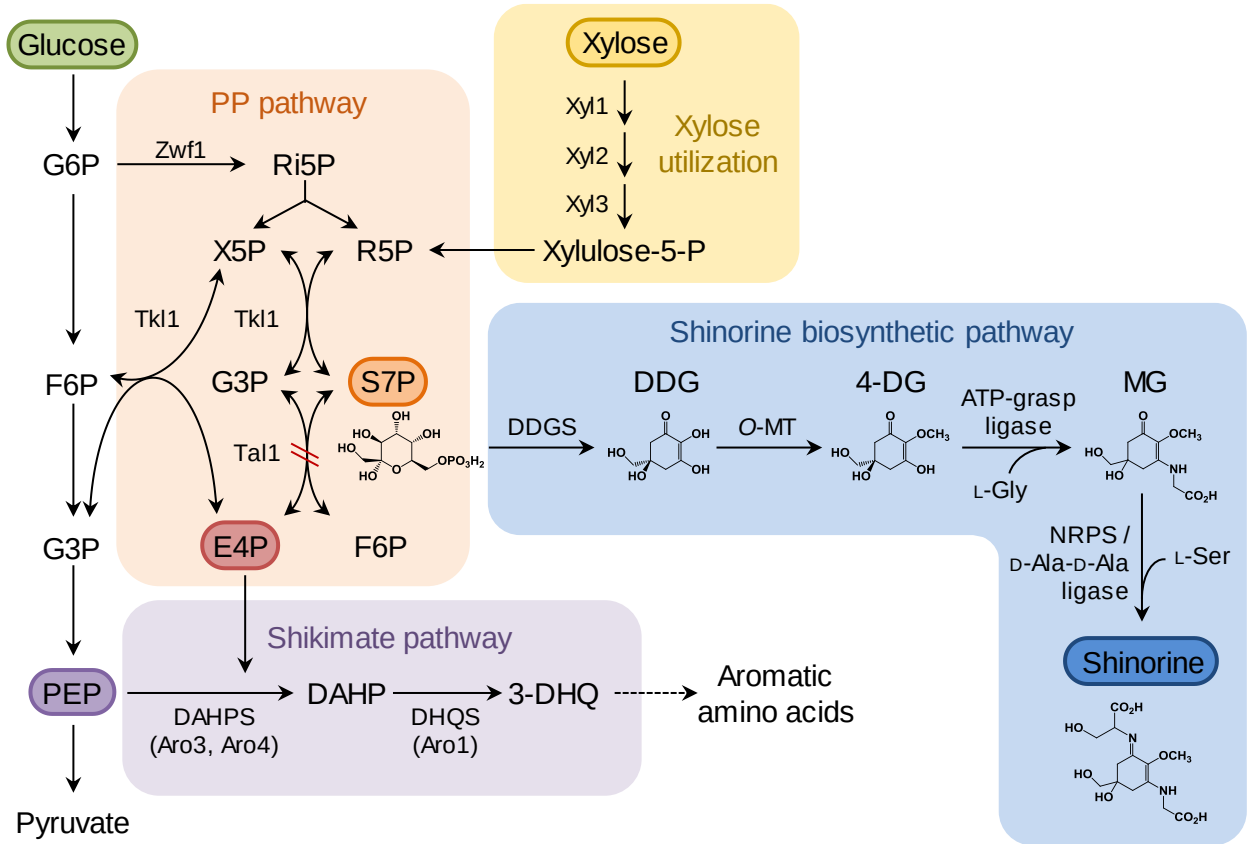
Glucose
G6P
F6P
G3P
PEP
Pyruvate
PP pathway
Zwf1
Ri5P
X5P
R5P
Tkl1
Tkl1
G3P
S7P
Tal1
E4P
F6P
Xylose
Xyl1
Xyl2
Xyl3
Xylose utilization
Xylulose-5-P
Shinorine biosynthetic pathway
DDG
4-DG
MG
DDGS
O-MT
ATP-grasp ligase
L-Gly
NRPS / D-Ala-D-Ala ligase
L-Ser
Shinorine
Shikimate pathway
DAHP
3-DHQ
DAHPS (Aro3, Aro4)
DHQS (Aro1)
Aromatic amino acids

Figure 7.1 Metabolic pathway for shinorine production used in this study

S7P is converted to shinorine via DDG, 4-DG, and MG by sequential catalytic reaction of DDG synthase (DDGS), O-methyl transferase (O-MT), ATP-grasp ligase, and non-ribosomal peptides synthetase (NRPS) or D-ala-D-ala ligase. Xylose reductase (Xyl1), xylitol dehydrogenase (Xyl2), and xylulokinase (Xyl3) catalyze the assimilation of xylose. Deleted gene is indicated by double slash (//) and dashed line indicate multiple enzymatic actions. S7P, sedoheptulose 7-phosphate; DDG, 2-demethyl 4-deoxygadusol; 4-DG, 4-deoxygadusol; MG, mycosporine-glycine; G6P, glucose-6-phosphate; Ri5P, ribulose-5-phosphate; X5P, xylulose-5-phosphate; R5P, ribose-5-phosphate; G3P, glyceraldhyde-3-phosphate; E4P, erythrose-4-phosphate; F6P, fructose-6-phosphate; PEP, phosphoenolpyruvate; DAHP, 3-deoxy-arabino-heptulosonate 7-phosphate; 3-DHQ, 3-dehydroquinate.

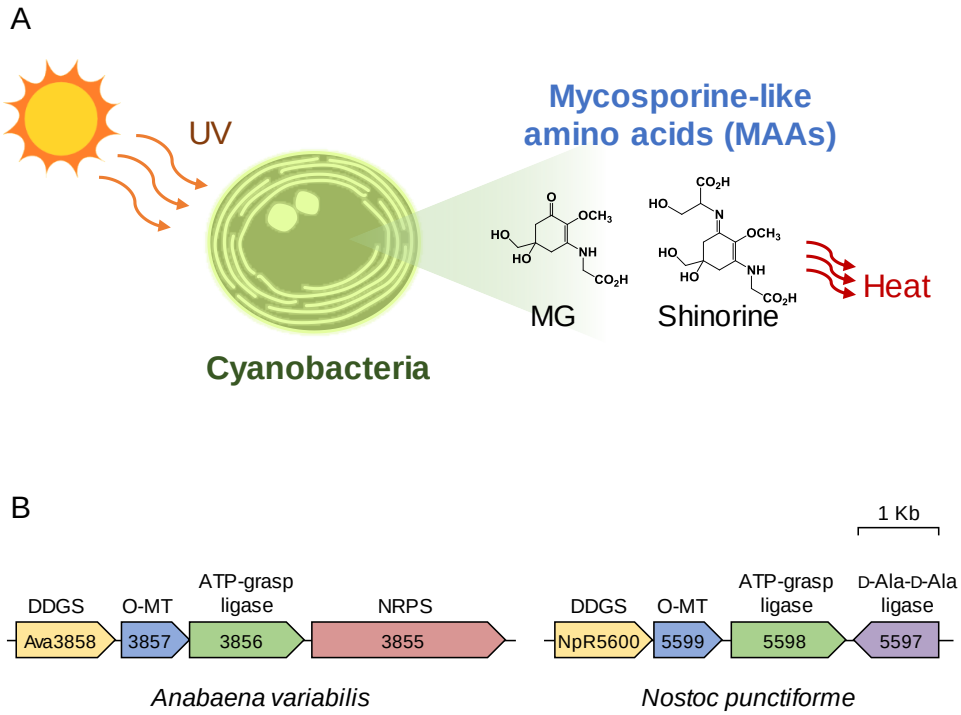

Figure 7.2 MAAs production in cyanobacteria.

A. MAAs production in cyanobacteria via inducing UV-ray.

B. Genes clusters involved in biosynthesis of shinorine in cyanobacteria, *A. variabilis* and *N. punctiforme*.

accumulation is required to mass-production of shinorine. However, cyanobacteria are not suitable strains for mass-production of shinorine, because cell culture is difficult and takes a long time and is difficult to genetically manipulate. Recently, introduction of heterologous gene from *Fischerella sp.* by tuning gene expression led to shinorine production (0.71 mg/L with 2.23 mg/gDCW) with a high production in cyanobacteria (Table 7.1) [103]. Shinorine was also produced in *E. coli* by introducing gene cluster from *A. valiabilis* but, its production was very low at 0.15 mg/L [99]. Meanwhile, engineered cyanobacteria by expressing gene cluster of *Synechocystis* produced quite a lot shinorine reaching at 19 mg/L (Table 7.1) [106].

Study on the production of shinorine using yeast have not been reported, but *S. cerevisiae* has been believed as a promising host for production of shinorine because of its safety and accumulated genetic technology [2,110]. *S. cerevisiae* has been used as a perfect host producing various non-natural metabolites, such as D-lactic acid, n-butanol, and terpenoids by introducing heterolous genes [172-174]. Moreover, charicteristics of genes involved in PP pathway and the production of various aromatic compounds derived via PP pathway have been reported. Especially, in yeast, there is transcriptional regulators (Stb5) of genes involved in the PP pathway and this enzyme is involved in regulating the transcription of target genes of PP pathway in response to oxidative stress and thereby regulating the amount of NADPH [175].

Alternatively, xylose can be used as a carbon source by the introduction of the xylose assimilation pathway to increase the carbon flux into the PP pathway (Fig. 7.1). Xylose assimilation requires the conversion of xylose into xylulose and

xylulose-5-phosphate which enters to PP pathway. In xylose-fermenting microorganisms, there are two kinds of xylose assimilation pathway (Fig. 2.11). In most bacteria, xylose is assimilated by xylose isomerase (XI) [114]. XI encoding genes are generally spread over bacterial genomes but it is difficult to express XI with maintaining function in yeast [115]. On the other hand, most of xylose-fermenting yeasts engage the pathway consisting of xylose reductase (XR), and xylitol dehydrogenase (XDH). Introducing XR-XDH pathway can offer high metabolic flux compared with introducing the XI pathway in *S. cerevisiae* [176]. There have been many studies to effectively utilize xylose in yeast, but most have been directed to ethanol production from xylose.

In this chapter I developed *S. cerevisiae* strain capable of producing shinorine by introducing shinorine biosynthetic pathways from *N. punctiforme* and *A. variabilis* (Fig. 7.2). Furthermore, as an effort to increase S7P pool, *XYL1* (xylose reductase), *XYL2* (xylitol dehydrogenase), and *XYL3* (xylulokinase) genes involved in xylose assimilation were introduced in *S. cerevisiae*, resulting in efficient production of shinorine using xylose as a carbon source and also competitive pathway that consume S7P was disrupted. Moreover, to enhancing PP pathway, transcriptional factor (Stb5) for PP pathway and transketolase (Tal1) was overexpressed in JHYS 17 strain resulting in the more improved shinorine production.

7.10. Construction of shinorine biosynthetic pathway in *S. cerevisiae*

S. cerevisiae does not naturally produce the shinorine. To produce shinorine in *S. cerevisiae*, heterologous shinorine biosynthetic pathway in cyanobacteria *N. punctiforme* consisting of DDGS (NpR5600), O-MT (NpR5599), ATP-grasp ligase (NpR5598), and D-ala-D-ala ligase (NpR5597), was introduced into wild type yeast strain (Fig. 7.2) [177]. S7P is sequentially converted to DDG, 4-DG, MG, and shinorine by NpR5600, NpR5599, NpR5598, and NpR5597, respectively (Fig. 7.1). There is no report on the production of shinorine by expressing this pathway in other organisms but the characterization of the enzymes has been already known in vitro.

To introduce genes responsible for shinorine biosynthesis, I used multigene-expression system previously constructed in my laboratory. NpR genes (*NpR5600, NpR5599, NpR5598,* and *NpR5597*) were cloned into multigene-expression vector and the resulting plasmid PL-NpR composing *NpR5600, NpR5599, NpR5598,* and *NpR5597* genes under the control of strong constitutive promoters, P_{TDH3} or P_{TEF1}, was constructed.

I confirmed the effect of introducing shinorine biosynthetic pathway of *N. punctiforme* into *S. cerevisiae* by transformation of PL-NpR plasmid into CEN.PK2-1C strain. The control strain is CEN. PK2-1C strain harboring p413GPD plasmid (WT-1) and JHYS10 strain is CEN. PK2-1C harboring PL-NPR plasmid. The HPLC analysis of cell extracts confirmed shinorine production by comparison with the

shinorine standard (Fig. 7.3A). As a result of HPLC analysis, WT-1 strain did not produce shinorine, while JHYS10 strain produced a trace amount of shinorine (459.03 μg/L and 84.57 μg/gDCW) using glucose as carbon source (Fig. 7.3).

7.11. Generation of shinorine-producing *S. cerevisiae* strain by random multi-copy delta-integration

Recently, developed delta integration using antibiotic selection enables construction of large biosynthetic pathway in one-step in *S. cerevisiae* [178] [24]. In *S. cerevisiae* genome, there are hundreds of retrotransposon Ty1 long terminal repeats (LTR) sequences known as delta-sequence [71,72]. By performing gene integration using these delta sites, a large number of genes can be rapidly and randomly introduced into the yeast chromosome. Therefore, I tried to integrate all of the NpR genes as multi-copy number into *S. cerevisiae* chromosome by delta site integration for production of shinorine.

To construct integration donor DNA fragments for delta integration of NpR genes, I developed Delta6M-NPR1 and Delta6M-NpR2 plasmids. Delta6M-NpR1 is composed of *NpR5597* and *NpR5600* genes under control of promoter, P_{TEF1} and P_{TDH3}, respectively, and Delta6M-NpR2 is composed of *NpR5598* and *NpR5599* genes under control of promoter, P_{TEF1} and P_{TDH3}, respectively. The mixture of these two plasmids treated with restriction enzyme *Swa*I to obtain integration donor DNA,

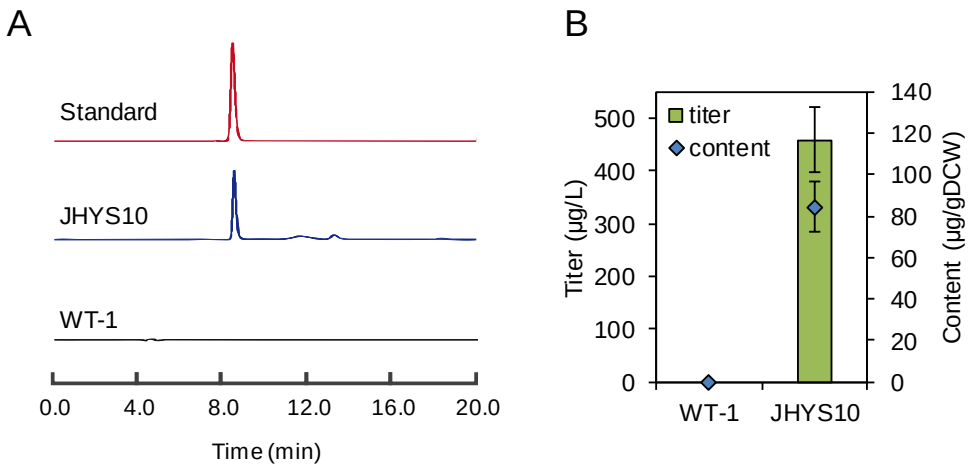

Figure 7.3 Detection of shinorine in *S. cerevisiae* carrying shinorine biosynthetic gene from *N. punctiforme*

A. HPLC spectra of shinorine of authentic standard and cell extracts of WT-1 and JHYS10 cells.

B. Quantitative value of shinorine production in yeast strains. WT-1 and JHYS10 cells were grown in SC-His medium containing 2 % glucose for 48 h. Each value indicates the average ± SD of triplicate experiments. Shinorine titer (bar) and content of shinorine (diamond) are shown.

consisting of delta sequence at both ends, was transformed into yeast cell (Fig. 7.4). Wild type strain, CEN. PK2-1C, was used as parental strains for delta-integration. G418 was chosen as a selective antibiotic. 18 colonies that could grow on the medium containing antibiotics, G418 (2000 μg/ml) were obtained. Among them, selected two strains, JHYS12 and JHYS13 produced more shinorine. JHYS13 strain produced 671.6 μg/L shinorine with 125.4 μg/gDCW content which was higher production compared with shinorine production of JHYS12 strain (508.1 μg/L shinorine with 106.3 μg/gDCW content) (Fig. 7.5A).

These shinorine production tendencies correspond to qPCR results (Fig. 7.5B). The status of the introduced genes in the chromosomes of two strains was analyzed by qPCR. As a result, it was confirmed that the amounts of introduced genes were different according to each strain. JHYS12 genome contains 5 copies of *NpR5600* and *NpR5597* and 2 copies of *NpR5599* and *NpR5598* compared with control strain JHYS11 in which only one copy of the NpR genes was introduced (Fig. 7.5B). Whereas, genome of JHYS13 strain contains 4 copies of *NpR5600* and *NpR5597* and 9 copies of *NpR5599* and *NpR5598*, resulting in more shinorine production than JHYS12 (Fig. 7.5A). This result also indicates the amount of *NpR5600* is important for shinorine production because the amount of *NpR5599* and *NpR5598* genes differs greatly in both stains, but there is no significant difference in shinorine production.
Using delta integration, large amounts of genes required for shinorine production were introduced into yeast strains, resulting in construction of yeast capable of

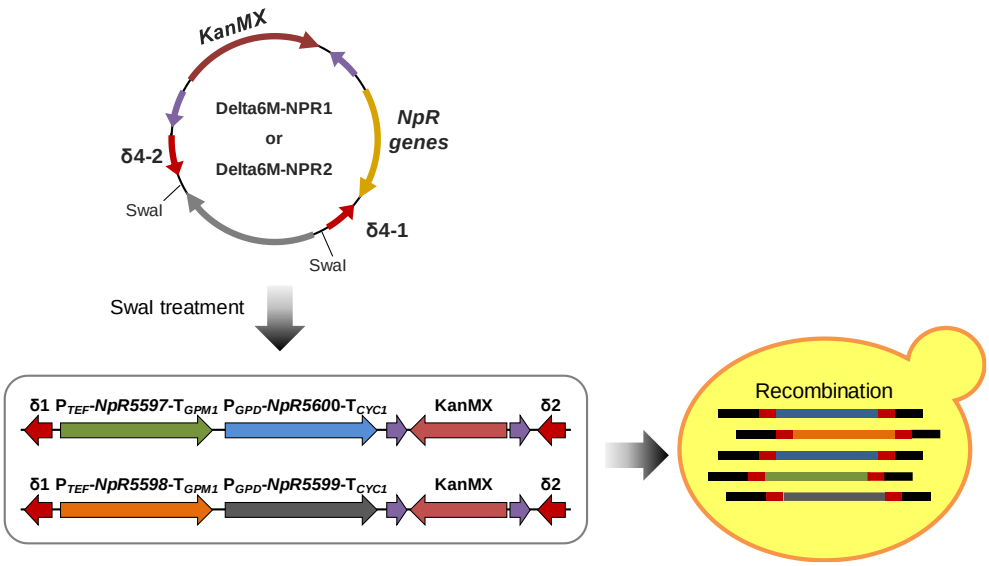

Figure 7.4 Schematic illustration of procedure of delta integration of NpR genes into *S. cerevisiae*

To integrate NpR genes into yeast, Delta6M-NPR1 and Delta6M-NPR2 plasmids, possessing a sequence recognized by the SwaI restriction enzyme, was constructed, at first. Both plasmids were randomly mixed and then treated with restrictional enzyme, SwaI, resulting in construction of donor DNA fragments for delta-site integration. The mixture was introduced into *S. cerevisiae*.

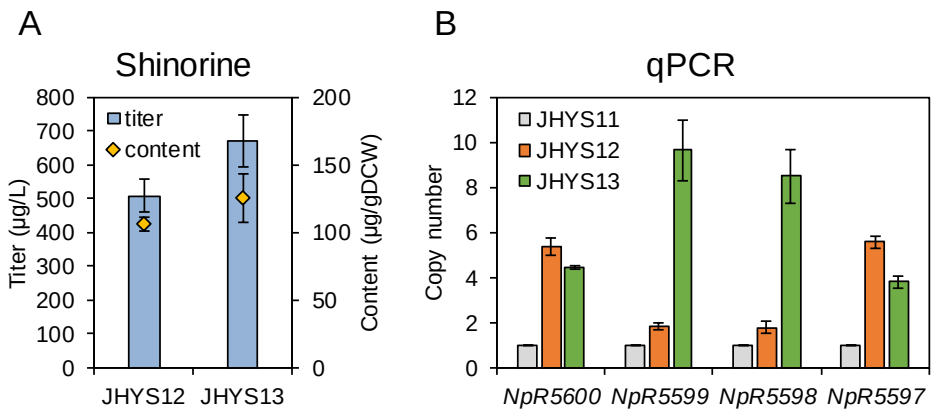

Figure 7.5 Construction of shinorine producing yeast by delta integration of NpR genes

A. Shinorine production. The selected strains, JHYS12 and JHYS13, were grown in SC mix medium containing 2 % glucose for 48 h. Each value indicates the average ± SD of triplicate experiments. Shinorine titer (bar) and content of shinorine (diamond) are shown.

B. Quantitative PCR (qPCR) for calculation of copy numbers of integrated genes. Each value indicates the average ± SD of duplicate experiments.

producing shinorine but production is still very low. This is because the glucose flux of *S. cerevisiae* is mostly used to make ethanol through glycolysis. Therefore, shinorine production is expected to be low because the pool of S7P, an important intermediate for shinorine production, is small. Therefore, it is essential to increase the carbon flux to the pentose phosphate pathway in order to increase shinorine production

7.12. Using xylose as carbon source for shinorine production in *S. cerevisiae* by introducing xylose assimilation pathway

In JHYS13 strain, shinorine production is still low. Therefore, to further improve shinorine production, it is critical to direct the carbon flux to the pentose phosphate pathway. So, here, xylose was used as carbon sources for shinorine production. However, *S. cerevisiae* does not have xylose assimilation enzymes, so xylose assimilation genes in *Scheffersomyces stiptis*, consisting of xylose reductase (Xyl1), xylitol dehydrogenase (Xyl2), and xylulokinase (Xyl3) were introduced into *S. cerevisiae* [179]. Xylose is sequentially converted to xylitol and xylulose by Xyl1 and Xyl2, respectively, and then xylulose is entered into pentose phosphate pathway by Xyl3 (Fig. 7.1).

The availability of xylose was verified and its effect on shinorine production by introducing genes required for xylose assimilation. The *XYL1, XYL2,* and *XYL3* genes under control of strong constitutive promoter, P_{TDH3}, was cloned into

p416GPD plasmid, generating coex416-XYL plasmid. JHYS13-1 and JHYS13-2 strain, which is JHYS13 strains harboring empty vector, p416GPD and coex416-XYL plasmid, respectively, were cultured in four different media with different ratios of glucose and xylose (Fig. 7.6 and Table 7.1). In the case of the strain JHYS13-1, it was observed that xylose was not consumed at all, and consequently, the production of shinorine in JHYS13-1 strain was low (<1 mg/L) (Fig. 7.6). On the other hand, JHYS13-2 strain was not only grown by consuming xylose, but also greatly increased shinorine production (Fig. 7.6). When both strains cultured in media 1 containing only glucose, glucose consumption rate, cell density, and the shinorine production is similar (Fig. 7.6A, E). When JHYS13-1 was cultured in media2 and media3, shinorine production was decreased (<0.1 mg/L) as the concentration of glucose was decreased (Fig. 7.6B, C, E). Furthermore, culturing in media4 containing only xylose as carbon source, JHYS13-1 strain could not assimilate xylose, resulting in not producing shinorine (Fig. 7.6D, E). By contrast, shinorine production in JHYS13-2 strain cultured in media2 and media3 was greatly increased depending on increasing xylose concentration in media (Fig. 7.6B, C, E). In particular, the shinorine production in JHYS13-2 strain was improved about 44.1 times when grown on media3 (17. 99 mg/L with 4.75 mg/gDCW content), compared to grown on media 1 (0.41 mg/L with 0.11 mg/gDCW content) (Fig. 7.6E). Also it was observed that shinorine was released out of the cell depending on increasing shinorine production in the cell (Fig. 7.6E). When the JHYS13-2 strain was cultured in medium containing only xylose (media 4), the shinorine content was high (2.74

mg/gDCW) but the produced shinorine concentration was low (2.64 mg/L) because the lag phase of the cell was long and the xylose was not consumed quickly (Fig. 7.6D, E). Therefore, even if xylose was used as a carbon source, adding a small amount of glucose to the medium could increase xylose consumption rate.

7.13. Construction of xylose-fermenting yeast strain by random multi-copy NTS-site integration

In the previous experiment, I confirmed that shinorine production was increased by using xylose as carbon source via overexpressing *XYL1, XYL2,* and *XYL3* (Fig. 7). It was then proceeded to integrate the genes required for xylose assimilation *XYL1, XYL2,* and *XYL3* into rDNA repetitive unit of *S. cerevisiae* genome, because yeast transformants not only keeps the p416GPD vector with a low copy number (1-2 copies per cell), but also was burdened by maintaining the vector. In *S. cerevisiae*, the ribosomal DNA (rDNA) is encoded on chromosome XII, an approximately 1-2 Mb region, consisting of about 150 tandem copies of a 9.1 kb repeat unit containing nontranscribed spacers (*NTS1* and *NTS2*). Some attempts has been already reported about integrating foreign genes into yeast rDNA site with multi-copy [78,80,81]. So, in this study, rDNA, especially NTS site, was used as a homologous recombination site for multi-copy integration of XYL genes (*XYL,1 XYL2,* and *XYL3*) into yeast.

To construct integration donor DNA fragments for NTS-site integration of XYL genes, NTS66M-XYL plasmids composed of *XYL1, XYL2,* and *XYL3* genes under

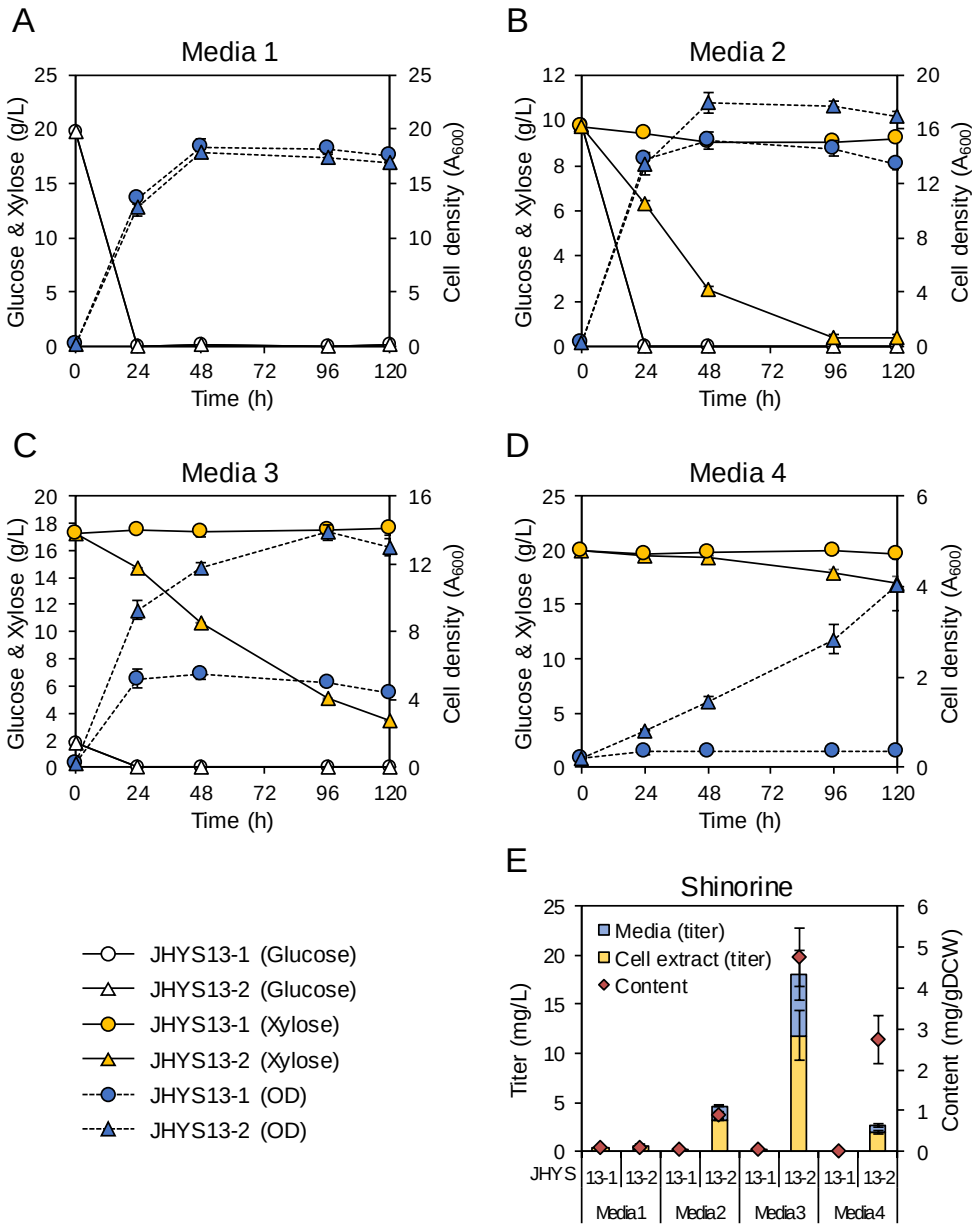
A
Media 1
B
Media 2
C
Media 3
D
Media 4
E
Shinorine
Glucose & Xylose (g/L)
Cell density (A600)
Time (h)
Titer (mg/L)
Content (mg/gDCW)
Media (titer)
Cell extract (titer)
Content
JHYS
13-1
13-2
Media1
Media2
Media3
Media4
JHYS13-1 (Glucose)
JHYS13-2 (Glucose)
JHYS13-1 (Xylose)
JHYS13-2 (Xylose)
JHYS13-1 (OD)
JHYS13-2 (OD)

Figure 7.6 Improvement of shinorine production by introducing xylose assimilation pathway and using xylose as carbon source

JHYS13-1 and JHYS13-2 cells were cultured in SC-Ura mediums containing different ratio of glucose and xylose for 120 h. Cell growth, the amount of glucose and xylose remaining in the media 1 containing 20 g/L glucose (A), media 2 containing 10 g/L glucose and 10 g/L xylose (B), media 3 containing 2 g/L glucose and 18 g/L xylose (C), and media 4 containing 20 g/L xylose (D). (E) Shinorine production. Each value indicates the average ± SD of triplicate experiments.

Table 7.1 Shinorine production of JHYS13-1 and JHYS13-2 strains cultured in various medium containing xylose and glucose

strain	Production Titer (mg/L) [Content (g/gDCW)]			
	Media 1	**Media 2**	**Media 3**	**Media 4**
JHYS13-1	0.41±0.083 [0.11±0.01]	0.14±0.012 [0.04±0.001]	0.03±0.001 [0.04±0.002]	ND
JHYS13-2	0.60±0.097 [0.08±0.004]	4.61±0.76 [1.39±0.02]	17.99±4.59 [4.75±0.52]	2.64±0.62 [2.74±0.01]

ND (No detected)

control of strong constitutive promoter, P_{TDH3} was developed. The integration donor DNA fragment obtained by restriction enzyme treatment of NTS66M-XYL vector, consisting of NTS sequence at both ends, was transformed into JHYS13 strain (Fig. 7.7). Zeocin was chosen as a selective antibiotic. I obtained 5 colonies with improved shinorine production based on viability on the YP medium containing only xylose as carbon source and 500 μg/ml zeocin. The selected 5 strains, JHYS14, JHYS15, JHYS16, JHYS17, and JHYS18, showed various production levels of shinorine from xylose. Among the transformants, JHYS14 and JHYS18 strains were grown the best and also consumed xylose most rapidly, but showed low level of shinorine production, 6.21 mg/L and 6.19 mg/L, respectively. JHYS17 strain produced 17.72 mg/L shinorine with 8.7 mg/gDCW content, which was higher production compared with shinorine production in JHYS15 strain (15.79 mg/L shinorine with 3.25 mg/gDCW content) and JHYS16 strain (14.91 mg/L shinorine with 3.24 mg/gDCW content) (Fig. 7.8). JHYS15 and JHYS17 genomes contains one copy of *XYL1*, *XYL2*, and *XYL3* resulting from qPCR analysis. The subtle difference in the production of shinorine between the both strains are believed to be due to differences in the expression of genes depending on integrating of the genes into different sites among numerous NTS sites.

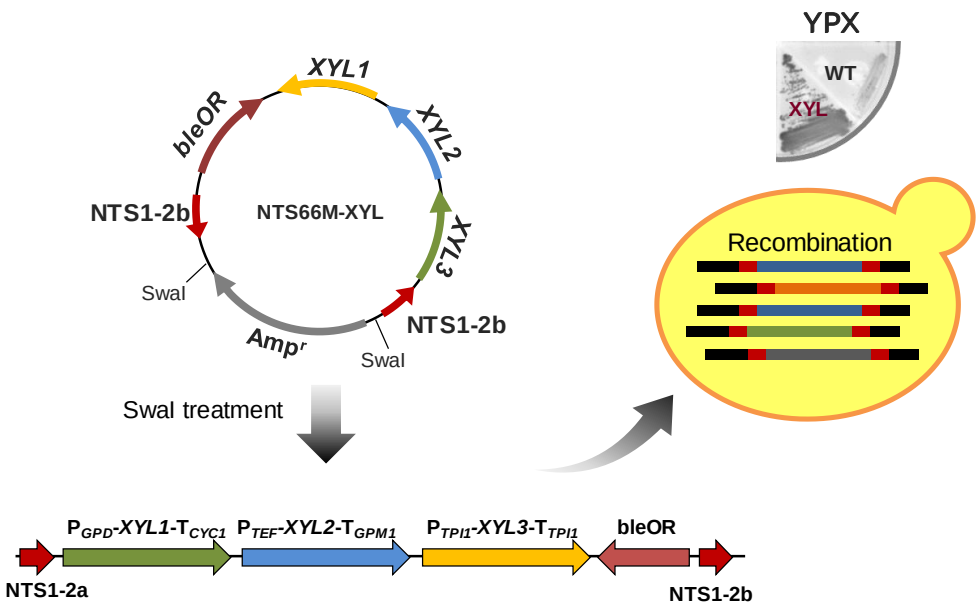

Figure 7.7 Schematic diagram of the overall prodedure of XYL genes integration

NTS66M-XYL plasmid treated with SwaI was introduced into yeast and then the strains capable of growing in YPX medium containing 500 μg/ml zeocin was selected.

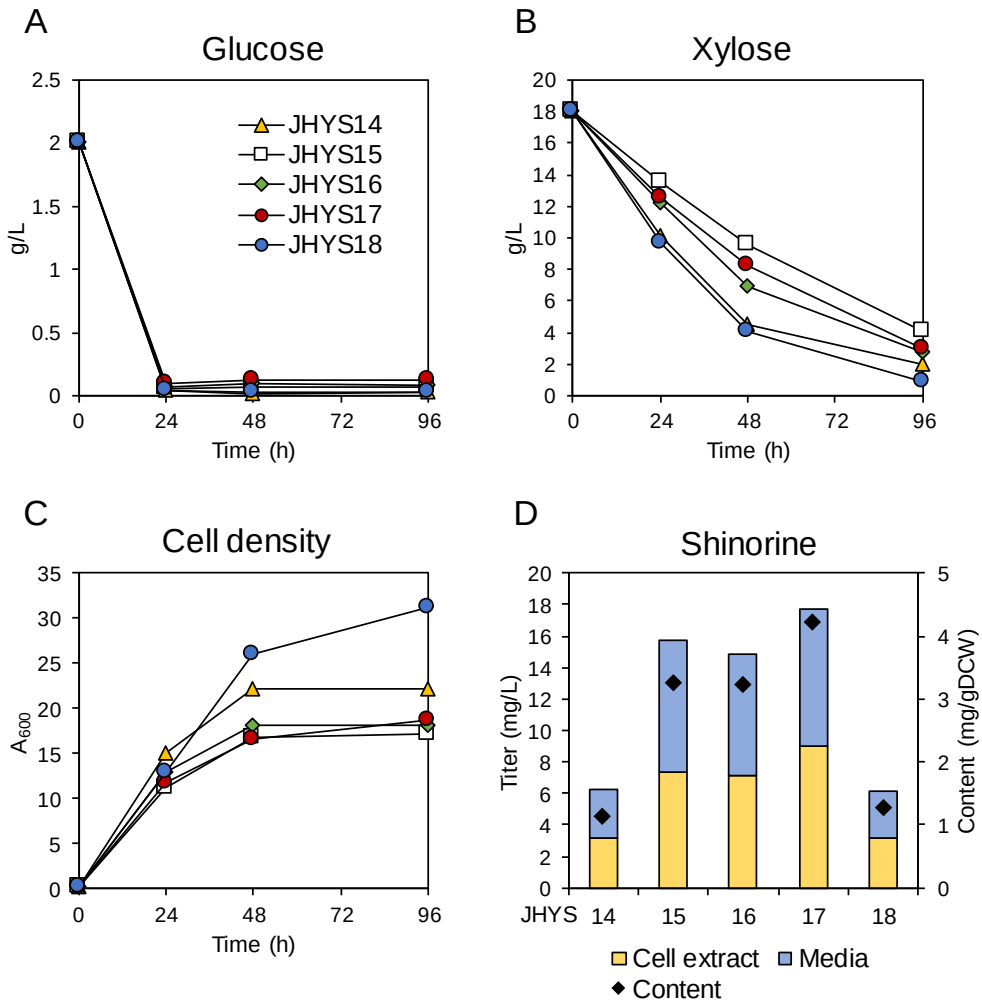

Figure 7.8 Construction of xylose consuming *S. cerevisiae* by NTS-site integration of xylose assimilation genes

The selected strains, JHYS14, JHYS15, JHYS16, JHYS17 and JHYS18 were cultured in SC mix medium containing 2 g/L glucose and 18 g/L xylose for 96 h. The amount of glucose (A) and xylose (B) remaining in the medium. (C) Cell growth. (D) Shinorine production of selected strains. Each value indicates the average ± SD of triplicate experiments.

7.14. Overexpressing genes related to shinorine production from *A. variabilis* in *S. cerevisiae*

There are a lot of cyanobacteria producing shinorine to protect against UV. Especially, cyanobacteria *A. variabilis* has shinorine production pathway and the characteristics of the enzymes involved in this shinorine production pathway was already well understood. The gene cluster required for shinorine production in *A. variabilis* consists of Ava genes, Ava3858 (DDGS), Ava3857 (O-MT), Ava3856 (ATP-grasp ligase), and Ava3855 (NRPS) (Fig. 7.2). There have been report of the production of shinorine by expressing these genes in *E. coli*.

To compare NpR genes in *N. punctiforme* and Ava genes in *A. variabilis*, each gene was expressed by strong promoter, P_{TDH3}, in wild yeast, CEN. PK2-1C, in various combinations. JHYS1-1 strain overexpressed only NpR genes produced 330.1 μg/L shinorine (Fig. 7.9A). CEN. PK2-1C strain overexpressed the only Ava genes did not produce shinorine and furthermore transformants could not be observed when the genes were overexpressed in combination with *Ava3858*, *Ava3857*, *Ava3856*, and *NpR5597* (data was not shown). Whereas shinorine production in CEN. PK2-1C strain harboring p413GPD-Ava3858, p414GPD-Ava3857, p415GPD-NpR5598, and p416GPD-NpR5597 plasmids (JHYS1-2) was significantly improved about 2.9-fold (944.94 μg/L) compared with JHYS1-1 strain (Fig. 7.9A). CEN. PK2-1C strain harboring p413GPD-Ava3858, p414GPD-NpR5599, p415GPD-NpR5598, and p416GPD-NpR5597 (JHYS1-3) showed 993. 7

μg/L shinorine production, which is similar to the shinorine production in the JHYS1-2 strain (Fig. 7.9A). Thus, the activity of the first gene in the production of shinorine is important and the activity of Ava3858 is better than that of NpR5600, resulting in increased shinorine production. It is also believed that the last gene of shinorine production from *A. variabilis*, Ava3855 is not active in yeast. It is known that NpR5597 is a D-ala-D-ala ligase and Ava3855 is an NRPS-like ligase (Fig. 7.2). These two enzymes have different domains and are involved in the production of shinorine by different mechanisms (Fig. 7.10) [99,177]. Furthermore, the catalytic activity of NRPS like Ava3855, requires a posttranslational modification on its peptidyl carrier protein (PCP) domain, which is facilitated by a phosphopantetheinyl transferase (PPT) [180]. So it is presumed that the activation of Ava3855 in yeast requires the introduction of an appropriate PPT enzyme.

The effect of overexpression of *Ava3858*, which is effective in the production of shinorine, was investigated in JHYS17 strain. JHYS17 harboring p413GPD (JHYS17-1) is control strain and JHYS17-2 strain is transformant harboring p413GPD-Ava3858 plasmid. The JHYS17-2 strain consumed xylose faster than the control strain, and thus the growth rate was fast (Fig. 7.9C). Shinorine production of JHYS17-2 increased by 3.1-fold, reaching 16.62 mg/L (3.68 mg/gDCW), compared with JHYS17-1 strain (5.38 mg/L) (Fig. 7.9B). It is believed that the activity of Ava3858 enzyme was better than NpR5600 and thus an additional overexpression of Ava3858 effectively redirected the carbon flux toward shinorine production.

In order to further improve the fermentation performance to produce shinorine

in JHYS17-2 strain, fed-batch fermentation was carried out in 250 mL flask containing 25 mL of SC-His. Fermentation of JHYS17-2 strain achieved the highest shinorine concentration and content, reaching 64.2 mg/L and 14.3 mg/gDCW, ever reported in microbes (Fig. 7.9D).

7.15. Disruption of competing pathway to enhance shinorine production

Shinorine is produced from S7P. Therefore, to further improve shinorine production, it is critical to increase the pool of S7P in yeast. It was chosen to be deletion of transaldorase, Tal1, which is involved in the accumulation of its substrate, S7P in pentose phosphate pathway (PPP) (Fig. 7.1) [181]. Especially, Pho13 deletion significantly reduced S7P, because *TAL1* upregulated by *pho13Δ* promoted consuming S7P [182].

Since S7P is a substrate of transaldolase (Tal1) in the PPP, *TAL1* deletion strain (JHYS19) was constructed into JHYS17 strain as parental strain by CRISPR-Cas9 system. JHYS19 strain showed severe growth defect in xylose rich-medium containing 2 g/L glucose and 18 g/L xylose (Fig. 7.11). It has been already known that *TAL1*-deficient strain did not grow well in the xylose medium but JHYS19 strain promoting the consumption of S7P through the introduction of the shinorine pathway was expected to consume xylose well. The problem of defection of cell growth in JHYS19 (*tal1Δ*) can be solved by increasing the glucose ratio in the medium. The

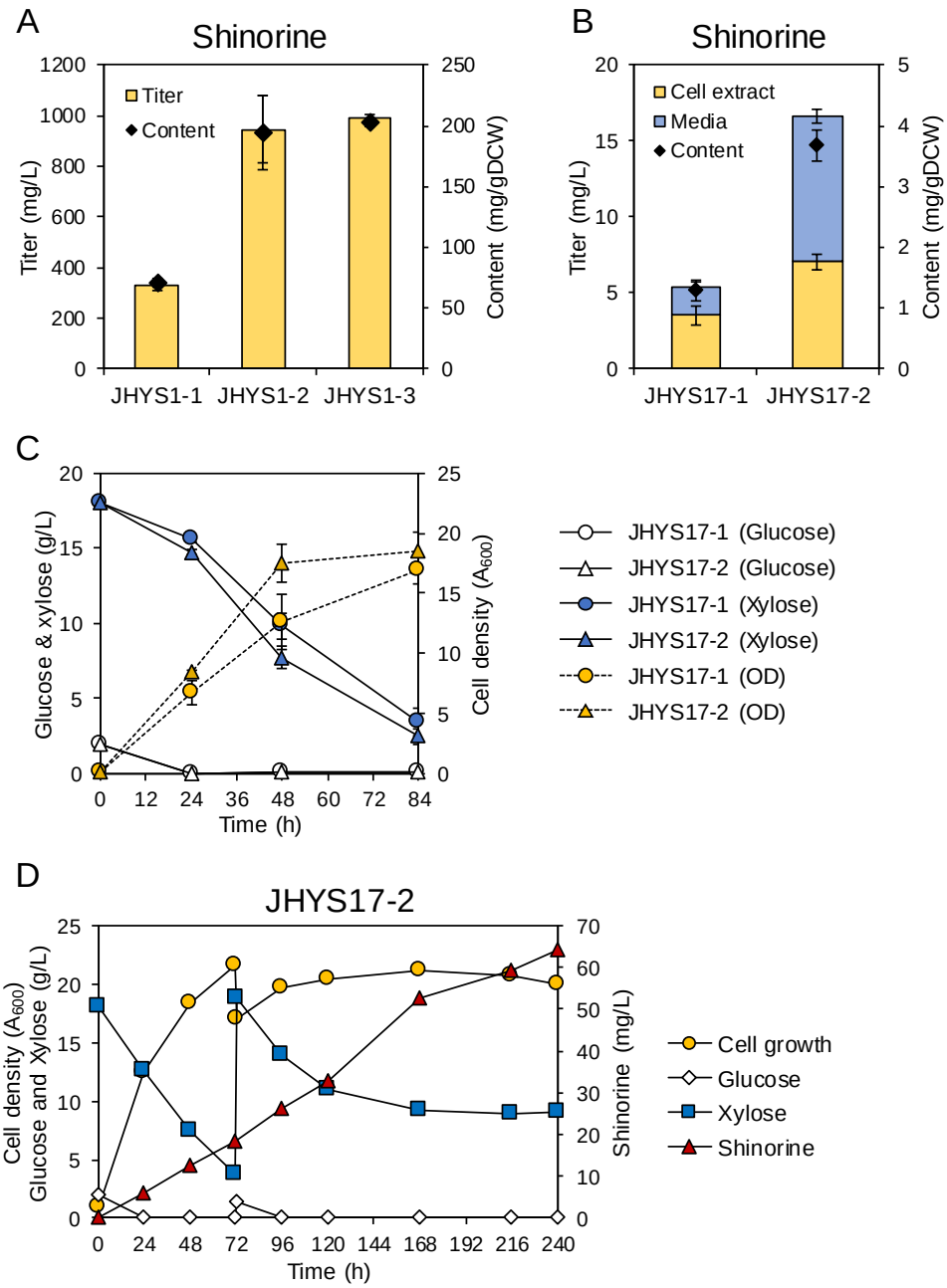
A
Shinorine
Titer
Content
Titer (mg/L)
Content (mg/gDCW)
JHYS1-1
JHYS1-2
JHYS1-3
B
Shinorine
Cell extract
Media
Content
Titer (mg/L)
Content (mg/gDCW)
JHYS17-1
JHYS17-2
C
Glucose & xylose (g/L)
Cell density (A600)
Time (h)
JHYS17-1 (Glucose)
JHYS17-2 (Glucose)
JHYS17-1 (Xylose)
JHYS17-2 (Xylose)
JHYS17-1 (OD)
JHYS17-2 (OD)
D
JHYS17-2
Cell density (A600)
Glucose and Xylose (g/L)
Shinorine (mg/L)
Time (h)
Cell growth
Glucose
Xylose
Shinorine

Figure 7.9 The effect of overexpressing shinorine biosynthetic genes derived from *A. variabilis*

(A) Shinorine production. JHYS1-1, JHYS1-2 and JHYS1-3 strains were cultured in SC-His, Trp, Leu, Ura medium containing 20 g/L glucose for 48 h. Shinorine production (B), cell growth, and glucose and xylose concentration (C) of JHYS17-1 and JHYS17-2 cultured in SC-His medium containing 2 g/L glucose and 18 g/L xylose for 84 h. Each value indicates the average ± SD of triplicate experiments. (D) Shinorine fermentation profile in fed-batch culture with glucose and xylose feeding. JHYS17-2 strain was grown in SC-His containing 18 g/L xylose and 2 g/L glucose with initial inoculation OD_{600} of 1. The feeding solution (600 g/L xylose and 200 g/L glucose) was added to culture medium when xylose concentration was about 5 g/L.

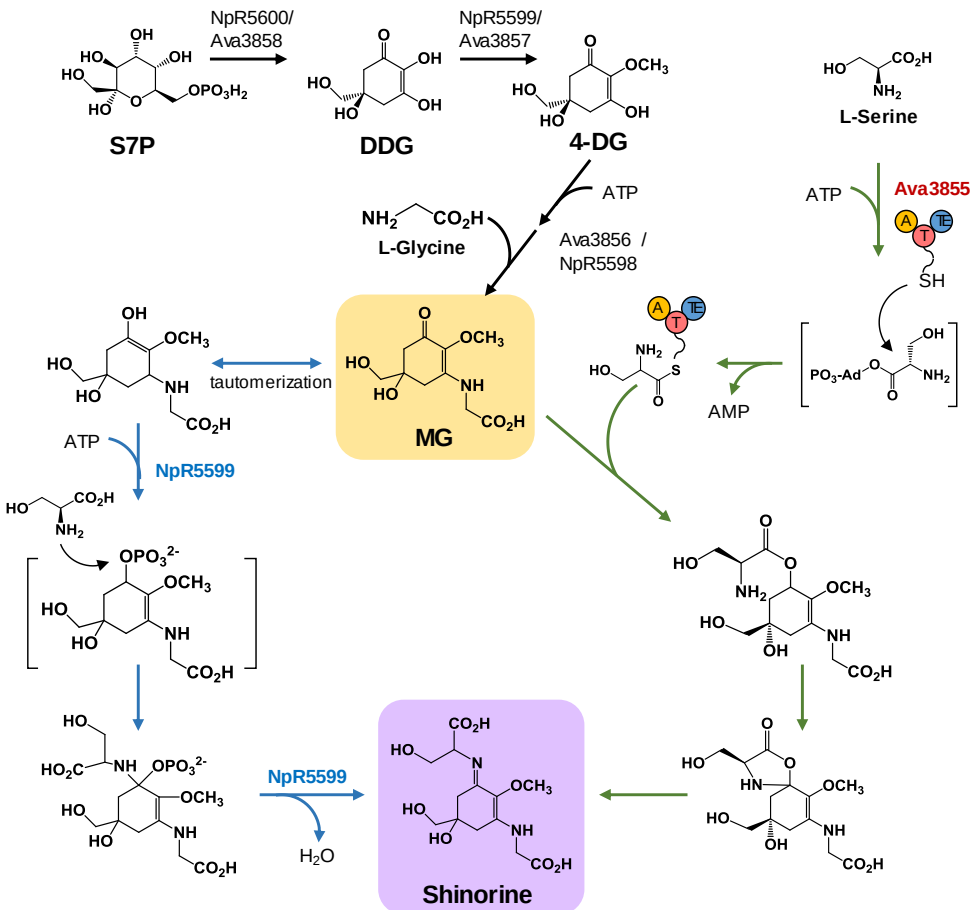

Figure 7.10 Alternative mechanisms of production of shinorine from mycosporine-glycine (MG)

Shinorine biosynthetic pathway in cyanobacteria describing the two alternative routes to the iminomycosporines from MG, catalyzing with D-ala-D-ala ligase from *N. punctiforme* (NpR5599) and NRPS-like ligase from *A. variabilis* (Ava3855). Although Ava3855 and NpR5597 are enzymes that play a similar role, they are completely different proteins in sequence, functional domain, and enzymatic mechanism. Ava3855 composed of adenylation (A), thiolation (T or peptidyl carrier protein (PCP) domain), and thioesterase (TE) domains. Clearly, the NpR5597 works differently with the Ava3855 because NpR5597 contains none of the domains typical of NRPSs.

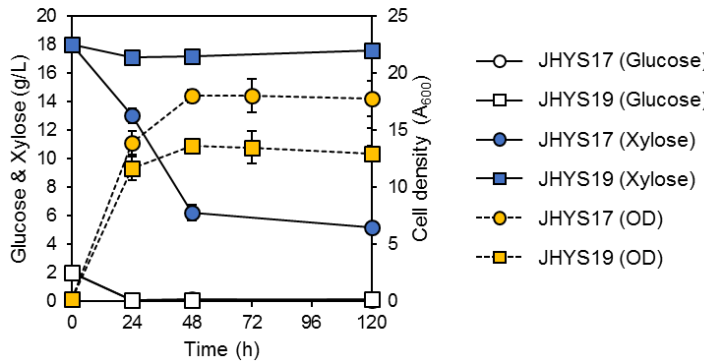

Figure 7.11 The effect of deleting competing pathway on shinorine production in xylose rich medium

JHYS17 and JHYS19 strains were grown in SC mix medium containing 2 g/L glucose and 18 g/L xylose for 120 h. Each value indicates the average ± SD of triplicate experiments.

JHYS17 and JHYS19 strains were cultured in SC medium, containing 10 g/L glucose and 10 g/L xylose (Fig. 7.12). The JHYS17 strain decreased shinorine production from 17.72 mg/L (Fig. 7.8D) to 6.62 mg/L (Fig. 7.12B) as the amount of xylose in the medium was decreased. On the other hand, JHYS19 strain showed significant improvement in shinorine production by 3.3-fold, reaching 21.9 mg/L with 7.67 mg/gDCW content, compared with JHYS17 strain, even though JHYS19 strain consumed only half of xylose in medium (Fig. 7.12).

The effect was also verified about additional overexpression of *Ava3858* in JHYS19 strain. JHYS19 strain used as parental strain to construct JHYS19-1 and JHYS19-2 strains by transformed p413GPD empty vector and p413GPD-Ava3858, respectively. JHYS19-2 strain produced 23.56 mg/L shinorine with 6.66 mg/gDCW content and JHYS19-2 showed 3.7% increased shinorine production (24.44 mg/L, 7.14 mg/gDCW) compared with JHYS19-1 strain, which was very similar (Fig. 7.13). Although Ava3838 gene overexpression was effective in shinorine production in the previous experiments (Fig. 7.9), overexpression of Ava3858 was not effective in *TAL1*-deficient strains. The reason for this result is considered that the *tal1Δ* increased the pool of S7P, so that offset ability of the Ava3858 to occupy S7P competing with Tal1.

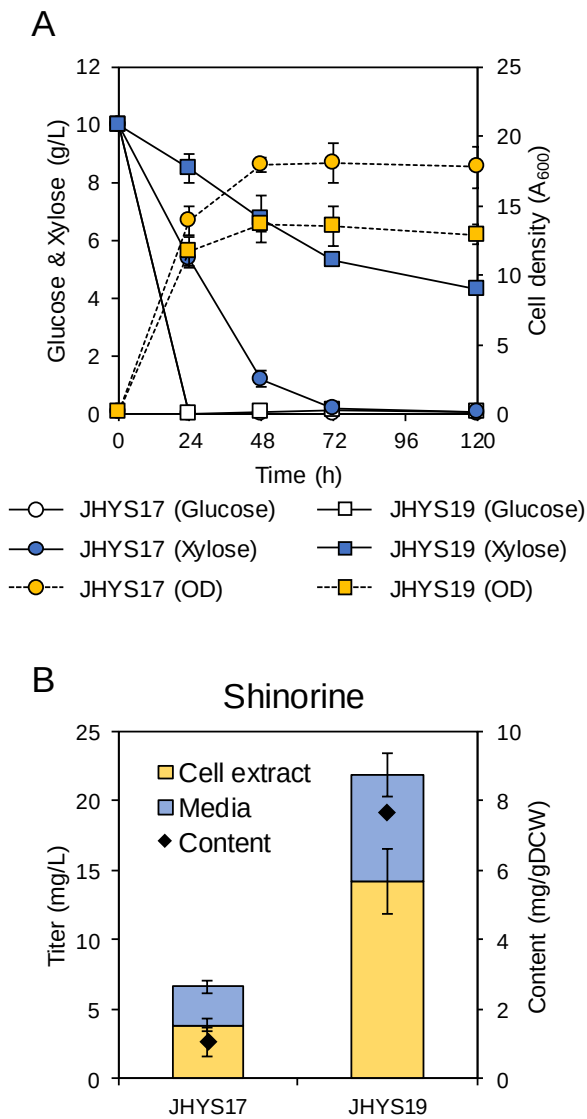

Figure 7.12 The effect of disruption of competing pathway on shinorine production

(A) Cell growth, glucose and xylose concentration, cell growth, and (B) shinorine production. JHYS17 and JHYS19 strains were grown in SC mix medium containing 10 g/L glucose and 10 g/L xylose for 120 h. Each value indicates the average ± SD of triplicate experiments.

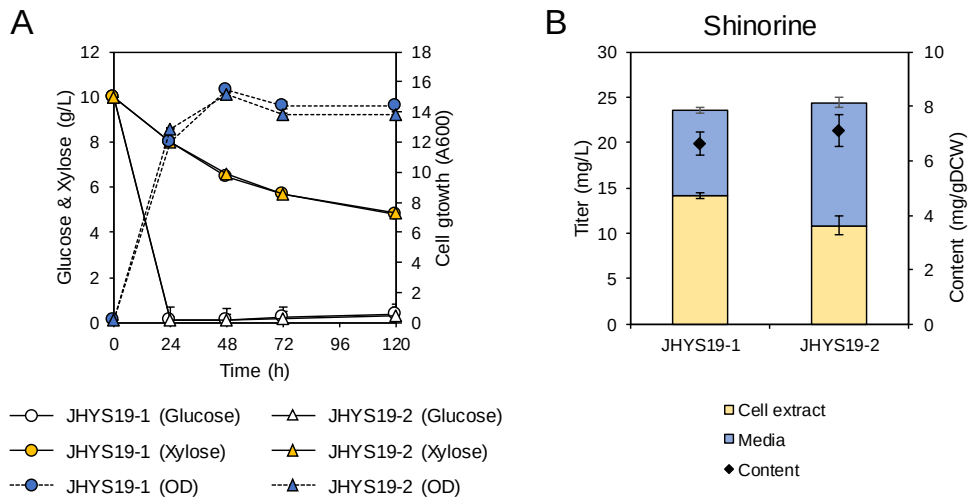

Figure 7.13 The effect of overexpression of Ava3858 in JHYS19 strain (*tal1Δ*)

A. Cell growth, glucose and xylose concentration and cell growth.

B. Shinorine production.

JHYS19-1 harboring empty vector, p413GPD, and JHYS19-2 strains harboring p413GPD-Ava3858 plasmid were grown in SC mix medium containing 10 g/L glucose and 10 g/L xylose for 120 h. Each value indicates the average ± SD of triplicate

7.16. Enhancing carbon flux to pentose phosphate pathway by overexpressing transcriptional factor Stb5 and transketolase Tkl1

To increase the production of shinorine by using xylose as a carbon source, it is necessary to reinforce the pentose phosphate pathway (PPP). Therefore, I overexpressed genes related to PPP, transcriptional factor Stb5 and transketolase Tkl1. Stb5 has dual function as activator and repressor required for PPP regulation [175]. It is known that the Stb5 binding site exists in the promoter region of the genes of the PPP pathway, such as *ZWF1* (glucose-6-phophate dehtdoregenase), *GND1* (phosphogluconate dehydrogenase), and *TKL1*. Since these enzymes are involved in the production of NADPH in the PPP and the generated NADPH plays an important role in oxidative stress resistance, Stb5, which regulates the expression of these genes plays an important role in the oxidative stress response. Especially, expression of Tkl1 which is create a reversible connection between two main metabolic pathways, the PPP and glycolysis is critical, when yeast is cultured with xylose as a carbon source [183,184].

To verify the effect of overexpressing Stb5 and Tkl1, genes expression plasmids, p414ADH-STB5, p414GPD-TKL1, and coex414-STB5-TKL1 were constructed. The *STB5* gene was overexpressed under control of relatively weak promoter, P_{ADH1}, because of expression using strong promoter like P_{TEF1} resulted in growth inhibition, while *TKL1* was overexpressed using strong promoter, P_{TDH3}. The p414ADH-STB5 and p414GPD-TKL1 is plasmid for overexpressing *STB5* and *TKL1*, respectively,

and coex414-STB5-TKL1 plasmid is a vector for expressing both genes.

The JHYS19-3, control strain harboring empty vector, p414GPD, produced 22.53 mg/L shinorine with 6.51 mg/gDCW content (Fig. 7.14D). JHYS19-4 and JHYS19-5 strain, which is JHYS19 strain harboring p414ADH-STB5 and p414GPD-TKL1, respectively, showed improved shinorine production up to 26.82 mg/L and 25.14 mg/L, respectively, compared with JHY462 indicating that overexpression of *STB5* or *TKL1* can contribute to shinorine production by enhancing PPP (Fig. 7.14D). Cells overexpressing *STB5* and *TKL1* (JHYS19-6) showed the highest level of shinorine production, reaching 31.55 mg/L, which is a 1.4-fold higher level than that produced in JHYS19-3. Furthermore, JHYS19-6 strain showed increase in xylose consumption rate compared with other strains, JHYS19-3, JHYS19-4, and JHYS19-5 (Fig. 7.14B). This result indicates that overexpression of *STB5* and *TKL1* together induced synergistic effect on improvement of shinorine production.

7.17. Conclusions

In this chapter *S. cerevisiae* strain capable of producing shinorine was developed by introducing shinorine biosynthetic pathways from *N. punctiforme* and *A. variabilis*. Furthermore, as an effort to increase S7P pool, *XYL1* (xylose reductase), *XYL2* (xylitol dehydrogenase), and *XYL3* (xylulokinase) genes involved in xylose assimilation were introduced in *S. cerevisiae*, resulting in efficient production of

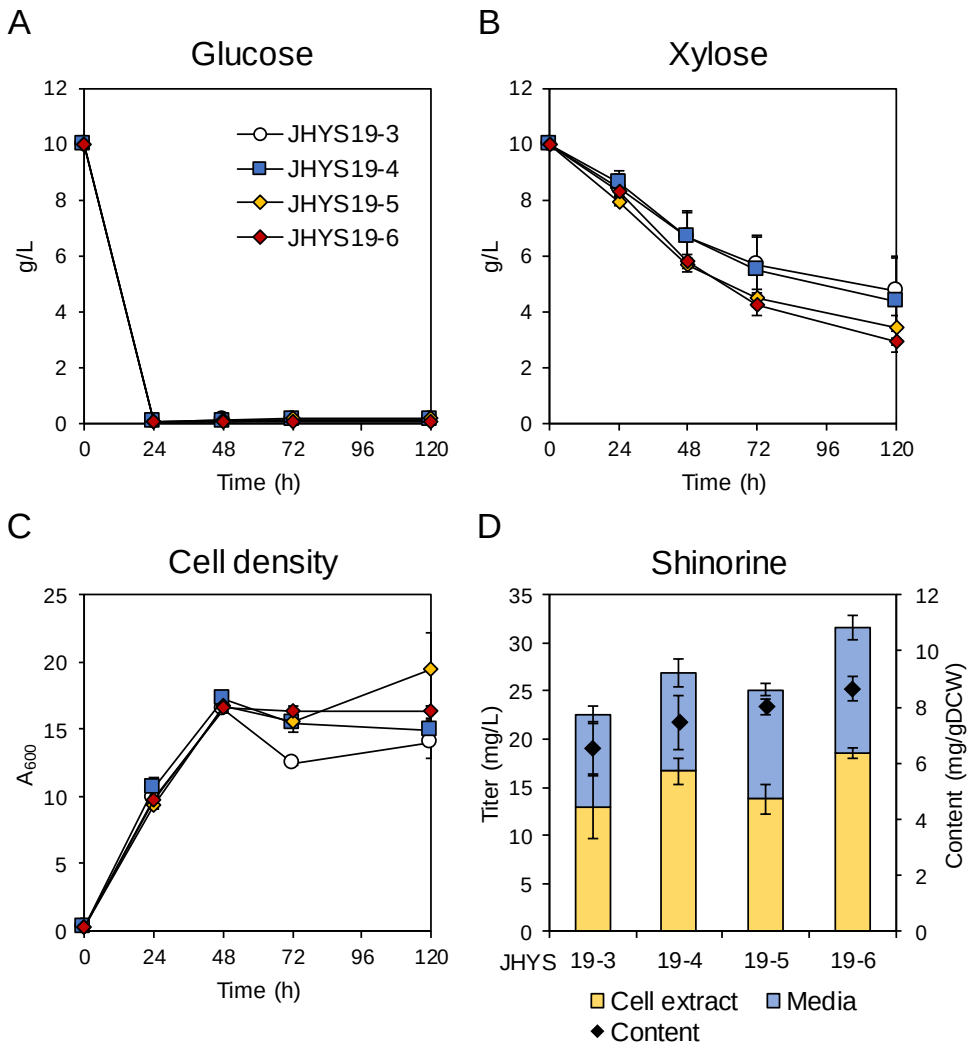

Figure 7.14 Improvement of shinorine production by overexpressing *STB5* and *TKL1*

The amount of glucose (A) and xylose (B) remaining in the medium. (C) Cell growth. (D) Shinorine production. All strains were grown in SC-Trp medium containing 10 g/L glucose and 10 g/L xylose for 120 h. Each value indicates the average ± SD of triplicate experiments

shinorine using xylose as a carbon source and also competitive pathway that consume S7P was disrupted. Moreover, to enhancing PP pathway, transcriptional factor (Stb5) for PP pathway and transketolase (Tal1) was overexpressed in JHYS17 strain, resulting in the more improved shinorine production. In engineered JHYS17-2 strain, shinorine was produced up to 64.2 mg/L with the highest content 14.3 mg/gDCW, reported ever before in fed-batch cultivation.

Chapter 8.

Overall discussion and recommendations

In this dissertation, a variety of genetic engineering tools for metabolic engineering, including rational pathway manipulation, multi-copy integration, and promoter engineering were applied to increase isobutanol production in *S. cerevisiae*. Based on the accumulated genetic engineering technology through the study of isobutanol production, it was further applied to the production of shinorine, a UV blocking material, as a new target material.

In the first part, the production of isobutanol increased by enhancing the innate isobutanol production pathway of yeast. In particular, overexpression of the transcription factor of the enzymes involved in the pathway effectively increased isobutanol production. Overexpression of the pathway-specific genes is the most readily accessible strategies in metabolic engineering. Overexpression of multiple genes in the metabolic pathway can be achieved not only by overexpressing individual genes, but also by overexpressing major regulatory transcription factors governing the metabolic pathway. In this study, both strategies was used to increase the production of isobutanol and 3-mehtyl-1-butanol in *S. cerevisiae*. Leu3 is the major transcription factor regulating branched-chain amino acid biosynthesis [43]. Leu3 is activated by 2-IPM, an intermediate of the leucine biosynthetic pathway, but represses its target genes in the absence of 2-IPM [138]. Leu3 targets include *ILV2* and *ILV5* [43,140], which are commonly required for isobutanol and 3-methyl-1-butanol production and *LEU4*, *LEU1*, and *LEU2* genes only involved in 3-methyl-1-butanol production [43,139]. In this study, the expression of Leu3Δ601 a constitutively active form of Leu3 was successfully applied [46], for the enhanced

production of isobutanol and 3-methyl-1-butanol, in combination with other strategies such as deleting *BAT1* and *ALD6* in competing pathways and overexpressing pathway-specific genes from heterologous promoters [6,142]. The potential targets of Leu3 also include other genes which could be beneficial for the production of isobutanol and 3-methyl-1-butanol. For example, *MAE1* encoding malic enzyme is also a potential target of Leu3, thus the expression of *MAE1* can also be induced by Leu3Δ601 [42]. Mae1 converting malate to pyruvate in mitochondria might contribute to providing mitochondrial pyruvate that serve as a substrate for isobutanol and 3-methyl-1-butanol production as well as providing NADPH, the cofactor required for Ilv5 activity [185]. In fact, recently *MAE1* was overexpressed to increase isobutanol production by resolving cofactor imbalance [28].

Although several efforts have been made to produce isobutanol in yeast, this study is the first demonstration of metabolic engineering approach to produce 3-methyl-1-butanol in yeast. Since 2-KIV is a common intermediate for the production of isobutanol and 3-methyl-1-butanol, I tried to shift the flux of 2-KIV to 3-methyl-1-butanol production in the isobutanol-production strain by additional overexpression of genes involved in 2-KIC synthesis. As previously shown in *E. coli* [186], overexpression of $LEU4^{D578Y}$, a feedback-insensitive mutant of *LEU4* [144], as well as *LEU2* gene was successful in increasing 3-methyl-1-butanol production while reducing isobutanol titers. However, unexpectedly, further overexpression of *LEU1* decreased 3-methyl-1-butanol production. Since I overexpressed 8 genes from

heterologous strong promoters, additional expression of *LEU1* might cause metabolic burden, resulting in reduced protein expression levels of essential enzymes in the metabolic pathways. Otherwise, since Leu1 requires iron-sulfur cluster as a cofactor, overexpression of *LEU1* might cause problems in iron-sulfur cluster availability for Ilv3, a mitochondrial iron-sulfur protein involved in isobutanol and 3-methyl-1-butanol production [187].

In the second part, mitochondrial isobutanol biosynthetic pathway was further developed for improvement of isobutanol production in *S. cerevisiae*. Subcellular compartmentalization of isobutanol biosynthetic pathway is one of the bottlenecks preventing efficient production in yeast. The natural isobutanol biosynthetic pathway in *S. cerevisiae* requires import of pyruvate into the mitochondria and export of 2-KIV into the cytoplasm. Previously, it has been shown that construction of mitochondrial pathway by re-localizing the last two cytosolic enzymes, KDC and ADH, into the mitochondria could improve isobutanol production [23]. Mitochondrial pathway might not only solve the problem of 2-KIV transport across the membrane, but also provide additional advantages such as increasing reaction rates through concentration of substrates. In addition, iron-sulfur cluster is synthesized exclusively in the mitochondria, making it more available for Ilv3, an iron-sulfur protein [188]. However, since *S. cerevisiae* has reduced mitochondrial function and pyruvate transport into mitochondria at high glucose concentrations or during anaerobic conditions [25,154], it is essential to increase mitochondrial pyruvate pool to improve mitochondrial isobutanol synthesis.

Therefore, isobutanol production was improved via mitochondrial pathway by increasing mitochondrial uptake of pyruvate through MPC. I first generated *S. cerevisiae* strain having mitochondrial isobutanol biosynthetic pathway based on previous studies [23,28]. Isobutanol production was improved by deleting competing pathway enzymes (Bat1, Ald6, and Lpd1), overexpressing all biosynthetic enzymes (Ilv2, Ilv5, Ilv3, Aro10, and Adh2) in the mitochondria by re-locating Aro10 and Adh2 into the mitochondria and overexpressing a constitutively active transcription factor Leu3Δ601. Although *LEU4* deletion was also effective in increasing isobutanol production in the *bat1Δald6Δ* background, it exerted a negative effect in combination with *lpd1Δ*. The reasons for these results are not clear yet, but since 2-IPM synthesized by Leu4 activates endogenous transcription factor Leu3, deleting *LEU4* gene might cause reduced expression levels of Leu3 target genes including *ILV2* and *ILV5* [43,138,140], affecting isobutanol synthesis.

MPC in the mitochondrial inner membrane is necessary for pyruvate uptake into the mitochondrial matrix [147,148]. *S. cerevisiae* has three homologous proteins, Mpc1, Mpc2, and Mpc3 forming two types of hetero-oligomeric complex, MPC_{FERM} and MPC_{OX} [154]. Mpc1, a common subunit of MPC, is constitutively expressed, but Mpc2 and Mpc3 are expressed under fermentative and respiratory conditions, respectively, forming MPC_{FERM} and MPC_{OX} [154]. Previously, overexpression of *MPC1* and *MPC2* from *S. cerevisiae* was shown to improve acetoin production via reconstructed mitochondrial pathway in *Candida glabrata* [189]. But I compared the effects of overexpressing Mpc1, MPC_{FERM} (Mpc1 and Mpc2) or MPC_{OX} (Mpc1 and

Mpc3) on mitochondrial isobutanol production. Overexpression of MPC_{OX} was most effective in increasing isobutanol production, followed by overexpression of Mpc1 alone. Overexpression of MPC_{FERM} was least effective. These results agree with a recent finding showing that MPC_{OX} has about 2-fold higher rate of pyruvate import than MPC_{FERM} [154]. Since fermentation pathway is dominant during the growth of *S. cerevisiae* on glucose, pyruvate flux to the mitochondria through the low-affinity MPC_{FERM} might not be sufficient for isobutanol production. Overexpression of the high-affinity MPC_{OX} using a strong constitutive promoter might increase pyruvate pool in the mitochondria even under fermentative conditions, leading to an improved isobutanol production. Overexpression of MPC_{OX} might also be a useful strategy for the production of other pyruvate-derived chemicals in mitochondria. However, even in cells overexpressing MPC_{OX}, pyruvate is mainly used for ethanol production. Therefore, further studies might be necessary for more efficient redirection of pyruvate flux into the mitochondria.

In addition, isobutanol was further improved via mitochondrial isobutanol biosynthetic pathway with overexpressing genes involved in iron-sulfur cluster assembly. Dihyroxyacid dehydratase (Ilv3) involved in valine catabolism is Fe-S protein that needs Fe-S cluster for its activation. In yeast, Fe-S cluster assembly exclusively occurs in mitochondria, which involves an iron donor, a sulfur donor, and a scaffold. The iron is delivered by Yfh1 (iron chaperone) and the sulfur is donated by Nfs1 (cysteine desulfurase) onto the scaffold protein Isu1 [155]. Especially, overexpression of *NFS1* and *ISD11* (Nfs1 activator) among them was

effective in enhancing isobutanol production.

In the third part, *S. cerevisiae* was engineered to improvement of isobutanol production by construction of artificial cytosolic isobutanol biosynthetic pathway using integration of related genes into multiple delta site and rDNA repeats in *S. cerevisiae* genome. Overexpression of bacterial *alsS* significantly improved isobutanol production with additional introduction of cytosol targeted Ilv5 (Ilv5ΔN48) and Ilv3 (Ilv3ΔN19) with kozak sequence.

I found that overexpressing *alsS* from *B. subtilis* in *S. cerevisiae* encourages severe cell growth hindrance, but this problem was solved by *alsS* expression controlled with the copper inducible promoter and additional overexpressing the *ILV5ΔN48* and *ILV3ΔN19* genes involved in subsequent reactions of alsS for production isobutanol. Furthermore, this phenomenon applied to development of novel screening system combining with multi-copy delta- and rDNA- integration for selecting strains into which a large amount of genes were introduced (Figure 1B). Using this system, I successfully generated JHY43D24 strain containing 4-copy alsS and 3-copy of *ILV5ΔN48* and *ILV3ΔN19* with 227.2 mg/L isobutanol titer. My final engineered strain JHY43D24-3 overexpressing *ILV5ΔN48*, *ILV3ΔN19*, *kivd*, and *ADH2* via plasmid showed a significant increase in isobutanol titer.

To further improve the production of isobutanol, future studies should be focused on increasing pool of NADPH and iron-sulfur cluster for improving activity of Ilv5ΔN49 and Ilv3ΔN19 enzymes, respectively, since they require NADPH and ISC as cofactor for its activity. Especially, since the copper and iron regulations for

homeostasis are closely linked to each other in yeast, it is expected that further investigation of Fe-S assembly is needed in the engineered strain expressing *alsS* using copper induction system.

Despite many attempts and strategies for increasing isobutanol in *S. cerevisiae*, the production of isobutanol in yeast is much lower than with bacteria. Although the production titers of isobutanol are still lower compared with those produced in engineered bacteria, the robustness and safety of *S. cerevisiae* system might provide some advantages as an industrial strain producing higher alcohols and other alcohol derivatives.

In the fourth part, an engineered *S. cerevisiae* strain capable shinorine production was developed by combining introduction of shinorine biosynthetic pathway from cyanobacteria and metabolic pathway engineering by introducing shinorine biosynthetic pathway consisting NpR5600, NpR5599, NpR5598, and NpR5597 from *N. punctiforme* and Ava3858 from *A. variabilis*. Furthermore, I also improved production of shinorine in *S. cerevisiae* by introducing xylose assimilation pathway consisting Xyl1, Xyl2, and Xyl3 from *S. stiptis* and then using xylose as carbon source. Deleting competing pathway consuming S7P, and overexpression of gene related to pentose phosphate pathway, *STB5* and *TKL1*, contributed to increasing production of shinorine. In previous reports to produce shinorine, most studies have been focused on using cyanobacteria like identifying cyanobacteria capable of producing shinorine or increasing shinorine accumulation through exposure to UV. However, production of shinorine using cyanobacteria is still very

low due to the difficulties of gene manipulation and cultivation of cyanobacteria. Although, recently some attempts have been made to produce shinorine in *E. coli* and *C. glutamicum*, it is an early research stage [99,106]. However, in this dissertation, I first reported the possibility of producing sunscreen material shinorine in a yeast strain and successfully increased shinorine production by enhancing pentose phosphate pathway. To further improve the production of shinorine, further studies should be focused on fine tuning of expression of *TAL1* gene because of deficiency of cell growth in *tal1*Δ strain cultured in medium containing xylose and constructing a strain that consumes xylose more efficiently by evolutional approach.

Bibliography

1. Woolston BM, Edgar S, Stephanopoulos G: **Metabolic engineering: past and future**. *Annu Rev Chem Biomol Eng* 2013, **4**:259-288.
2. Liu LQ, Redden H, Alper HS: **Frontiers of yeast metabolic engineering: diversifying beyond ethanol and *Saccharomyces***. *Current Opinion in Biotechnology* 2013, **24**:1023-1030.
3. Peralta-Yahya PP, Zhang F, del Cardayre SB, Keasling JD: **Microbial engineering for the production of advanced biofuels**. *Nature* 2012, **488**:320-328.
4. Ting CN, Wu J, Takahashi K, Endo A, Zhao H: **Screened butanol-tolerant *Enterococcus faecium* capable of butanol production**. *Appl Biochem Biotechnol* 2012, **168**:1672-1680.
5. Hazelwood LA, Daran JM, van Maris AJ, Pronk JT, Dickinson JR: **The Ehrlich pathway for fusel alcohol production: a century of research on *Saccharomyces cerevisiae* metabolism**. *Appl Environ Microbiol* 2008, **74**:2259-2266.
6. Lilly M, Bauer FF, Styger G, Lambrechts MG, Pretorius IS: **The effect of increased branched-chain amino acid transaminase activity in yeast on the production of higher alcohols and on the flavour profiles of wine and distillates**. *FEMS Yeast Res* 2006, **6**:726-743.
7. Prohl C, Kispal G, Lill R: **Branched-chain-amino-acid transaminases of yeast *Saccharomyces cerevisiae***. *Methods Enzymol* 2000, **324**:365-375.
8. Dickinson JR, Harrison SJ, Hewlins MJ: **An investigation of the metabolism of valine to isobutyl alcohol in *Saccharomyces cerevisiae***. *J Biol Chem* 1998, **273**:25751-25756.
9. ter Schure EG, Flikweert MT, van Dijken JP, Pronk JT, Verrips CT: **Pyruvate decarboxylase catalyzes decarboxylation of branched-chain 2-oxo acids but is not essential for fusel alcohol production by *Saccharomyces cerevisiae***. *Appl Environ Microbiol* 1998, **64**:1303-1307.
10. Vuralhan Z, Luttik MA, Tai SL, Boer VM, Morais MA, Schipper D, Almering MJ, Kotter P, Dickinson JR, Daran JM, et al.: **Physiological characterization of the *ARO10*-dependent, broad-substrate-specificity 2-oxo acid decarboxylase activity of *Saccharomyces cerevisiae***. *Appl Environ Microbiol* 2005, **71**:3276-3284.
11. Dickinson JR, Lanterman MM, Danner DJ, Pearson BM, Sanz P, Harrison SJ, Hewlins MJ: **A ^{13}C nuclear magnetic resonance investigation of the metabolism of leucine to isoamyl alcohol in *Saccharomyces cerevisiae***. *J Biol Chem* 1997, **272**:26871-26878.

12. Leuchtenberger W, Huthmacher K, Drauz K: **Biotechnological production of amino acids and derivatives: current status and prospects**. *Applied Microbiology and Biotechnology* 2005, **69**:1-8.

13. Blombach B, Riester T, Wieschalka S, Ziert C, Youn JW, Wendisch VF, Eikmanns BJ: ***Corynebacterium glutamicum*** **tailored for efficient isobutanol production**. *Applied and Environmental Microbiology* 2011, **77**:3300-3310.

14. Atsumi S, Hanai T, Liao JC: **Non-fermentative pathways for synthesis of branched-chain higher alcohols as biofuels**. *Nature* 2008, **451**:86-U13.

15. Bastian S, Liu X, Meyerowitz JT, Snow CD, Chen MM, Arnold FH: **Engineered ketol-acid reductoisomerase and alcohol dehydrogenase enable anaerobic 2-methylpropan-1-ol production at theoretical yield in *Escherichia coli***. *Metab Eng* 2011, **13**:345-352.

16. Hong KK, Nielsen J: **Metabolic engineering of *Saccharomyces cerevisiae*: a key cell factory platform for future biorefineries**. *Cellular and Molecular Life Sciences* 2012, **69**:2671-2690.

17. Sellis D, Callahan BJ, Petrov DA, Messer PW: **Heterozygote advantage as a natural consequence of adaptation in diploids**. *Proceedings of the National Academy of Sciences, USA* 2011, **108**:20666-20671.

18. Nielsen J, Jewett MC: **Impact of systems biology on metabolic engineering of *Saccharomyces cerevisiae***. *Fems Yeast Research* 2008, **8**:122-131.

19. Nevoigt E: **Progress in metabolic engineering of *Saccharomyces cerevisiae***. *Microbiology and Molecular Biology Reviews* 2008, **72**:379-412.

20. Li SS, Wen JP, Jia XQ: **Engineering *Bacillus subtilis* for isobutanol production by heterologous Ehrlich pathway construction and the biosynthetic 2-ketoisovalerate precursor pathway overexpression**. *Applied Microbiology and Biotechnology* 2011, **91**:577-589.

21. Miao R, Liu X, Englund E, Lindberg P, Lindblad P: **Isobutanol production in *Synechocystis* PCC 6803 using heterologous and endogenous alcohol dehydrogenases**. *Metabolic Engineering Communications* 2017, **5**:45-53.

22. Chen X, Nielsen KF, Borodina I, Kielland-Brandt MC, Karhumaa K: **Increased isobutanol production in *Saccharomyces cerevisiae* by overexpression of genes in valine metabolism**. *Biotechnology for Biofuels* 2011, **4**.

23. Avalos JL, Fink GR, Stephanopoulos G: **Compartmentalization of metabolic pathways in yeast mitochondria improves the production of branched-chain alcohols**. *Nat Biotechnol* 2013, **31**:335-341.

24. Yuan J, Ching CB: **Combinatorial assembly of large biochemical pathways into yeast chromosomes for improved production of value-added compounds**. *ACS Synth Biol* 2015, **4**:23-31.

25. Brat D, Weber C, Lorenzen W, Bode HB, Boles E: **Cytosolic re-localization and optimization of valine synthesis and catabolism enables inseased isobutanol production with the yeast *Saccharomyces cerevisiae***. *Biotechnol Biofuels* 2012, **5**:65.

26. Matsuda F, Kondo T, Ida K, Tezuka H, Ishii J, Kondo A: **Construction of an artificial pathway for isobutanol biosynthesis in the cytosol of *Saccharomyces cerevisiae***. *Bioscience, Biotechnology, and Biochemistry* 2012, **76**:2139-2141.

27. Lee WH, Seo SO, Bae YH, Nan H, Jin YS, Seo JH: **Isobutanol production in engineered *Saccharomyces cerevisiae* by overexpression of 2-ketoisovalerate decarboxylase and valine biosynthetic enzymes**. *Bioprocess and Biosystems Engineering* 2012, **35**:1467-1475.

28. Matsuda F, Ishii J, Kondo T, Ida K, Tezuka H, Kondo A: **Increased isobutanol production in *Saccharomyces cerevisiae* by eliminating competing pathways and resolving cofactor imbalance**. *Microbial Cell Factories* 2013, **12**.

29. Ikeda M: **Amino acid production processes**. *Adv Biochem Eng Biotechnol* 2003, **79**:1-35.

30. Park JH, Lee KH, Kim TY, Lee SY: **Metabolic engineering of *Escherichia coli* for the production of L-valine based on transcriptome analysis and in silico gene knockout simulation**. *Proceedings of the National Academy of Sciences of the United States of America* 2007, **104**:7797-7802.

31. Sahm H, Eggeling L, Eikmanns B, Kramer R: **Metabolic design in amino-acid producing bacterium *Corynebacterium glutamicum***. *Fems Microbiology Reviews* 1995, **16**:243-252.

32. Kondo T, Tezuka H, Ishii J, Matsuda F, Ogino C, Kondo A: **Genetic engineering to enhance the Ehrlich pathway and alter carbon flux for increased isobutanol production from glucose by *Saccharomyces cerevisiae***. *Journal of Biotechnology* 2012, **159**:32-37.

33. Ng CY, Jung MY, Lee J, Oh MK: **Production of 2,3-butanediol in *Saccharomyces cerevisiae* by in silico aided metabolic engineering**. *Microbial Cell Factories* 2012, **11**.

34. Dickinson JR: **Pathways of leucine and valine catabolism in yeast**. *Methods Enzymol* 2000, **324**:80-92.

35. Pang SS, Duggleby RG: **Expression, purification, characterization, and reconstitution of the large-and small subunits of yeast acetohydroxyacid synthase**. *Biochemistry* 1999, **38**:5222-5231.

36. Lill R: **Function and biogenesis of iron-sulphur proteins**. *Nature* 2009, **460**:831-838.

37. Colon M, Hernandez F, Lopez K, Quezada H, Gonzalez J, Lopez G, Aranda C, Gonzalez A: ***Saccharomyces cerevisiae*** **Bat1 and Bat2 aminotransferases have functionally diverged from the ancestral-like** ***Kluyveromyces lactis*** **orthologous enzyme**. *Plos One* 2011, **6**.

38. Yoshimoto H, Fukushige T, Yonezawa T, Sone H: **Genetic and physiological analysis of branched-chain alcohols and isoamyl acetate production in** ***Saccharomyces cerevisiae***. *Applied Microbiology and Biotechnology* 2002, **59**:501-508.

39. Holmberg S, Petersen JGL: **Regulation of isoleucine-valine biosynthesis in** ***Saccharomyces cerevisiae***. *Current Genetics* 1988, **13**:207-217.

40. Casalone E, Barberio C, Cavalieri D, Polsinelli M: **Identification by functional analysis of the gene encoding alpha-isopropylmalate synthase II (*LEU9*) in *Saccharomyces cerevisiae***. *Yeast* 2000, **16**:539-545.

41. Wallace MA, Liou LL, Martins J, Clement MHS, Bailey S, Longo VD, Valentine JS, Gralla EB: **Superoxide inhibits 4Fe-4S cluster enzymes involved in amino acid biosynthesis. Cross-compartment protection by CuZn-superoxide dismutase**. *Journal of Biological Chemistry* 2004, **279**:32055-32062.

42. Kohlhaw GB: **Leucine biosynthesis in fungi: Entering metabolism through the back door**. *Microbiology and Molecular Biology Reviews* 2003, **67**:1-15.

43. Friden P, Schimmel P: ***LEU3*** **of** ***Saccharomyces cerevisiae*** **activates multiple genes for branched-chain amino acid biosynthesis by binding to a common decanucleotide core sequence**. *Mol Cell Biol* 1988, **8**:2690-2697.

44. Todd RB, Andrianopoulos A: **Evolution of a fungal regulatory gene family: the Zn(II)2Cys6 binuclear cluster DNA binding motif**. *Fungal Genet Biol* 1997, **21**:388-405.

45. Remboutsika E, Kohlhaw GB: **Molecular architecture of a Leu3p-DNA complex in solution: a biochemical approach**. *Mol Cell Biol* 1994, **14**:5547-5557.

46. Friden P, Reynolds C, Schimmel P: **A large internal deletion converts yeast *LEU3* to a constitutive transcriptional activator**. *Mol Cell Biol* 1989, **9**:4056-4060.

47. Wang D, Zheng F, Holmberg S, Kohlhaw GB: **Yeast transcriptional regulator Leu3p. Self-masking, specificity of masking, and evidence for regulation by the intracellular level of Leu3p**. *J Biol Chem* 1999, **274**:19017-19024.

48. Mamane Y, Hellauer K, Rochon MH, Turcotte B: **A linker region of the yeast zinc cluster protein leu3p specifies binding to everted repeat DNA**. *J Biol Chem* 1998, **273**:18556-18561.

49. Zhou KM, Bai YL, Kohlhaw GB: **Yeast regulatory protein *LEU3*: a structure-function analysis**. *Nucleic Acids Res* 1990, **18**:291-298.

50. Sze JY, Woontner M, Jaehning JA, Kohlhaw GB: **In vitro transcriptional activation by a metabolic intermediate: activation by Leu3 depends on alpha-isopropylmalate**. *Science* 1992, **258**:1143-1145.

51. Cavalieri D, Casalone E, Bendoni B, Fia G, Polsinelli M, Barberio C: **Trifluoroleucine resistance and regulation of alpha-isopropyl malate synthase in *Saccharomyces cerevisiae***. *Mol Gen Genet* 1999, **261**:152-160.

52. Kirkpatrick C, Schimmel P: *Detection of leucine-independent DNA site occupancy of the yeast Leu3p transcriptional activator in vivo*; 1995.

53. Friden P, Reynolds C, Schimmel P: **A large internal deletion converts yeast Leu3 to a constitutive transcriptional activator**. *Molecular and Cellular Biology* 1989, **9**:4056-4060.

54. Beinert H, Holm RH, Munck E: **Iron-sulfur clusters: nature's modular, multipurpose structures**. *Science* 1997, **277**:653-659.

55. Frazzon J, Fick JR, Dean DR: **Biosynthesis of iron-sulphur clusters is a complex and highly conserved process**. *Biochem Soc Trans* 2002, **30**:680-685.

56. Lill R, Diekert K, Kaut A, Lange H, Pelzer W, Prohl C, Kispal G: **The essential role of mitochondria in the biogenesis of cellular iron-sulfur proteins**. *Biol Chem* 1999, **380**:1157-1166.

57. Schilke B, Voisine C, Beinert H, Craig E: **Evidence for a conserved system for iron metabolism in the mitochondria of *Saccharomyces cerevisiae***. *Proc Natl Acad Sci U S A* 1999, **96**:10206-10211.

58. Muhlenhoff U, Gerber J, Richhardt N, Lill R: **Components involved in assembly and dislocation of iron-sulfur clusters on the scaffold protein Isu1p**. *Embo j* 2003, **22**:4815-4825.

59. Webert H, Freibert SA, Gallo A, Heidenreich T, Linne U, Amlacher S, Hurt E, Muhlenhoff U, Banci L, Lill R: **Functional reconstitution of mitochondrial Fe/S cluster synthesis on Isu1 reveals the involvement of ferredoxin**. *Nat Commun* 2014, **5**:5013.

60. Muhlenhoff U, Balk J, Richhardt N, Kaiser JT, Sipos K, Kispal G, Lill R: **Functional characterization of the eukaryotic cysteine desulfurase Nfs1p from *Saccharomyces cerevisiae***. *J Biol Chem* 2004, **279**:36906-36915.

61. Adam AC, Bornhovd C, Prokisch H, Neupert W, Hell K: **The Nfs1 interacting protein Isd11 has an essential role in Fe/S cluster biogenesis in mitochondria**. *Embo j* 2006, **25**:174-183.

62. Kato S, Mihara H, Kurihara T, Takahashi Y, Tokumoto U, Yoshimura T, Esaki N: **Cys-328 of IscS and Cys-63 of IscU are the sites of disulfide bridge formation in a covalently bound**

IscS/IscU complex: implications for the mechanism of iron-sulfur cluster assembly. *Proc Natl Acad Sci U S A* 2002, **99**:5948-5952.

63. Majewska J, Ciesielski SJ, Schilke B, Kominek J, Blenska A, Delewski W, Song JY, Marszalek J, Craig EA, Dutkiewicz R: **Binding of the chaperone Jac1 protein and cysteine desulfurase Nfs1 to the iron-sulfur cluster scaffold Isu protein is mutually exclusive**. *J Biol Chem* 2013, **288**:29134-29142.
64. Li H, Gakh O, Smith DYt, Isaya G: **Oligomeric yeast frataxin drives assembly of core machinery for mitochondrial iron-sulfur cluster synthesis**. *J Biol Chem* 2009, **284**:21971-21980.
65. Yamaguchi-Iwai Y, Dancis A, Klausner RD: ***AFT1*: a mediator of iron regulated transcriptional control in *Saccharomyces cerevisiae***. *Embo j* 1995, **14**:1231-1239.
66. Rodriguez-Manzaneque MT, Tamarit J, Belli G, Ros J, Herrero E: **Grx5 is a mitochondrial glutaredoxin required for the activity of iron/sulfur enzymes**. *Mol Biol Cell* 2002, **13**:1109-1121.
67. Kispal G, Csere P, Guiard B, Lill R: **The ABC transporter Atm1p is required for mitochondrial iron homeostasis**. *FEBS Lett* 1997, **418**:346-350.
68. Johnson DC, Dean DR, Smith AD, Johnson MK: **Structure, function, and formation of biological iron-sulfur clusters**. *Annu Rev Biochem* 2005, **74**:247-281.
69. Woolston BM, Edgar S, Stephanopoulos G: **Metabolic Engineering: Past and Future**. *Annual Review of Chemical and Biomolecular Engineering* 2013, **4**:259-288.
70. Keasling JD: **Manufacturing molecules through metabolic engineering**. *Science* 2010, **330**:1355-1358.
71. Kim JM, Vanguri S, Boeke JD, Gabriel A, Voytas DF: **Transposable elements and genome organization: a comprehensive survey of retrotransposons revealed by the complete *Saccharomyces cerevisiae* genome sequence**. *Genome Res* 1998, **8**:464-478.
72. Lesage P, Todeschini AL: **Happy together: the life and times of Ty retrotransposons and their hosts**. *Cytogenet Genome Res* 2005, **110**:70-90.
73. Xie W, Gai X, Zhu Y, Zappulla DC, Sternglanz R, Voytas DF: **Targeting of the yeast Ty5 retrotransposon to silent chromatin is mediated by interactions between integrase and Sir4p**. *Mol Cell Biol* 2001, **21**:6606-6614.
74. Yamada R, Taniguchi N, Tanaka T, Ogino C, Fukuda H, Kondo A: **Cocktail δ-integration: a novel method to construct cellulolytic enzyme expression ratio-optimized yeast strains**. *Microbial Cell Factories* 2010, **9**:32.

75. Shi S, Liang Y, Zhang MM, Ang EL, Zhao H: **A highly efficient single-step, markerless strategy for multi-copy chromosomal integration of large biochemical pathways in *Saccharomyces cerevisiae***. *Metab Eng* 2016, **33**:19-27.

76. Venema J, Tollervey D: **Ribosome synthesis in *Saccharomyces cerevisiae***. *Annu Rev Genet* 1999, **33**:261-311.

77. Cox H, Mead D, Sudbery P, Eland RM, Mannazzu I, Evans L: **Constitutive expression of recombinant proteins in the methylotrophic yeast *Hansenula polymorpha* using the PMA1 promoter**. *Yeast* 2000, **16**:1191-1203.

78. Ganley AR, Kobayashi T: **Highly efficient concerted evolution in the ribosomal DNA repeats: total rDNA repeat variation revealed by whole-genome shotgun sequence data**. *Genome Res* 2007, **17**:184-191.

79. Voelkel-Meiman K, Keil RL, Roeder GS: **Recombination-stimulating sequences in yeast ribosomal DNA correspond to sequences regulating transcription by RNA polymerase I**. *Cell* 1987, **48**:1071-1079.

80. Fang C, Wang Q, Selvaraj JN, Zhou Y, Ma L, Zhang G, Ma Y: **High copy and stable expression of the xylanase XynHB in *Saccharomyces cerevisiae* by rDNA-mediated integration**. *Sci Rep* 2017, **7**:8747.

81. Sun H, Zang X, Liu Y, Cao X, Wu F, Huang X, Jiang M, Zhang X: **Expression of a chimeric human/salmon calcitonin gene integrated into the *Saccharomyces cerevisiae* genome using rDNA sequences as recombination sites**. *Appl Microbiol Biotechnol* 2015, **99**:10097-10106.

82. Afaq F, Mukhtar H: **Botanical antioxidants in the prevention of photocarcinogenesis and photoaging**. *Exp Dermatol* 2006, **15**:678-684.

83. McKenzie RL, Bjorn LO, Bais A, Ilyasad M: **Changes in biologically active ultraviolet radiation reaching the Earth's surface**. *Photochem Photobiol Sci* 2003, **2**:5-15.

84. Jagger J: **Solar-UV actions on living cells**. *Praeger* 1985.

85. Lawrence KP, Long PF, Young AR: **Mycosporine-like Amino Acids for Skin Photoprotection**. *Curr Med Chem* 2017.

86. Shinzato C, Shoguchi E, Kawashima T, Hamada M, Hisata K, Tanaka M, Fujie M, Fujiwara M, Koyanagi R, Ikuta T, et al.: **Using the Acropora digitifera genome to understand coral responses to environmental change**. *Nature* 2011, **476**:320-323.

87. Singh SP, Klisch M, Sinha RP, Hader DP: **Genome mining of mycosporine-like amino acid (MAA) synthesizing and non-synthesizing cyanobacteria: A bioinformatics study**. *Genomics* 2010, **95**:120-128.

88. Singh SP, Kumari S, Rastogi RP, Singh KL, Sinha RP: **Mycosporine-like amino acids (MAAs): chemical structure, biosynthesis and significance as UV-absorbing/screening compounds**. *Indian J Exp Biol* 2008, **46**:7-17.

89. Nakamura H, Kobayashi Ji, Hirata Y: **Separation of mycosporine-like amino acids in marine organisms using reversed-phase high-performance liquid chromatography**. *Journal of Chromatography A* 1982, **250**:113-118.

90. Favre-Bonvin J, Arpin N, Brevard C: **Structure de la mycosporine (P 310)**. *Canadian Journal of Chemistry* 1976, **54**:1105-1113.

91. Torres A, Hochberg M, Pergament I, Smoum R, Niddam V, Dembitsky VM, Temina M, Dor I, Lev O, Srebnik M, et al.: **A new UV-B absorbing mycosporine with photo protective activity from the lichenized ascomycete *Collema cristatum***. *Eur J Biochem* 2004, **271**:780-784.

92. Carreto JI, Carignan MO: **Mycosporine-like amino acids: relevant secondary metabolites. Chemical and ecological aspects**. *Mar Drugs* 2011, **9**:387-446.

93. Wada N, Sakamoto T, Matsugo S: **Mycosporine-like amino acids and their derivatives as natural antioxidants**. *Antioxidants (Basel)* 2015, **4**:603-646.

94. Conde FR, Churio MS, Previtali CM: **The deactivation pathways of the excited-states of the mycosporine-like amino acids shinorine and porphyra-334 in aqueous solution**. *Photochem Photobiol Sci* 2004, **3**:960-967.

95. Favre-Bonvin J, Bernillon J, Salin N, Arpin N: **Biosynthesis of mycosporines: Mycosporine glutaminol in *Trichothecium roseum***. *Phytochemistry* 1987, **26**:2509-2514.

96. Shick JM, Dunlap WC: **Mycosporine-like amino acids and related Gadusols: biosynthesis, acumulation, and UV-protective functions in aquatic organisms**. *Annu Rev Physiol* 2002, **64**:223-262.

97. Rastogi RP, Richa, Sinha RP, Singh SP, Hader DP: **Photoprotective compounds from marine organisms**. *J Ind Microbiol Biotechnol* 2010, **37**:537-558.

98. Osborn AR, Kean KM, Alseud KM, Almabruk KH, Asamizu S, Lee JA, Karplus PA, Mahmud T: **Evolution and distribution of C7-cyclitol synthases in prokaryotes and eukaryotes**. *ACS Chem Biol* 2017, **12**:979-988.

99. Balskus EP, Walsh CT: **The genetic and molecular basis for sunscreen biosynthesis in cyanobacteria**. *Science* 2010, **329**:1653-1656.

100. Bebout BM, Garcia-Pichel F: **UV B-induced vertical migrations of cyanobacteria in a microbial mat**. *Applied and Environmental Microbiology* 1995, **61**:4215-4222.

101. Becker K, Hartmann A, Ganzera M, Fuchs D, Gostner MJ: **Immunomodulatory effects of the mycosporine-like amino acids shinorine and porphyra-334**. *Marine Drugs* 2016, **14**.
102. Mushir S, Fatma T: **Ultraviolet Radiation-absorbing Mycosporine-like Amino Acids in Cyanobacterium *Aulosira fertilissima*: Environmental perspective and characterization**; *J phycol* 2011, **43**:418-430.
103. Yang G, Cozad MA, Holland DA, Zhang Y, Luesch H, Ding Y: **Photosynthetic production of sunscreen shinorine using an engineered cyanobacterium**. *ACS Synthetic Biology* 2018, **7**:664-671.
104. Hartmann A, Murauer A, Ganzera M: **Quantitative analysis of mycosporine-like amino acids in marine algae by capillary electrophoresis with diode-array detection**. *J Pharm Biomed Anal* 2017, **138**:153-157.
105. Nozzi NE, Oliver JWK, Atsumi S: **Cyanobacteria as a platform for biofuel production**. *Frontiers in bioengineering and biotechnology* 2013, **1**:7.
106. Tsuge Y, Kawaguchi H, Yamamoto S, Nishigami Y, Sota M, Ogino C, Kondo A: **Metabolic engineering of *Corynebacterium glutamicum* for production of sunscreen shinorine**. *Biosci Biotechnol Biochem* 2018:1-8.
107. Miyamoto KT, Komatsu M, Ikeda H: **Discovery of gene cluster for mycosporine-like amino acid biosynthesis from *Actinomycetales* microorganisms and production of a novel mycosporine-like amino acid by heterologous expression**. *Appl Environ Microbiol* 2014, **80**:5028-5036.
108. WHITWORTH DA, RATLEDGE C: **Phosphoketolase in *Rhodotorula graminis* and other yeasts**. *Microbiology* 1977, **102**:397-401.
109. Auesukaree C, Damnernsawad A, Kruatrachue M, Pokethitiyook P, Boonchird C, Kaneko Y, Harashima S: **Genome-wide identification of genes involved in tolerance to various environmental stresses in *Saccharomyces cerevisiae***. *J Appl Genet* 2009, **50**:301-310.
110. Hong KK, Nielsen J: **Metabolic engineering of *Saccharomyces cerevisiae*: a key cell factory platform for future biorefineries**. *Cell Mol Life Sci* 2012, **69**:2671-2690.
111. Harhangi HR, Akhmanova AS, Emmens R, van der Drift C, de Laat WT, van Dijken JP, Jetten MS, Pronk JT, Op den Camp HJ: **Xylose metabolism in the anaerobic fungus Piromyces sp. strain E2 follows the bacterial pathway**. *Arch Microbiol* 2003, **180**:134-141.
112. Madhavan A, Tamalampudi S, Ushida K, Kanai D, Katahira S, Srivastava A, Fukuda H, Bisaria VS, Kondo A: **Xylose isomerase from polycentric fungus *Orpinomyces*: gene sequencing, cloning, and expression in *Saccharomyces cerevisiae* for bioconversion of xylose to ethanol**. *Appl Microbiol Biotechnol* 2009, **82**:1067-1078.

113. Stincone A, Prigione A, Cramer T, Wamelink MM, Campbell K, Cheung E, Olin-Sandoval V, Gruning NM, Kruger A, Tauqeer Alam M, et al.: **The return of metabolism: biochemistry and physiology of the pentose phosphate pathway**. *Biol Rev Camb Philos Soc* 2015, **90**:927-963.

114. Bhosale SH, Rao MB, Deshpande VV: **Molecular and industrial aspects of glucose isomerase**. *Microbiol Rev* 1996, **60**:280-300.

115. Sarthy AV, McConaughy BL, Lobo Z, Sundstrom JA, Furlong CE, Hall BD: **Expression of the *Escherichia coli* xylose isomerase gene in *Saccharomyces cerevisiae***. *Appl Environ Microbiol* 1987, **53**:1996-2000.

116. Zhou H, Cheng JS, Wang BL, Fink GR, Stephanopoulos G: **Xylose isomerase overexpression along with engineering of the pentose phosphate pathway and evolutionary engineering enable rapid xylose utilization and ethanol production by *Saccharomyces cerevisiae***. *Metab Eng* 2012, **14**:611-622.

117. Li X, Park A, Estrela R, Kim SR, Jin YS, Cate JH: **Comparison of xylose fermentation by two high-performance engineered strains of *Saccharomyces cerevisiae***. *Biotechnol Rep (Amst)* 2016, **9**:53-56.

118. Kim SR, Skerker JM, Kang W, Lesmana A, Wei N, Arkin AP, Jin YS: **Rational and evolutionary engineering approaches uncover a small set of genetic changes efficient for rapid xylose fermentation in *Saccharomyces cerevisiae***. *PLoS One* 2013, **8**:e57048.

119. Runquist D, Hahn-Hagerdal B, Bettiga M: **Increased ethanol productivity in xylose-utilizing *Saccharomyces cerevisiae* via a randomly mutagenized xylose reductase**. *Appl Environ Microbiol* 2010, **76**:7796-7802.

120. Cadete RM, de Las Heras AM, Sandstrom AG, Ferreira C, Girio F, Gorwa-Grauslund MF, Rosa CA, Fonseca C: **Exploring xylose metabolism in *Spathaspora* species: XYL1.2 from *Spathaspora passalidarum* as the key for efficient anaerobic xylose fermentation in metabolic engineered *Saccharomyces cerevisiae***. *Biotechnol Biofuels* 2016, **9**:167.

121. Gueldener U, Heinisch J, Koehler GJ, Voss D, Hegemann JH: **A second set of *loxP* marker cassettes for Cre-mediated multiple gene knockouts in budding yeast**. *Nucleic Acids Research* 2002, **30**.

122. Gueldener U, Heinisch J, Koehler GJ, Voss D, Hegemann JH: **A second set of *loxP* marker cassettes for Cre-mediated multiple gene knockouts in budding yeast**. *Nucleic Acids Res* 2002, **30**:e23.

123. Mumberg D, Muller R, Funk M: **Yeast vectors for the controlled expression of heterologous proteins in different genetic backgrounds**. *Gene* 1995, **156**:119-122.

124. Kim S, Hahn JS: **Efficient production of 2,3-butanediol in *Saccharomyces cerevisiae* by eliminating ethanol and glycerol production and redox rebalancing**. *Metab Eng* 2015, **31**:94-101.

125. Baek SH, Kwon EY, Bae SJ, Cho BR, Kim SY, Hahn JS: **Improvement of D-lactic acid production in *Saccharomyces cerevisiae* Under acidic conditions by evolutionary and rational metabolic engineering**. *Biotechnol J* 2017, **12**.

126. Gietz RD, Woods RA: **Transformation of yeast by lithium acetate/single-stranded carrier DNA/polyethylene glycol method**. *Methods Enzymol* 2002, **350**:87-96.

127. Connor MR, Liao JC: **Microbial production of advanced transportation fuels in non-natural hosts**. *Curr Opin Biotechnol* 2009, **20**:307-315.

128. Weber C, Farwick A, Benisch F, Brat D, Dietz H, Subtil T, Boles E: **Trends and challenges in the microbial production of lignocellulosic bioalcohol fuels**. *Appl Microbiol Biotechnol* 2010, **87**:1303-1315.

129. Blombach B, Eikmanns BJ: **Current knowledge on isobutanol production with *Escherichia coli*, *Bacillus subtilis* and *Corynebacterium glutamicum***. *Bioeng Bugs* 2011, **2**:346-350.

130. Atsumi S, Wu TY, Eckl EM, Hawkins SD, Buelter T, Liao JC: **Engineering the isobutanol biosynthetic pathway in *Escherichia coli* by comparison of three aldehyde reductase/alcohol dehydrogenase genes**. *Appl Microbiol Biotechnol* 2010, **85**:651-657.

131. Yamamoto S, Suda M, Niimi S, Inui M, Yukawa H: **Strain optimization for efficient isobutanol production using *Corynebacterium glutamicum* under oxygen deprivation**. *Biotechnol Bioeng* 2013, **110**:2938-2948.

132. Hohmann S: **Osmotic adaptation in yeast--control of the yeast osmolyte system**. *Int Rev Cytol* 2002, **215**:149-187.

133. Nevoigt E: **Progress in metabolic engineering of *Saccharomyces cerevisiae***. *Microbiol Mol Biol Rev* 2008, **72**:379-412.

134. Porro D, Gasser B, Fossati T, Maurer M, Branduardi P, Sauer M, Mattanovich D: **Production of recombinant proteins and metabolites in yeasts: when are these systems better than bacterial production systems?** *Appl Microbiol Biotechnol* 2011, **89**:939-948.

135. Ryan ED, Kohlhaw GB: **Subcellular localization of isoleucine-valine biosynthetic enzymes in yeast**. *J Bacteriol* 1974, **120**:631-637.

136. Kispal G, Steiner H, Court DA, Rolinski B, Lill R: **Mitochondrial and cytosolic branched-chain amino acid transaminases from yeast, homologs of the myc oncogene-regulated Eca39 protein**. *J Biol Chem* 1996, **271**:24458-24464.

137. Schoondermark-Stolk SA, Tabernero M, Chapman J, Ter Schure EG, Verrips CT, Verkleij AJ, Boonstra J: **Bat2p is essential in *Saccharomyces cerevisiae* for fusel alcohol production on the non-fermentable carbon source ethanol**. *FEMS Yeast Res* 2005, **5**:757-766.

138. Baichwal VR, Cunningham TS, Gatzek PR, Kohlhaw GB: **Leucine biosynthesis in yeast : Identification of two genes (*LEU4*, *LEU5*) that affect alpha-Isopropylmalate synthase activity and evidence that *LEU1* and *LEU2* gene expression is controlled by alpha-Isopropylmalate and the product of a regulatory gene**. *Curr Genet* 1983, **7**:369-377.

139. Friden P, Schimmel P: ***LEU3* of *Saccharomyces cerevisiae* encodes a factor for control of RNA levels of a group of leucine-specific genes**. *Mol Cell Biol* 1987, **7**:2708-2717.

140. Boer VM, Daran JM, Almering MJ, de Winde JH, Pronk JT: **Contribution of the *Saccharomyces cerevisiae* transcriptional regulator Leu3p to physiology and gene expression in nitrogen- and carbon-limited chemostat cultures**. *FEMS Yeast Res* 2005, **5**:885-897.

141. Eden A, Simchen G, Benvenisty N: **Two yeast homologs of *ECA39*, a target for c-Myc regulation, code for cytosolic and mitochondrial branched-chain amino acid aminotransferases**. *J Biol Chem* 1996, **271**:20242-20245.

142. Buijs NA, Siewers V, Nielsen J: **Advanced biofuel production by the yeast *Saccharomyces cerevisiae***. *Curr Opin Chem Biol* 2013, **17**:480-488.

143. Romagnoli G, Luttik MA, Kotter P, Pronk JT, Daran JM: **Substrate specificity of thiamine pyrophosphate-dependent 2-oxo-acid decarboxylases in *Saccharomyces cerevisiae***. *Appl Environ Microbiol* 2012, **78**:7538-7548.

144. Oba T, Nomiyama S, Hirakawa H, Tashiro K, Kuhara S: **Asp578 in LEU4p is one of the key residues for leucine feedback inhibition release in sake yeast**. *Biosci Biotechnol Biochem* 2005, **69**:1270-1273.

145. Ida K, Ishii J, Matsuda F, Kondo T, Kondo A: **Eliminating the isoleucine biosynthetic pathway to reduce competitive carbon outflow during isobutanol production by *Saccharomyces cerevisiae***. *Microb Cell Fact* 2015, **14**:62.

146. Milne N, van Maris AJ, Pronk JT, Daran JM: **Comparative assessment of native and heterologous 2-oxo acid decarboxylases for application in isobutanol production by *Saccharomyces cerevisiae***. *Biotechnol Biofuels* 2015, **8**:204.

147. Bricker DK, Taylor EB, Schell JC, Orsak T, Boutron A, Chen YC, Cox JE, Cardon CM, Van Vranken JG, Dephoure N, et al.: **A Mitochondrial pyruvate carrier required for pyruvate uptake in yeast, drosophila, and humans**. *Science* 2012, **337**:96-100.

148. Herzig S, Raemy E, Montessuit S, Veuthey JL, Zamboni N, Westermann B, Kunji ERS, Martinou JC: **Identification and functional expression of the mitochondrial pyruvate carrier**. *Science* 2012, **337**:93-96.

149. Park SH, Kim S, Hahn JS: **Metabolic engineering of *Saccharomyces cerevisiae* for the production of isobutanol and 3-methyl-1-butanol**. *Applied Microbiology and Biotechnology* 2014, **98**:9139-9147.

150. Pronk JT, Steensma HY, vanDijken JP: **Pyruvate metabolism in *Saccharomyces cerevisiae***. *Yeast* 1996, **12**:1607-1633.

151. Kim S, Hahn JS: **Efficient production of 2,3-butanediol in *Saccharomyces cerevisiae* by eliminating ethanol and glycerol production and redox rebalancing**. *Metabolic Engineering* 2015, **31**:94-101.

152. Maarse AC, Van Loon AP, Riezman H, Gregor I, Schatz G, Grivell LA: **Subunit IV of yeast cytochrome c oxidase: cloning and nucleotide sequencing of the gene and partial amino acid sequencing of the mature protein**. *EMBO J* 1984, **3**:2831-2837.

153. Lee AC, Xu X, Blachly-Dyson E, Forte M, Colombini M: **The role of yeast VDAC genes on the permeability of the mitochondrial outer membrane**. *J Membr Biol* 1998, **161**:173-181.

154. Bender T, Pena G, Martinou JC: **Regulation of mitochondrial pyruvate uptake by alternative pyruvate carrier complexes**. *Embo Journal* 2015, **34**:911-924.

155. Balk J, Lill R: **The cell's cookbook for iron--sulfur clusters: recipes for fool's gold?** *Chembiochem* 2004, **5**:1044-1049.

156. Da Silva NA, Srikrishnan S: **Introduction and expression of genes for metabolic engineering applications in *Saccharomyces cerevisiae***. *FEMS Yeast Res* 2012, **12**:197-214.

157. Futcher B, Carbon J: **Toxic effects of excess cloned centromeres**. *Mol Cell Biol* 1986, **6**:2213-2222.

158. Lopes TS, de Wijs IJ, Steenhauer SI, Verbakel J, Planta RJ: **Factors affecting the mitotic stability of high-copy-number integration into the ribosomal DNA of *Saccharomyces cerevisiae***. *Yeast* 1996, **12**:467-477.

159. Semkiv MV, Dmytruk KV, Sibirny AA: **Development of a system for multicopy gene integration in *Saccharomyces cerevisiae***. *J Microbiol Methods* 2016, **120**:44-49.

160. Kozak M: **Point mutations define a sequence flanking the AUG initiator codon that modulates translation by eukaryotic ribosomes**. *Cell* 1986, **44**:283-292.

161. Hamilton R, Watanabe CK, de Boer HA: **Compilation and comparison of the sequence context around the AUG startcodons in *Saccharomyces cerevisiae* mRNAs**. *Nucleic Acids Res* 1987, **15**:3581-3593.

162. Li J, Liang Q, Song W, Marchisio MA: **Nucleotides upstream of the Kozak sequence strongly influence gene expression in the yeast *S. cerevisiae***. *J Biol Eng* 2017, **11**:25.

163. Zur H, Tuller T: **Strong association between mRNA folding strength and protein abundance in S. cerevisiae**. *EMBO Rep* 2012, **13**:272-277.

164. Dvir S, Velten L, Sharon E, Zeevi D, Carey LB, Weinberger A, Segal E: **Deciphering the rules by which 5'-UTR sequences affect protein expression in yeast**. *Proc Natl Acad Sci U S A* 2013, **110**:E2792-2801.

165. Butt TR, Sternberg EJ, Gorman JA, Clark P, Hamer D, Rosenberg M, Crooke ST: **Copper metallothionein of yeast, structure of the gene, and regulation of expression**. *Proc Natl Acad Sci U S A* 1984, **81**:3332-3336.

166. Thiele DJ: ***ACE1* regulates expression of the *Saccharomyces cerevisiae* metallothionein gene**. *Mol Cell Biol* 1988, **8**:2745-2752.

167. Etcheverry T: **Induced expression using yeast copper metallothionein promoter**. *Methods Enzymol* 1990, **185**:319-329.

168. Peng B, Williams TC, Henry M, Nielsen LK, Vickers CE: **Controlling heterologous gene expression in yeast cell factories on different carbon substrates and across the diauxic shift: a comparison of yeast promoter activities**. *Microbial Cell Factories* 2015, **14**:91.

169. de la Coba F, Aguilera J, de Galvez MV, Alvarez M, Gallego E, Figueroa FL, Herrera E: **Prevention of the ultraviolet effects on clinical and histopathological changes, as well as the heat shock protein-70 expression in mouse skin by topical application of algal UV-absorbing compounds**. *J Dermatol Sci* 2009, **55**:161-169.

170. M. Bandaranayake W: **Mycosporines: are they nature's sunscreens?** *Natural Product Reports* 1998, **15**:159-172.

171. Gao Q, Garcia-Pichel F: **Microbial ultraviolet sunscreens**. *Nat Rev Microbiol* 2011, **9**:791-802.

172. Curran KA, Leavitt JM, Karim AS, Alper HS: **Metabolic engineering of muconic acid production in *Saccharomyces cerevisiae***. *Metab Eng* 2013, **15**:55-66.

173. Chen Y, Bao J, Kim IK, Siewers V, Nielsen J: **Coupled incremental precursor and co-factor supply improves 3-hydroxypropionic acid production in *Saccharomyces cerevisiae***. *Metab Eng* 2014, **22**:104-109.

174. Xie W, Lv X, Ye L, Zhou P, Yu H: **Construction of lycopene-overproducing *Saccharomyces cerevisiae* by combining directed evolution and metabolic engineering**. *Metab Eng* 2015, **30**:69-78.

175. Larochelle M, Drouin S, Robert F, Turcotte B: **Oxidative stress-activated zinc cluster protein Stb5 has dual activator/repressor functions required for pentose phosphate pathway regulation and NADPH production**. *Mol Cell Biol* 2006, **26**:6690-6701.

176. Jin YS, Laplaza JM, Jeffries TW: ***Saccharomyces cerevisiae* engineered for xylose metabolism exhibits a respiratory response**. *Appl Environ Microbiol* 2004, **70**:6816-6825.

177. Gao Q, Garcia-Pichel F: **An ATP-grasp ligase involved in the last biosynthetic step of the iminomycosporine shinorine in *Nostoc punctiforme* ATCC 29133**. *J Bacteriol* 2011, **193**:5923-5928.

178. Lee FW, Da Silva NA: **Improved efficiency and stability of multiple cloned gene insertions at the delta sequences of *Saccharomyces cerevisiae***. *Appl Microbiol Biotechnol* 1997, **48**:339-345.

179. Dupreez JC, Prior BA: **A Quantitative screening of some xylose-fermenting yeast isolates**. *Biotechnology Letters* 1985, **7**:241-246.

180. Beld J, Sonnenschein EC, Vickery CR, Noel JP, Burkart MD: **The phosphopantetheinyl transferases: catalysis of a post-translational modification crucial for life**. *Nat Prod Rep* 2014, **31**:61-108.

181. Schaaff I, Hohmann S, Zimmermann FK: **Molecular analysis of the structural gene for yeast transaldolase**. *Eur J Biochem* 1990, **188**:597-603.

182. Xu H, Kim S, Sorek H, Lee Y, Jeong D, Kim J, Oh EJ, Yun EJ, Wemmer DE, Kim KH, et al.: ***PHO13* deletion-induced transcriptional activation prevents sedoheptulose accumulation during xylose metabolism in engineered *Saccharomyces cerevisiae***. *Metab Eng* 2016, **34**:88-96.

183. Lindqvist Y, Schneider G, Ermler U, Sundstrom M: **Three-dimensional structure of transketolase, a thiamine diphosphate dependent enzyme, at 2.5 A resolution**. *Embo j* 1992, **11**:2373-2379.

184. Kleijn RJ, van Winden WA, van Gulik WM, Heijnen JJ: **Revisiting the ^{13}C-label distribution of the non-oxidative branch of the pentose phosphate pathway based upon kinetic and genetic evidence**. *Febs j* 2005, **272**:4970-4982.

185. Boles E, de Jong-Gubbels P, Pronk JT: **Identification and characterization of *MAE1*, the *Saccharomyces cerevisiae* structural gene encoding mitochondrial malic enzyme**. *J Bacteriol* 1998, **180**:2875-2882.

186. Connor MR, Liao JC: **Engineering of an *Escherichia coli* strain for the production of 3-methyl-1-butanol**. *Appl Environ Microbiol* 2008, **74**:5769-5775.
187. Ihrig J, Hausmann A, Hain A, Richter N, Hamza I, Lill R, Muhlenhoff U: **Iron regulation through the back door: iron-dependent metabolite levels contribute to transcriptional adaptation to iron deprivation in *Saccharomyces cerevisiae***. *Eukaryot Cell* 2010, **9**:460-471.
188. Muhlenhoff U, Lill R: **Biogenesis of iron-sulfur proteins in eukaryotes: a novel task of mitochondria that is inherited from bacteria**. *Biochimica Et Biophysica Acta-Bioenergetics* 2000, **1459**:370-382.
189. Li SB, Liu LM, Chen J: **Compartmentalizing metabolic pathway in *Candida glabrata* for acetoin production**. *Metabolic Engineering* 2015, **28**:1-7.

Abstract in Korean

국 문 초 록

이소부탄올은 가지 사슬 고급 알코올로서 높은 에너지 밀도와 낮은 흡습성으로 현재 기반시설을 이용한 수송과 저장이 용이하기 때문에 에탄올을 대체할 수 있는 바이오 연료로서 각광받고 있다. 특히 가솔린에 높은 비율로 첨가할 수 있을 뿐만 아니라 수송 연료로 사용시 엔진의 노킹 현상을 감소시킨다는 장점이 존재한다. *Saccharomyces cerevisiae* 오랜기간 연구가 활발히 진행된 진핵 모델 시스템으로 알코올기를 가지는 화합물에 대한 저항성이 높을 뿐만 아니라, 산업적 발효 공정과 같은 극한의 환경에서도 잘 견디기 때문에 이소부탄올을 생산하기 위한 미생물 세포 공장으로써의 높은 효용성을 지닌다. 본 연구에서는 다양한 대사 공학적 전략을 이용하여 다양한 이소부탄올 생산 경로를 구축함으로써 이소부탄올 생산이 증대된 *S. cerevisiae* 균주를 제작하고자 하였고, 이를 통해 구축된 시스템을 자외선차단 물질인 시노린 생산에 적용하여 그 가능성을 확인하였다.

첫 번째로, 이소부탄올 생산 효모 균주를 개발하기 위하여 *S. cerevisiae* 내에 존재하는 이소부탄올 생산경로를 강화하였다. 효모 내에서 이소부탄올 발린 생합성 과정과 그의 분해 과정인 Ehrlich 경로에 의해 생산된다. 특히 발린 생합성 과정에 관여하는 효소들은 대사물질에 의해 활성이 조절되는 전사조절인자 Leu3 에 의해 발현이 조절된다. 따라서 대사물질의 유무에 관계없이 항상 활성을 가지는 Leu3 돌연변이를 제작 및 과발현 하였다. 이와 함께 이소부탄올 생산 관련 유전자들을 강한 프로모터를 이용하여 과발현함으로써 376.9 mg/L 의

이소부탄올 생산하였다. 또한, 본 균주에 류신 생합성 경로를 재건하고 류신에 의해 피드백 저해를 받지 않는 생합성 유전자를 과발현함으로써 또 다른 가지 사슬 고급알코올인 3-메틸-1-부탄올을 야생형 균주 대비 43 배 증가한 765.7 mg/L 생산하였다.

두 번째로, 이소부탄올 생산 경로를 조작하여 미토콘드리아 내부로 밀집시켜 이소부탄올 생산량이 증가된 효모 균주를 개발하였다. 효모는 다양한 막구조를 가지는 진핵 생물로서 이소부탄올 생산은 미톤콘드리아 안팍을 경유하는 경로를 통해 이루어진다. 따라서 이소부탄올 생산을 위해서는 중간체들의 미토콘드리아 내외로의 수송이 필수이고 이는 효모 내에서 이소부탄올 생산에 중요한 저해요소가 된다. 따라서 이를 극복하고자 효모의 이소부탄올 생산 경로에 관련된 효소들을 미토콘드리아 내부로 재배치 하였다. 이러한 미토콘드리아 기반의 이소부탄올 대사 경로에 의해 세포와 기질의 밀집이 유도되고 이는 빠른 반응 속도를 제공하기 때문에 이소부탄올 생산량이 증가하였다. 특히 미토콘드리아 내부에서 Fe-S 클러스터의 생산이 이루어지기 때문에 미토콘드리아 기질은 이소부탄올 생산 경로 3 번째에 관여하는 Fe-S 단백질인 Ilv3 의 활성을 증가시킬 수 있는 환경을 제공을 제공한다. 본 경로를 이용하여 이소부탄올 생산을 증가시키기 위해서는 세포질에 존재하는 피루브산을 다량 미토콘드리아 내부로 유입해야한다. 따라서 여기에 관여하는 미토콘드리아 피루브산 수송 단백질의 최적의 조합을 탐색하였고, 이의 과발현을 통해 이소부탄올을 야생형과 비교하여 22 배 증가시킨 338 mg/L 농도로 생산하였다. 추가적으로 Fe-S 클러스터의 결합에 관여하는 cysteine desulferase Nfs1, 그의 활성자 Isd11 을 과발현함으로써 최종적으로 435.2 mg/L 의 이소부탄올을 생산할 수 있었다. .

세 번째로, 세포질 기반의 이소부탄올 생산 경로의 구축을 통해

효모내에서 이소부탄올 생산을 증가시켰다. 미토콘드리아 기반의 대사 경로에서 MPC 유전자를 과발현하여 이소부탄올 생산을 증가시켰지만, 여전히 피루브산의 미토콘드리아로의 수송은 중요한 제한요소로 작용한다. 따라서 세포질에 존재하는 다량의 피루브산을 이용하기위해 박테리아 유래의 이소부탄올 생산 관련 유전자 (*alsS*) 를 도입하고 효모의 미토콘드리아 발린 생합성 유전자에 코작 시퀀스를 도입하여 세포질로 재배치함으로써 이소부탄올 생산이 증가함을 확인하였다. 특히 *B. subtilis* 유래의 alsS 과발현시 효모가 생장하지 않음을 관찰하였고 이를 구리에 의해 유도되는 프로모터를 이용하여 발현함으로써 이소부탄올 생산을 향상시켰다. 한편, 이소부탄올 생산 경로를 효모 염색체 내에 다량 도입하기 위해 델타-인터그레이션과 rDNA-인터그레이션을 이용하였다. 유전자가 염색체 내로 도입된 효모 균주의 라이브러리에서 최적의 균주 선별을 위하여 구리에 의한 alsS 의 유도성 과발현에 의해 나타나는 효모의 표현형을 이용하여 균주 선별 시스템을 개발하였고 이를 통해 다량의 유전자가 염색체 내로 도입된 효모 균주를 성공적으로 확보할 수 있었다.

마지막으로, 이소부탄올 생산에 이용한 유전자 조작 기법을 응용하여 새로운 타겟 물질인 자외선차단물질 시노린을 효모내에서 생산하였다. 기존에 널리 사용되는 화학적 물리적 자외선 차단 물질은 환경오염과 알레르기를 발생시키기 때문에 고효율로 자외선을 차단할 수 있는 천연 물질이 필요하다. 시노린은 일부 미세조류나 곰팡이에서 생산되는 자외선 차단물질로서 자외선 차단 효과뿐만 아니라, 안티에이징 효과가 입증되어 있는 고부가가치 물질이다. 하지만 자연적으로 시노린을 생산하는 미생물들은 배양조건이 까다롭고 유전자 조작이 힘들기 때문에 효모는 이를 극복할 수 있는 대안이라고 할 수 있다. 미세조류 *Nostoc punctiforme* 과 *Anabaena variabilis* 유래의 시노린

생산 경로를 효모내에 도입함으로써 시노린 생산 효모 균주를 재작하였다. 또한 시노린 생산은 오탄당인산경로를 통하기 때문에 자일로오스를 탄소원으로 도입하였고 이를 이용할 수 있는 효모 균주의 개발을 통해 시노린 생산량이 크게 증가함을 확인하였다. 특히 유가 배양을 통해 JHYS17-1 균주는 64.2 mg/L 의 시놀린을 생산하였고 지금까지 보고된 최고 함량 (14.3 mg/gDCW) 을 나타내었다. 추가적으로 경쟁 경로의 제거 및 오탄당인산경로의 전사조절인자 (Stb5) 와 트랜스케톨라아제 (Tkl1) 의 과발현을 통해 시놀린생산량이 더욱 증가할 수 있는 가능성을 확인하였다.

주요어 : 대사공학, 아미노산 대사, 이소부탄올, 미토콘드리아, 피루브산 수송체, 시노린, 자일로오스 대사, 델타-인터그레이션, rDNA-인터그레이션, *Saccharomyces cerevisiae*

학 번 : 2014-30253

감사의 글

끝이 올까 싶었던 학위 과정에도 마침표가 찍어지는 순간이 다가왔습니다. 졸업이라는 것이, 박사라는 학위가 이렇게 무거운 것임을 졸업하고서야 비로소 깨닫게 되는 것 같습니다. 6 년 반이라는 긴 시간동안 졸업만을 향해서 달려온 것 같지만 그 과정 속에서 스스로 성장하고 단단해질 수 있었습니다. 돌이켜 생각해보면 좋은 일, 힘든 일, 소소했지만 행복했던 순간들이 참 많았습니다. 이 순간 순간들을 함께해주신 감사한 분들께 짧게나마 감사의 마음을 전하고자 합니다.

먼저 학위 과정동안 부족한 저에게 가르침을 주시고 믿어주시고 끝까지 성장할 수 있도록 지지해주신 지도 교수님, 한지숙 교수님께 진심으로 감사드립니다. 스승으로, 리더로, 연구자로서뿐만 아니라 인생의 멘토로서 교수님께 많은 것을 배웠고, 이는 제 인생의 큰 지침이 되었습니다. 학위 과정 동안 무럭무럭 성장할 수 있도록 든든한 버팀목이 되어 주셔서 감사합니다. 교수님의 가르침에 보답할 수 있도록 언제, 어디서든 최선을 다하겠습니다. 또한 바쁘신 와중에도 논문 심사에 힘써주신 서진호 교수님, 김병기 교수님, 오민규 교수님, 그리고 서상우 교수님께도 다시 한번 감사드립니다.

학위 과정 동안 가족보다 더 많은 시간을 함께 했던 우리 생물분자공학 연구실 식구들에게도 이 기회를 빌어 감사의 인사를 전합니다. 생물분자공학 연구실 선배님 모두 저의 사수였다고해도 과언이 아닙니다. 인턴 기간동안 큰 힘이 되어준 베드로 오빠, 연구에 꾸준히 지원해주신 규성오빠, 항상 따뜻하고 너그러웠던 태준오빠, 언제나 말벗이 되어주시고 격려해주신 보람오빠, 옆자리에서 말 많은 후배때문에 힘드셨을텐데 항상 잘 챙겨주신 승호오빠에게 감사합니다. 그리고 많은 것을 가르쳐 주시고, 항상 힘이 되고 의지가 되어준 수진언니에게 감사의 말을 전합니다. 동갑인 후배 때문에 많이 힘들었을 대희에게도 감사합니다. 이제 아기 엄마가 되는 아람언니, 같이 박사과정을 마무리하는 상민 오빠에게도 감사합니다. 언니 오빠들 덕분에 학위 과정 내내 든든했고, 동기부여가 많이 되었던 것 같습니다. 많은 배려를 해준 후배들에게도 고맙습니다. 후배이지만 때로는 친구처럼, 언니처럼 옆에서 많이 도와준 상정이에게 고맙습니다. 미국에 있는 윤정이에게도 고맙고 원하는 것을 꼭 이루길 바랍니다. 첫 후배였던 지수, 착한 우훈이와 똑부러지는 주현이에게도 고맙습니다. 또한 광현이, 승우, 시화, 종관이, 수민이, 한결이, 용훈이

모두 고맙고, 각자 학위 과정에 임했던 초심을 되새기며 후회가 남지 않는 학위 과정을 보냈으면 좋겠습니다.

학위 과정동안 다른 연구실에 신세를 많이 졌습니다. 많은 것을 함께 공유하며 살뜰히 챙겨주셨던 은영언니, 귀찮은 부탁들을 흔쾌히 들어준 준원이, 평강이에게 고맙습니다. 그리고 같은 연구실처럼 편안하게 대해 주신 유영제 교수님 연구실분들, 김병기 교수님 연구실분들에게도 감사합니다.

서울이라는 타지에서 외롭지 않도록 함께해준 많은 친구들에게도 감사드립니다. 우선 눈이오나 비가오나 기쁘거나 힘든 순간에도 항상 함께해준 민숙이, 엄마처럼 언니처럼 항상 걱정해준 수미, 대장부 효주, 철없던 십대 시절부터 서른이 넘도록 많은 추억을 함께 공유했고. 서로를 이해해가며 더욱 단단한 우정을 쌓았다고 생각합니다. 너무 고맙습니다. 벌써 십년지기가 된 우리 벤젠, 국희, 지은이, 예슬이, 경아, 정민이 고맙습니다. 자랑스러운 친구 경은이, 자기개발을 게을리하지 않는 미희에게도 고마운 마음을 전합니다. 영어뿐만 아니라 무엇보다 내적으로 단단해 질 수 있도록 스스로를 바라보는 시각을 길러주신 레바 선생님과 쓸데있는 영어 연구소 식구들에게도 고맙습니다. 영어를 계속 공부할 수 있도록 시작부터 함께 열심히 해준 예지에게도 고마운 마음을 전합니다.

그리고 우리 할머니, 손녀가 제대로 효도할 때까지 건강하게 더 오래 사셨으면 좋겠습니다. 나이 많은 조카 용돈 챙겨주신다고 고생하신 친척분들께도 모두 감사드립니다. 아무쪼록 다들 건강하셨으면 좋겠습니다.

마지막으로 우리 가족들, 다른 누구보다 동생을 살뜰히 챙긴 든든한 우리 오빠, 멀리 떨어져 있는딸 대신 더 부모님을 챙겨주는 완선 언니, 너무 고맙습니다. 그리고 올해 우리 집의 큰 선물인 사랑스러운 마로, 우리 수호 덕분에 졸업 마무리를 힘내서 할 수 있었습니다. 그리고 사랑하는 우리 엄마 아빠, 남들보다 오래 공부하는 딸 뒷바라지 하느라 고생하셨습니다. 말로는 다 전하지 못할 만큼 감사하고 사랑합니다. 우리 가족 모두 행복하고 건강했으면 좋겠습니다.

감사합니다.

2018 년 여름

감사의 마음을 담아, 성희 올림.